UNIVERSIDADE FEDERAL DE SANTA MARIA
CENTRO DE CIÊNCIAS NATURAIS E EXATAS
PROGRAMA DE PÓS-GRADUAÇÃO EM CIÊNCIAS BIOLÓGICAS:
BIOQUÍMICA TOXICOLÓGICA

James Eduardo Lago Londero

AVALIAÇÃO DA IMPORTÂNCIA DO FOTORREPARO DE DNA EM ANFÍBIOS

Santa Maria, RS
2019

James Eduardo Lago Londero

AVALIAÇÃO DA IMPORTÂNCIA DO FOTORREPARO DE DNA EM ANFÍBIOS

Dissertação apresentada ao Curso de Pós-Graduação em Ciências Biológicas: Bioquímica Toxicológica, da Universidade Federal de Santa Maria (UFSM, RS), como requisito parcial para a obtenção do título de **Mestre em Ciências Biológicas: Bioquímica Toxicológica**.

Orientador: Prof. Dr. André Passaglia Schuch

Santa Maria, RS
2019

Londero, James Eduardo Lago
Avaliação da importância do fotorreparo de DNA em anfíbios / James Eduardo Lago Londero.- 2019.
84 p.; 30 cm

Orientador: André Passaglia Schuch
Dissertação (mestrado) - Universidade Federal de Santa Maria, Centro de Ciências Naturais e Exatas, Programa de Pós-Graduação em Ciências Biológicas: Bioquímica Toxicológica, RS, 2019

1. Declínio de anfíbios 2. Radiação UV 3. Dano de DNA 4. Reparo de DNA 5. Fotoliase I. Schuch, André Passaglia II. Título.

Sistema de geração automática de ficha catalográfica da UFSM. Dados fornecidos pelo autor(a). Sob supervisão da Direção da Divisão de Processos Técnicos da Biblioteca Central. Bibliotecária responsável Paula Schoenfeldt Patta CRB 10/1728.

James Eduardo Lago Londero

AVALIAÇÃO DA IMPORTÂNCIA DO FOTORREPARO DE DNA EM ANFÍBIOS

Dissertação apresentada ao Curso de Pós-Graduação em Ciências Biológicas: Bioquímica Toxicológica, da Universidade Federal de Santa Maria (UFSM, RS), como requisito parcial para a obtenção do título de **Mestre em Ciências Biológicas: Bioquímica Toxicológica**.

Aprovado em 19 de fevereiro de 2019:

André Passaglia Schuch

André Passaglia Schuch, Dr. (UFSM)
(Presidente/Orientador)

Tiago Antonio de Souza, Dr. (USP)

Daniel Mendes Pereira Ardisson-Araújo

Daniel Mendes Pereira Ardisson-Araújo, Dr. (UFSM)

Santa Maria, RS
2019

AGRADECIMENTOS

Começarei esta seção citando a cientista Marie Curie, a única pessoa a receber por duas vezes o prêmio Nobel em categorias científicas distintas até hoje (Física em 1903; Química em 1911):

"Cada pessoa deve trabalhar para o seu aperfeiçoamento e, ao mesmo tempo, participar da responsabilidade coletiva por toda a humanidade".

Na universidade somos capazes de impactar a sociedade, seja com as nossas aulas e palestras ministradas, as pesquisas desenvolvidas e as atividades que nós universitários propomos para a sociedade não universitária. Na presente dissertação encontram-se descobertas e novas discussões científicas que possuem alcance global. Tudo isso só foi possível por causa da manutenção de uma universidade pública e gratuita. Que nós como sociedade possamos melhorar a sua qualidade cada vez mais. Obrigado UFSM, PPGBTox e órgãos de fomento (PROEX CAPES – 8882.182173/2018-01).

Agradeço ao André pela sua orientação, prestatividade e por dar o seu melhor para que nós do Lab Fotobio tenhamos a oportunidade de desenvolver estudos originais, legais e com relevância ambiental/social. Gratidão, André, Maurício, Rayana, Bruno, Bruna, Marcelo, Cassiano, Ana Lúcia, Victor, Ismália, Sophia, Caroline e Lucas pelas trocas de experiências no Lab Fotobio que puderam me levar a um maior aperfeiçoamento pessoal, como diria Curie. Não poderia deixar de agradecê-los pelas risadas, conversas aleatórias e também pelos almoços/jantas e comemorações com os salgados!!!

Obrigado a todos que de alguma forma contribuíram para que eu pudesse chegar onde cheguei, incluindo familiares, amigos, professores escolares e universitários.

Gratidão especial aos meus pais, Cleusa e Carlos, à minha irmã, Dinah, e à minha namorada, Júlia, pelo amor, companheirismo, carinho e suporte; e também ao Marco, pela amizade nestes dois anos. Vocês são a minha base. Eu amo muito vocês!!!

RESUMO

AVALIAÇÃO DA IMPORTÂNCIA DO FOTORREPARO DE DNA EM ANFÍBIOS

AUTOR: James Eduardo Lago Londero
ORIENTADOR: André Passaglia Schuch

Os anfíbios têm sofrido um declínio populacional generalizado em todo o globo. Em torno de 40% das espécies de anfíbios existentes estão ameaçadas de extinção. A radiação ultravioleta (UV) solar (280-400 nm) possui a capacidade de formar lesões citotóxicas e mutagênicas no genoma de anfíbios, as quais podem comprometer o desempenho e aptidão destes animais. Fatores como o decréscimo do ozônio estratosférico, mudanças climáticas, desmatamento e diminuição de matéria orgânica em corpos de água, têm aumentado a incidência de radiação UV solar em sítios reprodutivos de anfíbios. Em contrapartida, a fim de minimizar os efeitos prejudiciais das lesões induzidas pela UV em seu genoma, anfíbios possuem mecanismos capazes de repará-las, tais como o fotorreparo (ou fotorreativação), o qual envolve a absorção de luz (350-700 nm) por meio de enzimas chamadas fotoliases e a transferência de elétrons às lesões, assim removendo-as. No entanto, a capacidade de fotorreparo varia entre espécies, sendo a ineficiência deste mecanismo um possível fator determinante para o declínio populacional de espécies sensíveis à radiação solar. Levando isto em consideração, o objetivo geral deste trabalho consistiu em avaliar a importância do fotorreparo de DNA em anfíbios. Primeiramente, as respostas biológicas de anfíbios aos danos de DNA induzidos pela UV, as quais incluem a capacidade de fotorreparo, foram discutidas através de uma revisão ampla da literatura existente sobre este tópico. Os resultados demonstram que apenas três trabalhos dos 21 encontrados avaliaram diretamente as lesões de DNA induzidas pela UV *in vivo*. Como consequência, os mecanismos de reparo de DNA são pouquíssimos estudados e compreendidos. Desta forma, a importância do fotorreparo de DNA para a manutenção do desempenho alimentar de girinos especialistas florestais previamente expostos a uma baixa dose ambiental de radiação UVB (280-315 nm) foi avaliada através de um estudo experimental controlado com girinos de uma espécie de perereca ameaçada de extinção [*Boana curupi* (Garcia, Faivovich e Haddad, 2007); Anura; Hylidae]. Os resultados demonstram que a radiação UVB impactou negativamente no peso dos girinos devido a uma redução do consumo de alimento, que por sua vez foi consequência do impacto genotóxico da UVB. O tratamento adicional com luz visível (pós UVB) sugeriu uma baixa eficiência do fotorreparo de DNA nesta espécie, uma vez que o peso corporal e a atividade de consumo de alimento permaneceram afetados. Adicionalmente, análises *in silico* foram conduzidas com o objetivo de compreender as bases moleculares das fotoliases de anfíbios. Análises de homologia foram realizadas com sequências de fotoliases de anfíbios. Apenas sequências anotadas e acuradas foram obtidas a partir do GenBank, BLASTp e tBLASTn (NCBI). Os resultados demonstram variações interespecíficas na ocorrência destas enzimas e a possível má anotação de algumas sequências. A partir destes resultados, perspectivas futuras são discutidas. A presente dissertação demonstra que há ainda uma falta de compreensão do fotorreparo em anfíbios, e que possíveis novas avenidas sobre este tema devem ser traçadas, a fim de melhor elucidar o papel do fotorreparo em anfíbios. Portanto, a contribuição da radiação UV solar para o declínio de anfíbios e a importância do fotorreparo de DNA para evitar os efeitos genotóxicos induzidos pela radiação UV em espécies de anfíbios pode se tornar mais evidente em um futuro próximo.

Palavras-chave: Radiação UV. Luz solar. Declínio de anfíbios. Danos de DNA. Lesões de DNA. Reparo de DNA. Fotorreparo de DNA. Fotorreativação. Fotoliases. Girinos. Performance alimentar. Floresta. Mata Atlântica.

ABSTRACT

ASSESSMENT OF THE IMPORTANCE OF DNA PHOTOREPAIR IN AMPHIBIANS

AUTHOR: JAMES EDUARDO LAGO LONDERO
ADVISOR: ANDRÉ PASSAGLIA SCHUCH

Amphibians have suffered a widespread population decline across the globe. About 40% of existing amphibian species are threatened with extinction. Solar ultraviolet (UV) radiation (280-400 nm) has the capacity to form cytotoxic and mutagenic lesions in the amphibian genome, which may compromise the performance and fitness of these animals. Factors such as the decrease of stratospheric ozone, climate changes, deforestation and decrease of organic matter in water bodies have increased the incidence of solar UV radiation upon amphibian breeding sites. In contrast, in order to minimize the harmful effects of UV-induced lesions on their genome, amphibians have mechanisms capable of repairing them, such as photorepair (or photoreactivation), which involves the absorption of light (350-700 nm) by means of enzymes called photolyases and the transfer of electrons to the lesions, thus removing them. However, photorepair capacity varies among species, and the inefficiency of this mechanism is a possible determinant factor for population decline of UV-sensitive species. Taking this into account, the general objective of this work was to evaluate the importance of DNA photorepair in amphibians. First, the biological responses of amphibians to UV-induced DNA damage, which include photorepair capability, have been discussed through a broad review of existing literature on this topic. The results show that only three out the 21 studies found directly evaluated the UV-induced DNA lesions *in vivo*. As a consequence, DNA repair mechanisms are very few studied and understood. Thus, the importance of DNA photorepair for the maintenance of the feeding performance of forest specialist tadpoles previously exposed to a low environmental dose of UVB radiation (280-315 nm) was evaluated through a controlled experimental study with a species of treefrog threatened with extinction [*Boana curupi* (Garcia, Faivovich and Haddad, 2007); Anura; Hylidae]. The results demonstrate that UVB radiation negatively impacted tadpole weight due to reduced food consumption, which in turn was a consequence of the genotoxic impact of UVB. An additional treatment with visible light (post-UVB) suggested a low efficiency of DNA photorepair in this species, since body weight and food consumption activity remained affected. In addition, *in silico* analyzes were conducted with the objective of understanding the molecular basis of amphibian photolyases. Homology analyzes were performed with sequences of amphibian photolyases. Only annotated and accurate sequences were obtained from GenBank, BLASTp and tBLASTn (NCBI). The results demonstrate interspecific variations in the occurrence of these enzymes and the possible bad annotation of some sequences. From these results, future perspectives are discussed. The present dissertation demonstrates that there is still a lack of understanding of amphibian photolyases, and that possible new avenues on this subject must be traced in order to better elucidate the role of photorepair in amphibians. Therefore, the contribution of solar UV radiation to the decline of amphibians, and the importance of DNA photorepair to avoid the UV-induced genotoxic effects on amphibian species may become more evident in the near future.

Keywords: UV radiation. Sunlight. Amphibian decline. DNA lesions. DNA repair. DNA photorepair. Photoreactivation. Photolyases. Tadpoles. Feeding performance. Forest. Atlantic forest.

SUMÁRIO

1 INTRODUÇÃO

Nas últimas décadas têm se observado um fenômeno global de declínio de anfíbios, onde muitas espécies estão sofrendo reduções em suas distribuições naturais ou mesmo já foram extintas (STUART et al., 2004). Segundo a Lista Vermelha das Espécies Ameaçadas da União Internacional para Conservação da Natureza (IUCN), aproximadamente 40% das espécies existentes de anfíbios (~2676 de 6690 espécies) encontra-se ameaçada de extinção, mas esta proporção pode alcançar o alarmante valor de 54% (IUCN, 2018). Alarmantemente, mais de 200 espécies estão sofrendo rápidos declínios populacionais mesmo em hábitats aparentemente adequados e intocados, ou seja, sem interferência humana (STUART et al., 2004).

Anfíbios são componentes fundamentais da dinâmica trófica e fluxo de energia dentro dos ecossistemas e constituem uma significante proporção da biomassa de vertebrados (STEBBINS, 1995; WHILES 2006). Anfíbios são ectodérmicos dependentes de água para reprodução e são caracterizados pela pele permeável que pode absorver facilmente substancias do ambiente (DUELLMAN, 1994). Indivíduos que possuem ciclos de vida complexos, como muitos anuros (sapos, rãs e pererecas), possuem uma história de vida caracterizada pelos diferentes estágios de desenvolvimento: o ovo que contém o embrião; o girino ou larva; o imago ou juvenil; e o adulto. Ovos e girinos são fortemente dependentes de corpos de água, enquanto imagos e adultos são tipicamente terrestres (DUELLMAN, 1994). Os tipos de alimentação podem diferir entre as fases de vida, sendo a maioria dos girinos de hábito onívoro/micrófago com muitas adaptações no aparato locomotor e alimentar; e a maioria dos adultos possuindo hábito carnívoro (DUELLMAN, 1994; ALTIG e MCDIARMID, 1999). Notavelmente, a susceptibilidade a alterações ambientais pode variar entre indivíduos ou espécies (BLAUSTEIN e BELDEN, 2003).

A radiação ultravioleta (UV) solar, um importante estressor genotóxico ambiental, afeta negativamente a saúde e desempenho de embriões e larvas de anfíbios (SCHUCH et al., 2015a; ALTON e FRANKLIN, 2017). Alterações ambientais globais induzidas por humanos como o decréscimo da concentração de ozônio estratosférico e as mudanças climáticas, podem contribuir de forma significativa para o aumento dos níveis incidentes de radiação UV solar sobre os estágios iniciais do desenvolvimento de anfíbios (SCHUCH et al., 2015b; HADER et al., 2015; ALTON e FRANKLIN, 2017). Diferentes consequências biológicas têm sido verificadas em indivíduos expostos à radiação UV, tais como redução das taxas de crescimento e desenvolvimento, metamorfose atrasada, malformações, mudanças

comportamentais, susceptibilidade a infecções e predação, ou mesmo morte (BLAUSTEIN et al., 1998; ALTON et al., 2012; SCHUCH et al., 2015a; SCHUCH et al., 2015b, LIPINSKI et al., 2016).

O potencial genotóxico da radiação UV solar que incide na superfície terrestre [formada pelos comprimentos de onda do tipo B (UVB, 280−315 nm) e tipo A (UVA, 315−400 nm)] advém principalmente da energia de seus fótons, que é capaz de induzir ligações covalentes entre pirimidinas de nucleotídeos vizinhos em uma hélice do DNA (SCHUCH et al., 2017). A estrutura gerada é conhecida como dímero de pirimidina, um tipo de danos ou lesão de DNA, que pode ser chamado também de fotoproduto (SANCAR, 2008; SCHUCH et al., 2017). Uma vez formados, os dímeros de pirimidina proporcionam uma distorção na dupla hélice, que prejudica a replicação e a transcrição do DNA (SCHUCH et al., 2017). A radiação UVB é mais eficaz que a UVA para formar dímeros de pirimidina devido à maior absorção direta de fótons de UVB pelo DNA (SCHUCH et al., 2017). Os danos de DNA induzidos com maior frequência pela UV são conhecidos como dímeros de pirimidina ciclobutano (CPD), os quais constituem ~80–90% das lesões, e fotoprodutos (6-4) pirimidina-pirimidona (6-4PP), os quais correspondem a 10–20% das lesões (SANCAR, 2008). Ver detalhes estruturais destas lesões na p. 36.

As radiações UVB e UVA podem induzir morte celular, mutagênese e carcinogênese como consequências dos dímeros de pirimidina no DNA (FRIEDBERG, 2003; SCHUCH et al., 2017). Entretanto, as lesões induzidas pela radiação UV podem ser corrigidas por diferentes mecanismos de reparo de DNA, antes mesmo de desencadearem processos citotóxicos e mutagênicos (FRIEDBERG, 2003; RASTOGI et al., 2010). Em um processo conhecido como fotorreparo ou fotorreativação, enzimas chamadas como fotoliases utilizam UVA/luz visível (300 – 500 nm) como fonte de energia, e transferência de elétrons para reverter os dímeros de pirimidina (FRIEDBERG, 2003; SANCAR 2008). Desta forma, a luz solar têm sido um fator chave na evolução da vida, devido a sua ação prejudicial ou benéfica em sistemas vivos.

Dois tipos de fotoliases são capazes de reparar os fotoprodutos induzidos pela UV: as CPD fotoliases (CPD PHR) reparam lesões CPD; e as (6-4) fotoliases ((6-4) PHR) reparam lesões 6-4PP (SANCAR 2008). A seguir a dinâmica do fotorreparo realizado pela CPD PHR será detalhada. A dinãmica se inicia no escuro com a enzima fotoliase se ligando ionicamente com os resíduos de fosfato da fita de DNA danificada e liberando o dímero de pirimidina na cavidade do sítio ativo, de forma que o dímero esteja em contato com FADH– por meio de ligações de forças de Van der Waals. A reação catalítica é iniciada pela absorção de fótons de

UVA/luz visível (300-500 nm) pelo painel solar/fotoantena folato (MTHF). O estado singlete excitado do MTHF transfere a energia de excitação para FADH– por transferência de energia de ressonância (RET). O FADH–* excitado divide o anel ciclobutano pela reação redox cíclica e monomeriza o dímero de pirimidina, e em seguida o DNA reparado se dissocia da enzima. O fotociclo catalítico é completado pela restauração da forma ativa FADH- através do retorno de elétrons do dímero reparado (**Figura 1**). A reação fotoquímica inteira é ultra rápida (1,2 ns) e eficiente (rendimento quantum em torno de 0.9). O mecanismo de fotorreparo é similar em ambos os complexos CPD + CPD PHR e 6-4PP + 6-4 PHR (SANCAR, 2003; KAO et al., 2007;.LIU et al., 2011; ZHONG, 2015).

Figura 1 - Dinâmica do fotorreparo de DNA. (1) A enzima fotoliase se liga ao dímero de pirimidina (por exemplo, CPD) no escuro. (2) Através de uma reação térmica, (3) a enzima torce o dímero de pirimidina de dentro da dupla hélice do DNA para sua cavidade do sítio ativo. (4) Quando fótons de luz visível/UVA incidem na fotoliase e (5) alcançam o painel solar (ou fotoantena; por exemplo, MTHF), este se torna excitado. (6) Por meio de transferência de energia de ressonância (RET), o MTHF transfere sua energia de excitação para (7) FADH–, a coenzima catalítica. (8) O FADH–* excitado monomeriza (reverte) o dímero de pirimidina e ocorre o retorno de elétrons do dímero e restauração da forma ativa FADH. No entanto, pode ocorrer a excitação direta do FADH– pela luz visível/UVA. Legenda: CPD: cyclobutane pyrimidine dimer; MTHF: methenyltetrahydrofolate.

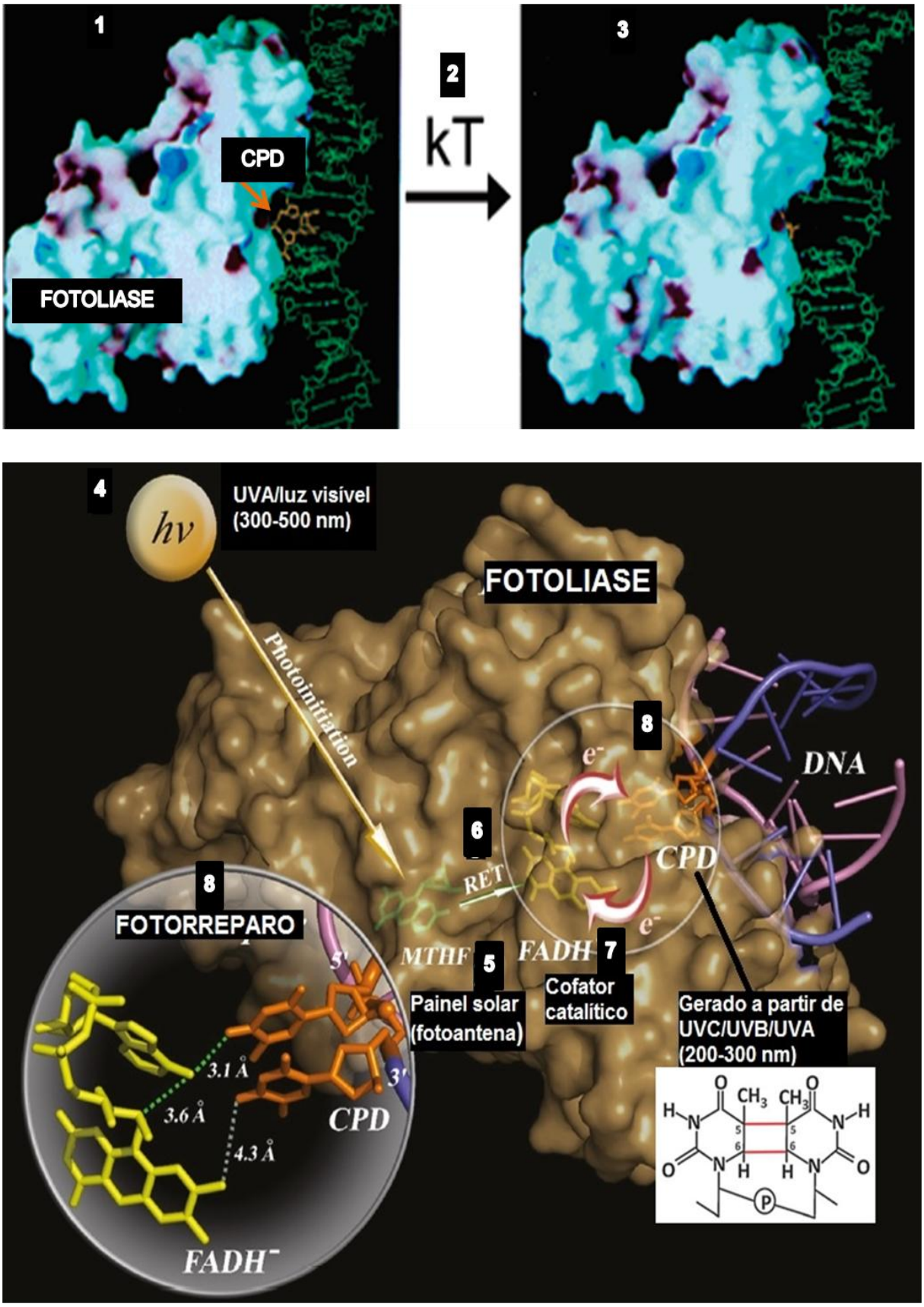

Fonte: Adaptado de SANCAR (2003) e KAO et al. (2007).

O fotorreparo de DNA é o principal e mais eficiente mecanismo de reparo dos dímeros de pirimidina induzidos pela UV presente no clado dos anfíbios (MENCK, 2002). Entretanto, de acordo com a hipótese da sensibilidade à UV, espécies de anfíbios com menor resistência à radiação UV solar possuem uma menor capacidade de reparar os dímeros de pirimidina gerados na molécula de DNA (BLAUSTEIN et al., 1994). Assim, os níveis de atividade das fotoliases diferem substancialmente entre espécies de anfíbios (BLAUSTEIN et al. 1994; VAN DE MORTEL et al., 1998; SANTOS e LONDERO et al., 2018).

O objetivo geral deste trabalho consistiu em avaliar a importância do fotorreparo de DMA em anfíbios. A sessão de texto da presente dissertação encontra-se dividida em seis capítulos, sendo esta sessão introdutória o primeiro capítulo. O segundo capítulo trata-se de uma revisão da literatura existente sobre o impacto da radiação UV solar em anfíbios, tendo com o foco as respostas biológicas destes animais, as quais incluem a eficiência do fotorreparo de DNA. O terceiro capítulo avalia a importância do fotorreparo de DNA para a manutenção do desempenho alimentar de girinos especialistas florestais expostos à radiação UVB. A espécie modelo utilizada neste trabalho, *Boana curupi* (Garcia, Faivovich and Haddad, 2007; Anura; Hylidae), está ameaçada de extinção a nível nacional e estadual (MINISTÉRIO DO MEIO AMBIENTE, 2014; GOVERNO DO ESTADO DO RIO GRANDE DO SUL, 2014), estando restrita aos remanescentes florestais de Mata Atlântica do sul do Brasil, a qual compõe o hotspot de biodiversidade Mata Atlântica (MYERS et al., 2000; LONDERO et al., 2018). Os dados sugerem uma alta susceptibilidade desta espécie à radiação UV solar devido à ineficiência do mecanismo de fotorreparo de DNA. A fim de compreender as bases moleculares subjacentes ao fotorreparo de DNA de anfíbios, o quarto capítulo lança uma perspectiva de estudo de caracterização computacional dos genes e proteínas das fotoliases de anfíbios a partir de sequências primárias de 28 espécies. Resultados preliminares demonstram que (1) a ocorrência de genes de fotoliases nas espécies não é uma regra ou (2) as sequências, em geral, são pouco conservadas dentro do clado dos anfíbios ou (3) as sequências utilizadas não foram obtidas e anotadas de maneira correta. Em seguida, os resultados adquiridos nos capítulos mencionados acima, as novidades científicas do presente trabalho, bem como perspectivas para estudos futuros, são discutidos em uma sessão única (quinto capítulo). A conclusão geral da dissertação encontra-se no sexto capítulo.

2 ARTIGO 1 - IMPACT OF SOLAR UV RADIATION ON AMPHIBIANS: FOCUS ON GENOTOXIC STRESS

Este estudo revisa os artigos de pesquisa existentes que têm como foco os danos de DNA (e respostas biológicas) induzidos por doses relevantes ambientalmente de UVB e UVA em espécies de anfíbios. Apenas 21 artigos foram encontrados nos bancos de dados, dos quais somente três mediram diretamente as lesões de DNA *in vivo*. A contribuição da genotoxicidade induzida pela radiação UV solar para o declínio de anfíbios pode estar sendo subestimada. Possíveis investigações futuras são discutidas.

Uma cópia do arquivo referente à última submissão para a revista *Mutation Research – Genetic Toxicology and Environmental Mutagenesis* tem início na página seguinte.

Manuscript Details

Manuscript number	MUTGEN_2018_242_R2
Title	Impact of solar UV radiation on amphibians: focus on genotoxic stress
Article type	Short review

Abstract

Genomic stability is critical for cellular and organismal function. The solar UV radiation is one of the most important environmental genotoxic factors, and its increased incidence due to stratospheric ozone depletion, climate changes, and deforestation plays a role in the worldwide decline of amphibians' populations. Even sublethal effects of UV-induced genotoxicity may cause drastic consequences in the performance and fitness of amphibians. We reviewed the existing literature searching for research papers focused on the induction of DNA damage (and responses) in amphibian species by environmental relevant UVB and UVA doses. We found twenty one papers relative to this topic, but only three of them focused on the direct measurement of DNA lesions induced in vivo. Finally, we identify knowledge gaps and provide recommendations for future investigations concerning the impact of the genotoxicity induced by sunlight on amphibians.

Keywords	Amphibian decline; Sunlight; DNA lesion; DNA damage responses; DNA repair; Genotoxicity.

Corresponding Author	André Schuch
Corresponding Author's Institution	Federal University of Santa Maria
Order of Authors	James Londero, Maurício dos Santos, André Schuch

Suggested reviewers	Carlos FM Menck, Rajeshwar Sinha, Donat Häder, Andrew Blaustein

Graphical abstract

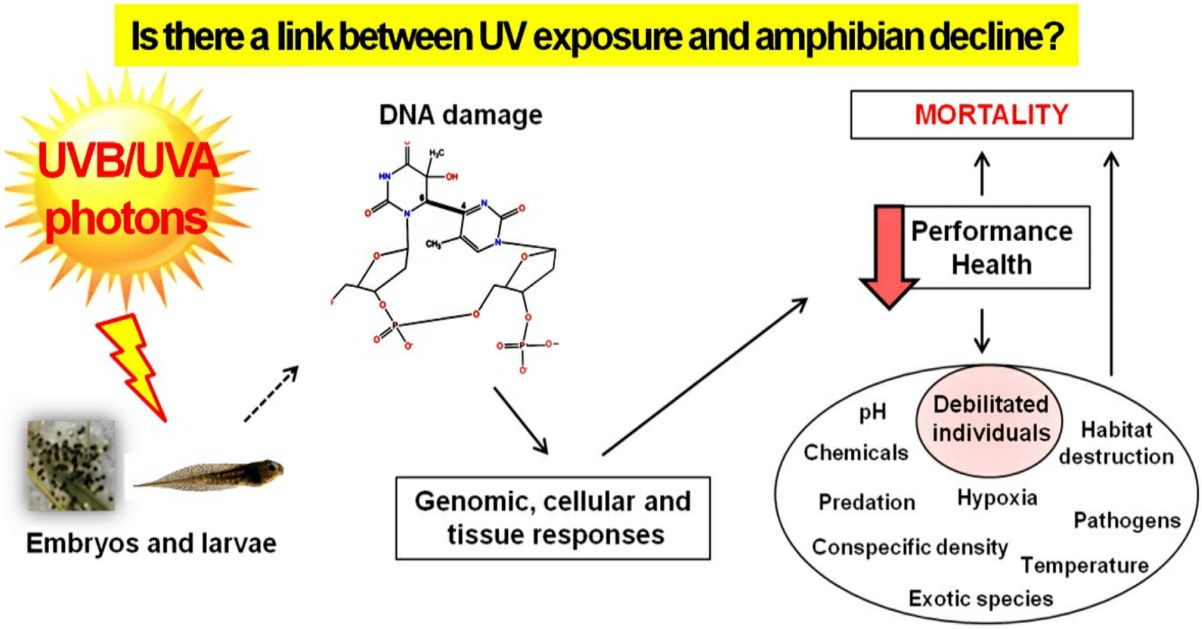

Impact of solar UV radiation on amphibians: focus on genotoxic stress

James Eduardo Lago Londero[1], Maurício Beux dos Santos[1] and André Passaglia Schuch[1]*

1. Federal University of Santa Maria, Department of Biochemistry and Molecular Biology, Post-Graduation Program in Biological Sciences: Toxicological Biochemistry, Santa Maria, RS, Brazil.

*Corresponding author: Roraima Av, 1000, P.O. Box 5021, room 3010, Camobi, Santa Maria, RS, 97110-970, Brazil. Phone: 55.55.3301-2024; Fax: 55.55.3301-2030; E-mail: schuchap@gmail.com.

Abstract

Genomic stability is critical for cellular and organismal function. The solar UV radiation is one of the most important environmental genotoxic factors, and its increased incidence due to stratospheric ozone depletion, climate changes, and deforestation plays a role in the worldwide decline of amphibians' populations. Even sublethal effects of UV-induced genotoxicity may cause drastic consequences in the performance and fitness of amphibians. We reviewed the existing literature searching for research papers focused on the induction of DNA damage (and responses) in amphibian species by environmental relevant UVB and UVA doses. We found twenty one papers relative to this topic, but only three of them focused on the direct measurement of DNA lesions induced *in vivo*. Finally, we identify knowledge gaps and provide recommendations for future investigations concerning the impact of the genotoxicity induced by sunlight on amphibians.

Keywords: Amphibian decline; Sunlight; DNA lesion; DNA damage responses; DNA repair; Genotoxicity.

1. Introduction

Amphibians are potential targets of environmental stressors due to their complex life cycle and skin permeability [1]. In the last decades, several species of amphibians have suffered population declines, and the extinction of many species has been recorded worldwide [2]. According to the IUCN Red List of Endangered Species, about 54% of the amphibian species are threatened with extinction [3]. Several hypotheses have been proposed to explain this phenomenon, including the isolated effects of solar ultraviolet (UV) radiation on embryonic and larval developmental stages, or the combination of exposure to UV radiation with other stressors [see reviews 4-9].

At the cellular level, both ultraviolet B (UVB; 280-315 nm) and ultraviolet A (UVA; 315-400 nm) radiation are capable of inducing damage in DNA, proteins and lipids via direct absorption of UV photons or through the production of reactive oxygen species (ROS) [10]. Notably, the most relevant deleterious effects of solar UV radiation are mediated by DNA damage (or lesions), given that the DNA is the primary target of this type of radiation in living cells [10]. The DNA damage plays an important role in the induction of lethal, mutagenic, tumorigenic and immunosuppressive effects after UV exposure, negatively affecting living systems [10, 11], especially those with complex life cycles, such as amphibians.

Several factors influence the UV radiation dose that reaches the chromosomes of embryos and larvae of amphibians in water bodies. The incidence of solar UV radiation on the aquatic surface is inversely proportional to the solar zenith angle, latitude, cloudiness, and the concentration of stratospheric ozone and other atmospheric UV-absorbing compounds (such as aerosols), and directly proportional to the altitude [12, 13]. The depth of the water column and the levels of dissolved organic matter (DOM) on freshwater ecosystems are factors that also attenuate UV penetrance [13-15].

Although chlorine- and bromine-containing ozone-depleting substances declined slowly after the 1987 Montreal Protocol, low levels of stratospheric ozone are still a reality [16, 17]. The loss of ozone has led to an increase in the surface UVB over the last decades. Additionally, in a scenario of changing climate, the dynamics of atmospheric UV-absorbing compounds, cloudiness, water column depth, and DOM levels became more complex, and changes in any of these factors may alter the exposure of amphibians to solar UV radiation [13, 18, 19]. Furthermore, human-induced wood extraction generates clearings within forests that ultimately allow the incidence of higher UV doses in the habitats of forest-specialist amphibian species [20].

Amphibians show interspecific differences regarding defense mechanisms against UV-induced DNA lesions [1]. The choice of suitable oviposition sites by adults, as well as the perception and avoidance of solar UV rays by tadpoles are among the behaviors reported for several species [1, 15, 21, 22]. However, it was also observed that certain environmental contaminants compromise the UV-avoidance behavior in tadpoles [23]. Furthermore, UV transmission properties of the jelly of eggs, mainly due to the presence of pigments and natural sunscreens, are also critical for DNA protection in embryos [1]. A representative diagram of the factors that influence the incidence of solar UV radiation on chromosomes of amphibian embryos and larvae is shown in Figure 1.

Even though the DNA damage induced by UV radiation may lead to sublethal and lethal effects on amphibians, which in turn can contribute to the decline of populations, UV radiation still remains an underestimated environmental stressor in amphibian ecology studies. Given the biological and the ecological relevance of this subject, we review the existing literature searching for research papers that address the sublethal and lethal effects of DNA damage (and responses) induced by solar UV radiation in amphibians. In addition, we discuss the key implications of UV-induced genotoxicity with regards to the performance and fitness of amphibians. We also identify knowledge gaps and provide recommendations for future investigations in this field.

2. Literature search

We conducted a comprehensive literature search in MedLine/PubMed (National Library of Medicine, http://www.ncbi.nlm.nih.gov/PubMed), SCOPUS (Elsevier, http://www.scopus.com), Thomson ISI's Web of Science (Thomson Reuters Corporation, http://apps.webofknowledge.com), and Google Scholar (Google, http://www.google.scholar.com) for articles published between January 1st, 1960 and June 15th, 2018. The terms used in the searches were as follows: UV DNA damage amphibian; UVB DNA damage amphibian; UVA DNA damage amphibian; sunlight DNA damage amphibian; UV genotoxicity amphibian; UVB genotoxicity amphibian; UVA genotoxicity amphibian; sunlight genotoxicity amphibian. The abstracts of the articles returned in the searches were analyzed to determine whether they met the following inclusion criteria: full abstract available online; articles written in English; and articles containing data about the biological responses to UV-induced DNA damage in amphibians.

3. UV-induced DNA damage and repair

UVB and UVA radiation induces DNA damage via photochemical reactions dependent on the direct absorption of energy from UV rays or through the indirect production of ROS [10, 12, 24].

Notably, the toxicity of UVB-induced DNA lesions is more detrimental than that induced by UVA because UVB induces a higher number of distortive DNA lesions, known as pyrimidine dimers [10, 12, 24]. These lesions result from direct absorption of UV photons by DNA pyrimidine bases, and are generally known as photoproducts. Cyclobutane pyrimidine dimers (CPDs) represent about 80-90% of these products, while pyrimidine-pyrimidone (6-4) photoproducts (6-4PPs) represent about 10-20% [25]. Both types of lesions compromise the DNA metabolism, blocking DNA replication and transcription leading to cell death or mutagenesis [26].

UV radiation can also indirectly cause the photosensitized formation of oxidative DNA damage through ROS production [10, 24]. UV-induced ROS act as oxidants that cause base oxidation, such as the highly mutagenic 8-oxo-7,8-dihydroguanine (8-oxoG), or single strand breaks (SSB) [10, 24]. Environmental doses of UVA radiation are more efficient than UVB in regard to ROS production. In addition, SSBs and double strand breaks (DSB) can be formed due to instability in the processes of DNA transcription/replication of unrepaired UV-induced DNA lesions [10, 24]. If not repaired, DNA strand breaks can result in cell death or mutations at the chromosome level [10].

In contrast, several DNA repair mechanisms work to reverse UV-induced DNA damage. The DNA repair by photolyase enzymes (also known as photorepair or photoreactivation) uses the energy of visible light and some UVA photons to directly remove pyrimidine dimers through its monomerization [24, 27]. Several taxa, including the amphibians, have two photolyases to deal with specific DNA lesions: CPD photolyase (CPD PHR), which repairs only CPDs; and 6-4 photolyase (6-4 PHR), which repairs only 6-4PPs [24]. On the other hand, pyrimidine dimers (and several other types of DNA lesion) can be removed by the nucleotide excision repair (NER), a process that requires several proteins and ATP consumption [24, 27]. Importantly, if a lesion is located in active regions for gene expression, transcription-coupled nucleotide excision repair (TC-NER) is directly triggered due to blockage of RNA-polimerase II. On the other hand, global genome nucleotide excision repair (GG-NER) is used to randomly remove DNA lesions throughout the entire genome [10, 27]. After damage recognition, the repair process follows the same path through the unwinding of damaged double helix, cleavage and excision of the damaged strand, filling the gap in the molecule by DNA synthesis and final ligation [10]. In addition, base excision repair (BER) is another process that involves several proteins and ATP consumption. However, this is the primary repair pathway for the correction of oxidized DNA bases, SSBs and abasic sites. Two pathways can be used: short-patch (SP-BER) and long-patch (LP-BER). The SP-BER pathway repairs the damage through the excision of a single nucleotide, whereas the LP-BER excises from two to ten nucleotides

to correct the damage [10]. A scheme about the DNA lesions induced directly or indirectly by UVB/UVA radiation, as well as their respective DNA repair mechanisms, is shown in Figure 2.

4. Search results

We identified a total of twenty one studies. Table 1 presents detailed information on the focal species, the study objective, the methodology used, and the main results and conclusions of each study.

Table 1 – Detailed information about the studies concerning the genotoxic stress induced on amphibians after UV exposure, and the responses to UV-induced DNA damage.

Species	Study objective	Type of methodology	Main results/conclusions	Ref.
Bufo boreas boreas	Detect a possible mitigation of the potentially lethal UVB damage to tadpoles.	Assessment of larval photorepair via phenotypic responses.	Photoreactivation following exposure to UVB mitigated the potentially lethal damage to tadpoles.	[28]
Bufo boreas boreas	Evaluate the effects of increased UVB radiation on the development and viability of tadpoles.	Assessment of larval photorepair via phenotypic responses.	Photoreactivation following exposure to UVB mitigated the potentially lethal damage to tadpoles.	[29]
Xenopus laevis, *Rana cascadae*, *Pseudacris regilla*, *Bufo boreas*, *Taricha granulosa*, *Ambystoma gracile*, *Ambystoma macrodactylum*, *Plethodon dunni*, *Plethodon vehiculum*, *Rhyacotriton variegatus*.	Determine photolyase activity in 10 amphibian species and evaluate if the differential UV-sensitivity among species contributes to population decline.	*In vitro* assessment of photorepair in embryos.	Photolyase activity varies >80-fold among species. There was a strong correlation between UVB exposure and photolyase activity among the amphibian species. The population status of three anuran species correlates strikingly with their repair proficiency.	[30]
Rana aurora	Assess DNA repair and resistance to solar radiation in eggs of a frog species whose populations appear to be in decline.	*In vitro* assessment of photorepair in embryos.	The photolyase activity in *R. aurora* was higher when compared with other amphibians, and the hatching success seems to be unaffected by UVB radiation in field experiments.	[31]
Litoria aurea, *Litoria dentata*, *Litoria peronii*	Determine if photolyase activity differs in three sympatric treefrog species.	*In vitro* assessment of photorepair in embryos.	The photolyase activity in *Litoria dentata* was 5-fold higher than in *L. aurea*, and 2-fold higher than in *L. peronii*. The relationship between photolyase activity and hatching success may not be simple to be assessed.	[32]
Xenopus laevis	Establish indicative sublethal endpoints (DNA photodamage, growth inhibition, and malformations) of UVB exposure.	*In vitro* assessment of photorepair in embryos.	Teratogenesis and growth inhibition were positively correlated with UVB dose. Teratogenesis was positively correlated with the frequency of DNA photodamage. There was variation in DNA photodamage between eggs clutches.	[33]

Rana pretiosa, Rana luteiventris.	Assess DNA repair and resistance to solar radiation in eggs of a frog species whose populations are suffering severe decline.	*In vitro* assessment of photorepair in embryos.	Photolyase activities were relatively high. In field experiments, hatching success was unaffected by UVB.	[34]
Rana sylvatica	Estimate *in vivo* induction of photolyase activity.	*In vivo* and *in vitro* assessment of photorepair in embryos.	The photolyase activity of embryos was altered by the exposure to ambient levels of sunlight. When photolyase activity is quantified via an *in vitro* assay it is crucial to remember that the *in vivo* conditions may significantly affect the estimation.	[35]
Ambystoma maculatum	Evaluate the oxidative stress, DNA damage, and expression of p53/p73 after exposure of embryos of a salamander species to UVB/UVA, both in laboratory and field experiments.	Assessment of photoproducts in embryos.	In laboratory experiments, embryos showed significant photoproducts and an increase in melanin production in response to UV. The production of ROS initiates the expression of p53/p73, which leads to DNA repair or apoptosis. The embryos showed less sensitivity and higher survivorship within vernal pools.	[36]
Ambystoma laterale, Ambystoma maculatum, Pseudacris crucifer, Rana clamitans, Rana pipiens, Rana sylvatica.	Estimate the level of photolyase activity of various tissue types in seven species of amphibians. Determine whether the level of photolyase activity was correlated with the expected UVB exposure.	*In vitro* assessment of photorepair in embryos.	*In vitro* measurements of photolyase activity in the seven species were significantly different and tended to be positively correlated with the expected *in vivo* UVB exposure.	[37]
Rana cascadae, *Pseudacris regilla*, *Ambystoma macrodactylum*, *Ambystoma gracile.*	Evaluate and combine data on the physiological sensitivity to UVB, and patterns of field exposure, across sites for embryos of two frog species and two salamander species.	Assessment of embryonic photorepair via phenotypic responses. Assessment of behaviors that avoid genomic instability.	Species with the highest physiological sensitivity to UVB (lower photorepair activity; higher mortality) were those with the lowest field exposures as a function of the location of embryos and the UVB attenuation properties of water at each site.	[14]
Rana temporaria	Test of tolerance variation to UVB and benzo[a]pyrene (BaP) among populations of a frog species, according to their natural exposure level in the field.	Assessment of nuclear abnormalities.	High-altitude populations showed the lowest number of micronucleated erythrocytes. The prevention and repair of UVB-induced DNA damage could also protect these populations against BaP-induced DNA damage.	[38]
Ambystoma maculatum	Determine if coal-tar sealant can have negative effects on the larvae of a salamander species, and if coal-tar toxicity is influenced by UV.	Assessment of nuclear abnormalities.	Exposure to UV affected the frequencies of leukocytes and increased the incidence of micronucleated erythrocytes. Coal-tar sealant and UV increased sublethal effects in salamanders.	[39]
Ambystoma macrodactylum	Examine the ability of a salamander species, at high- and low-elevation breeding sites, to cooperatively employ behavioral and physiological trait responses to mediate UVB damage.	*In vitro* assessment of photorepair in embryos. Assessment of behaviors that avoid genomic instability.	The oviposition behavior differed across populations. There was no difference in photolyase activity between populations at high and low elevations. For high-elevation populations, low physiological repair capabilities in embryos appear to be buffered by behavioral modifications to reduce UVB exposure and standardize developmental temperatures.	[40]

Xenopus laevis	Investigate the interactive effects of UVB, endosulfan, and cypermethrin on the induction of DNA photo-adducts and expression of DNA repair-related genes in embryos.	Assessment of photoproducts in embryos. *In vivo* assessment of NER gene expression in embryos.	XPC, HR23B, XPG, and GADD45α exhibited elevated mRNA concentrations, whereas the concentration of MUTL transcript reduced in UVB-alone treatments. Pesticides may increase the accumulation of UVB-induced DNA photo-adducts, and one likely mechanism is the alteration of critical NER gene expression.	[41]
Boana pulchella	Evaluate the genotoxic effects of UVB/UVA doses on the morphology and development of treefrog tadpoles, as well as on the induction of malformation after the conclusion of metamorphosis.	Assessment of nuclear abnormalities. Assessment of larval photorepair via phenotypic responses.	Tadpoles were much more sensitive to UVB than UVA, which reduces their survival and developmental rates. The rates of micronucleus formation by UVB were considerably higher compared to UVA, even after the activation of photolyases enzymes by a further photoreactivation treatment. Consequently, a higher occurrence of malformation was observed in UVB-irradiated individuals.	[16]
Boana pulchella	Evaluate the ability of treefrog tadpoles to behaviorally avoid UV rays, and the efficacy of DNA repair against UV photoproducts.	Assessment of photoproducts in larvae. *In vivo* assessment of photorepair in larvae. Assessment of nuclear abnormalities. Assessment of larval photorepair via phenotypic responses. Assessment of behaviors that avoid genomic instability.	Tadpoles were highly sensitive to UVB, which could be explained by the slow DNA repair rates for both CPDs and 6-4PPs, and the high rates of apoptosis induction. Tadpoles were resistant to UVA. A sensory mechanism that triggers their escape from UVB and UVA avoids the generation of DNA damage and helps to maintain the genomic integrity.	[22]
Physalaemus nattereri	Test the genotoxic effects of UV and assess the internal pigmentation in a Neotropical frog.	Assessment of nuclear abnormalities. Assessment of the importance of pigmentation for the maintenance of DNA integrity via phenotypic responses.	UV exposure at doses that activate mast cells resulted in skin darkening and increased internal pigmentation in hepatic melanomacrophages, testicular melanocytes, and in the liver. Only longer periods of exposure caused genotoxic effects.	[42]
Boana curupi	Investigate the effects of UVB on food consumption and body weight of tadpoles of a forest specialist species, evaluating the importance of photorepair to maintain the feeding and growth performances.	Assessment of nuclear abnormalities. Assessment of larval photorepair via phenotypic responses.	The body weight decrease induced by UVB occurred due to the reduction of tadpoles' food consumption. This behavior is related to the genotoxic impact of UVB, since the micronuclei frequency increased after treatments. The results indicate that a further photoreactivation treatment was ineffective in restoring the feeding and growth performances.	[43]
Lithobates catesbeianus	Evaluate the effects of UV exposure on immune cells and DNA integrity in pigmented and non-pigmented tadpoles.	Assessment of nuclear abnormalities. Assessment of the importance of pigmentation for the maintenance of DNA integrity.	Exposure to UV affected immune cells of both non-pigmented and pigmented tadpoles, although the genotoxic effects were more severe in non-pigmented tadpoles. Leukocyte responses were faster in non-pigmented tadpoles.	[44]

Boana pulchella	Evaluate the importance of photorepair to maintain the growth and locomotor performances, as well as survival of tadpoles after acute and chronic exposure to UVB and UVA radiation.	Assessment of larval photorepair via phenotypic responses.	Photorepair was fundamental for the maintenance of tadpole performance after chronic UVB exposures, but it was relatively inefficient after acute exposures to UVB, but not to UVA radiation. UVB impacted the skin and mouth structures, locomotion, body length, body mass, and the survival of tadpoles, while UVA affected only the body mass.	[45]

The references follow a chronological sequence: the first paper was published in 1975 and the last paper was published in 2018.

4. Knowledge gaps and recommendations for future investigations

The need of further studies to better understand the impact of solar UV radiation on amphibian decline is evident. Only three out of 21 papers measured the UV-induced DNA lesions during developmental phases [22, 36, 41]. Furthermore, only one study addressed the immediate molecular response after UV exposure through the expression of NER genes in embryos, although the main focus of the study was the interactive effects of UV and pesticides [41]. Eight papers concerned the photolyase activity in amphibian species through *in vitro* experiments of light-dependent removal of CPDs from exogenous UV-irradiated DNA samples incubated with egg/oocyte protein extracts [30-35, 37, 40]. However, Smith et al. [35] showed that these *in vitro* estimates may differ from *in vivo* situations. In addition, 12 papers evaluated the influence of UV genotoxic stress in some amphibian developmental stage [14, 16, 22, 28, 29, 38-40, 42-45]. Three studies deserve special mention. The most influential study was published by Blaustein et al. in 1994 [30], who pioneered the studies of UV genotoxicity and DNA repair in amphibians and addressed the UV-sensitivity hypothesis, which proposes that species with higher photolyase activity are more resistant to solar UV radiation than species with lower photolyase activity. Schuch et al. [22] addressed both the induction of DNA photoproducts and photorepair efficiency, as well as the phenotypic and behavioral responses in treefrog tadpoles exposed to UVB and UVA radiation. Finally, Lesser et al. [36] demonstrated that the molecular responses of salamander embryos to UV in laboratory and field conditions differed due to UV attenuation caused by DOM within the vernal pools.

The sublethal effects of solar UV have negative implications for amphibians in nature. Reduced growth and reduced developmental performances were observed in embryonic or larval developmental stages of several species after non-lethal UV exposure, and were primarily associated to UV genotoxicity [16, 22, 43]. UV genotoxicity leads to reduction in locomotor and feeding performances of larval stages [43, 45]. Interestingly, UVB-induced reduction in the number of skin cell layers of tadpoles has been associated with apoptosis. It may compromise skin respiration, as well as the inner cell layers, which may become more vulnerable to infections, dehydration, toxic substances and even to more UV radiation [45]. Additionally, carry-over negative effects from one life stage to another may be a source of fitness variation [16, 46, 47]. In an ecological context, less healthy and less mobile individuals may become more susceptible to diseases and predation, and disadvantaged in the competition for resources with normal individuals.

Little consideration has been given to the impact of UVA wavelengths and natural sunlight on amphibians. UVA radiation is less efficient in producing DNA photoproducts than UVB [10, 48]. However, solar UVA incidence is 20-fold more intense than UVB. Furthermore, UVA penetrates the

skin more deeply than UVB, and can induce apoptotic and mutagenic processes in deeper cells [10, 48]. Thus, the damage caused directly or indirectly by UVA in the DNA and other biomolecules may be underestimated. In addition, comparative investigations of the responses of amphibians to UV radiation in laboratory and field conditions are needed. A relevant question is the definition of ecologically relevant UV doses for amphibians in laboratory experiments. An alternative for these studies is to compare the UV-sensitivity of species using equivalent UV doses to quantify the amount of DNA damage generated in naked DNA samples *in vitro* [12]. Several ecological and biological factors (e.g., physical and biological UV attenuators or even behavioral mechanisms) could be excluded in order to compare the biological sensitivity of different species regarding DNA damage induced by solar UV wavelengths.

In aquatic ecosystems, the relationship between UV radiation, climate changes, DOM, chemicals, and organisms is complex. Although high DOM concentrations decrease the UV penetrance in water column, it can be converted to H_2O_2 as a consequence of UV exposure, increasing the exposure of aquatic organisms to ROS [49, 50]. Furthermore, UV-induced DOM degradation enables more UV penetrance [51]. Solar UV radiation also has the potential to energize molecules of environmental contaminants present in aquatic habitats, increasing the genotoxic stress [52]. Therefore, field experiments focused on the measurement of ambient UV incidence upon aquatic breeding sites of amphibians should take into account all these environmental variables.

Future studies should be better designed to access the UV-induced genotoxicity in amphibians, as well as to provide information about correlations between environmental variables, fitness, and molecular mechanisms of the target species [53]. Between-species and between-individual differences in the ability to deal with UV-induced DNA damage may help to explain the observed differences in the stability of amphibian populations. Several types of DNA damage responses (DDR), including DNA repair and cell-cycle checkpoint, have evolved because of the advantage in maintaining genomic integrity [see 24, 27, 54, 55]. If DNA lesions remain unrepaired in the genome, cells may enter apoptosis, senescence or autophagy, or develop mutations, which may lead to tumorigenesis, death or contribute for evolution [24, 27, 54, 55]. In addition, the mechanism underlying the immunosuppression linked to UV-induced DNA damage [56] constitute another example of biological response that require attention, since it has been demonstrated that UV radiation has a negative impact on amphibian immune system [11, 42, 44, 46].

It is still unclear whether the DNA damage formation or the energetic costs of DDR is the main determinant factor for the impact on amphibian health and survival [43, 57, 58]. More specifically, are the direct effects of DNA damage on the inhibition of DNA metabolism or the

energetic and nutritional demand for DDR the main factors that affect amphibian performance? More precise answers on the role of specific DDR proteins may be obtained through experiments with knockout individuals. For instance, the removal of specific repair proteins could reveal if UV-induced DNA lesions are determinant for differential phenotypic disadvantages observed in UV-exposed individuals.

In silico, in vitro and *in vivo* studies should be conducted together for the investigation of the molecular, genetic, biochemical and functional bases of DDR in amphibians. If proven, variations in the coding sequence and in post-transcriptional processing of mRNA of DNA repair genes, differences in the expression of DDR genes according to circadian cycles, differences in the expression of genes that modulate the DNA repair mechanisms, as well as changes in the structure and function of proteins, may help to explain variation in the sensibility to solar UV radiation between amphibian species. Notably, the advent of Next-Generation Sequencing technologies can help to understand the molecular bases of the impact generated by solar UV exposure on amphibian individuals and, ultimately, on populations.

5. Concluding remarks

Solar UV radiation is an important environmental stressor for amphibian populations, and has been defined as a driver of amphibian decline worldwide. Surprisingly, the most relevant deleterious effect of UV radiation, the induction of DNA damage, was directly measured in only 3 out of 21 papers. Consequently, the roles of molecular pathways that attenuate the impact of sunlight-induced DNA damage on amphibian species are poorly understood and deserve further attention. Multidisciplinary approaches are necessary in order to better understand the real biological impact of UV radiation on amphibian in nature. Therefore, the biological relevance of solar UV radiation in the phenomenon of amphibian decline may become more evident in the near future.

Competing interests

The authors declare no competing interest.

Acknowledgements

This study was supported by the Coordenação de Aperfeiçoamento de Pessoal de Nível Superior/Programa de Excelência Acadêmica – Brasil (CAPES/PROEX – 23038.005848/2018; 88882.182173/2018-01).

References

[1] A.R. Blaustein, L.K. Belden, Amphibian defenses against ultraviolet-B radiation, Evol. Dev. 5 (2003) 89–97. https://doi.org/10.1046/j.1525-142X.2003.03014.x

[2] S.N. Stuart, J.S. Chanson, N.A. Cox, B.E. Young, A.S.L. Rodrigues, D.L. Fischman, R.W. Waller, Status and trends of amphibian declines and extinctions worldwide, Science 306 (2004) 1783–1786. https://doi.org/10.1126/science.1103538

[3] IUCN, Summary statistics, International Union for Conservation of Nature and Natural Resources, (2018) Available at: http://www.iucnredlist.org/about/summary-statistics

[4] J.P. Collins, A. Storfer, Global amphibian declines: sorting the hypotheses, Divers. Distrib. 9 (2003) 89–98. https://doi.org/10.1046/j.1472-4642.2003.00012.x

[5] R.A. Alford, S.J. Richards, Global Amphibian Declines: A Problem in Applied Ecology, Annu. Rev. Ecol. Syst. 30 (1999) 133-165. https://doi.org/10.1146/annurev.ecolsys.30.1.133

[6] A.R. Blaustein, J.M. Kiesecker, Complexity in conservation: lessons from the global decline of amphibian populations, Ecol. Lett. 5 (2002) 597–608. https://doi.org/10.1046/j.1461-0248.2002.00352.x

[7] A.R. Blaustein, J.M. Romansic, J.M. Kiesecker, A.C. Hatch, Ultraviolet radiation, toxic chemicals and amphibian population declines, Divers. Distrib. 9 (2003) 123–140. https://doi.org/10.1046/j.1472-4642.2003.00015.x

[8] M.C. Croteau, M.A. Davidson, D.R.S. Lean, V.L. Trudeau, Global increases in ultraviolet B radiation: potential impacts on amphibian development and metamorphosis. Physiol. Biochem. Zool. 81 (2008) 743–761. https://doi.org/10.1086/591949

[9] L.A. Alton, C.E. Franklin, Drivers of amphibian declines: effects of ultraviolet radiation and interactions with other environmental factors, Clim. Chang. Responses 4 (2017) 6. https://doi.org/10.1186/s40665-017-0034-7

[10] A.P. Schuch, N.C. Moreno, N.J. Schuch, C.F.M. Menck, C.C.M. Garcia, Sunlight damage to cellular DNA: Focus on oxidatively generated lesions. Free Rad. Biol. Med. 107 (2017) 110–124. https://doi.org/10.1016/j.freeradbiomed.2017.01.029

[11] R.L. Cramp, C.E. Franklin. Exploring the link between ultraviolet B radiation and immune function in amphibians: implications for emerging infectious diseases, Conserv Physiol. 6 (2018). https://doi.org/10.1093/conphys/coy035

[12] A.P. Schuch, C.C. Garcia, K. Makita, C.F.M. Menck, DNA damage as a biological sensor for environmental sunlight, Photochem. Photobiol. Sci. 12 (2013) 1259–1272. https://doi.org/10.1039/c3pp00004d

[13] D.-P. Häder, C.E. Williamson, S.-Å. Wängberg, M. Rautio, K.C. Rose, K. Gao, E.W. Helbling, R.P. Sinha, R. Worrest, Effects of UV radiation on aquatic ecosystems and interactions with other environmental factors, Photochem. Photobiol. Sci.14 (2015) 108-126. https://doi.org/10.1039/c4pp90035a

[14] W.J. Palen, C.E. Williamson, A.A. Clauser, D.E. Schindler, Impact of UV-B exposure on amphibian embryos: linking species physiology and oviposition behaviour, Proc. R. Soc. London, Ser. B 272 (2005) 1227–1234. https://doi.org/10.1098/rspb.2005.3058

[15] W.J. Palen, D.E. Schindler, Water clarity, maternal behavior, and physiology combine to eliminate UV radiation risk to amphibians in a montane landscape, Proc. Natl. Acad. Sci. USA 107 (2010) 9701-9706. https://doi.org/10.1073/pnas.0912970107

[16] A.P. Schuch, M.B. Santos, V.M. Lipinski, L.V. Peres, C.P. Santos, S.Z. Cechin, N.J. Schuch, D.K. Pinheiro, E.L.S. Loreto, Identification of influential events concerning the Antarctic ozone hole over southern Brazil and the biological effects induced by UVB and UVA radiation in an endemic treefrog species, Ecotoxicol. Environ. Saf. 118 (2015) 190–198. https://doi.org/10.1016/j.ecoenv.2015.04.029

[17] M.P. Chipperfield, S.S. Dhomse, W. Feng, R.L. McKenzie, G.J.M. Velders, J.A. Pyle. Quantifying the ozone and ultraviolet benefits already achieved by the Montreal Protocol, Nat. Commun. 6 (2015) 7233. https://doi.org/10.1038/ncomms8233

[18] J.M. Kiesecker, A.R. Blaustein, L.K. Belden, Complex causes of amphibian population declines. Nature 410 (2001) 681–684. https://doi.org/10.1038/35070552

[19] C.E. Williamson, R.G. Zepp, R.M. Lucas, S. Madronich, A.T. Austin, C.L. Ballaré, M. Norval, B. Sulzberger, A.F. Bais, R.L. McKenzie, S.A. Robinson, D.-P. Häder, N. D. Paul, J.F.

Bornman, Solar ultraviolet radiation in a changing climate. Nat. Clim. Chang. 4 (2014) 434–441. https://doi.org/10.1038/nclimate2225

[20] V.M. Lipinski, T.G. Santos, A.P. Schuch, An UV-sensitive anuran species as an indicator of environmental quality of the Southern Atlantic Rainforest, J. Photochem. Photobiol. B 165 (2016) 174–181. https://doi.org/10.1016/j.jphotobiol.2016.10.025

[21] L.B. Kats, G.M. Bucciarelli, D.E. Schlais, A.R. Blaustein, B.A. Han, Ultraviolet radiation influences perch selection by a neotropical poisondart frog, PLoS ONE 7 (2012) e51364. https://doi.org/10.1371/journal.pone.0051364

[22] A.P. Schuch, V.M. Lipinski, M.B. Santos, C.P. Santos, S.S. Jardim, S.Z. Cechin, E.L.S. Loreto, Molecular and sensory mechanisms to mitigate sunlight-induced DNA damage in treefrog tadpoles, J. Exp. Biol. 218 (2015) 3059–3067. https://doi.org/10.1242/jeb.126672

[23] S. Yu, S.M. Weir, G.P. Cobb, J.D. Maul, The effects of pesticide exposure on ultraviolet-B radiation avoidance behavior in tadpoles. Sci. Total Environ. 481 (2014) 75-80. https://doi.org/10.1016/j.scitotenv.2014.02.018

[24] R.P. Rastogi, Richa, A. Kumar, M.B. Tyagi and R.P. Sinha, Molecular mechanisms of ultraviolet radiation-induced DNA damage and repair, J. Nucleic Acids (2010) 592980. http://dx.doi.org/10.4061/2010/592980

[25] A. Sancar, Structure and function of photolyase and in vivo enzymology: 50th anniversary, J. Biol. Chem. 283 (2008) 32153–32157. http://www.jbc.org/content/283/47/32153

[26] A.P. Schuch, C.F.M. Menck, The genotoxic effects of DNA lesions induced by artificial UV-radiation and sunlight, J. Photochem. Photobiol. B 99 (2010) 111–116. https://doi.org/10.1016/j.jphotobiol.2010.03.004

[27] E.C. Friedberg, DNA damage and repair, Nature 421 (2003) 436–440. https://doi.org/10.1038/nature01408

[28] R.C. Worrest, D.J. Kimeldorf, Photoreactivation of potentially lethal, UV-induced damage to boreal toad (*Bufo boreas boreas*) tadpoles, Life Sci. 17 (1975) 1545-1550. https://doi.org/10.1016/0024-3205(75)90175-7

[29] R.C. Worrest, D.J. Kimeldorf, Distortions in amphibian development induced by ultraviolet-B enhancement (290-315 nm) of a simulated solar spectrum, Photochem. Photobiol. 24 (1976) 377-382. https://doi.org/10.1111/j.1751-1097.1976.tb06840.x

[30] A.R. Blaustein, P.D. Hoffman, D.G. Hokit, J.M. Kiesecker, S.C. Walls, J.B. Hays, UV repair and resistance to solar UV-B in amphibian eggs: a link to population declines? Proc. Natl. Acad. Sci. U.S.A. 91 (1994) 1791–1795. https://doi.org/10.1073/pnas.91.5.1791

[31] A.R. Blaustein, P.D. Hoffman, J.M. Kiesecker, J.B. Hays, DNA repair activity and resistance to solar UV-B radiation in eggs of the red-legged frog, Conserv. Biol. 10 (1996) 1398–1402. https://doi.org/10.1046/j.1523-1739.1996.10051398.x

[32] T. van de Mortel, W. Buttemer, P. Hoffman, J. Hays, A.R. Blaustein, A comparison of photolyase activity in three Australian tree frogs. Oecologia 115 (1998), 366-369. https://doi.org/10.1007/s004420050529

[33] D.J. Bruggeman, J.A. Bantle, C. Goad, Linking teratogenesis, growth, and DNA photodamage to artificial ultraviolet B radiation in *Xenopus laevis* larvae, Environ. Toxicol. Chem. 17 (1998) 2114-2121. https://doi.org/10.1002/etc.5620171030

[34] A.R. Blaustein, J.B. Hays, P.D. Hoffman, D.P. Chivers, J.M. Kiesecker, W.P. Leonard, A. Marco, D.H. Olson, J.K. Reaser, R.G. Anthony. DNA repair and resistance to UV-B radiation in western spotted frogs. Ecol. Appl. 9 (1999) 1100–1105. https://doi.org/10.1890/1051-0761(1999)009[1100:DRARTU]2.0.CO;2

[35] M.A. Smith, C.M. Kapron, M. Berrill, Induction of photolyase activity in wood frog (*Rana sylvatica*) Embryos, Photochem. Photobiol. 72 (2000) 575-578. https://doi.org/10.1562/0031-8655(2000)0720575IOPAIW2.0.CO2

[36] M.P. Lesser, S.L. Turtle, J.H. Farrell, C.W. Walker, Exposure to ultraviolet radiation (290–400 nm) Causes Oxidative Stress, DNA Damage, and Expression of *p53/p73* in laboratory experiments on embryos of the spotted salamander, *Ambystoma maculatum*, Physiol. Biochem. Zool. 74 (2001) 733-741. https://doi.org/10.1086/322931

[37] M.A. Smith, M. Berrill, C.M. Kapron, Photolyase activity of the embryo and the ultraviolet absorbance of embryo jelly for several Ontario amphibian species. Can. J. Zool. 80 (2002) 1109–1116. https://doi.org/10.1139/z02-093

[38] O. Marquis, C. Miaud, G.F. Ficetola, A. Bocherc , F. Mouchetd , S. Guittonneauc, A. Devauxe, Variation in genotoxic stress tolerance among frog populations exposed to UV and pollutant gradients, Aquat. Toxicol. 95 (2009) 152–161. https://doi.org/10.1016/j.aquatox.2009.09.001

[39] T. Bommarito, D.W. Sparling, R.S. Halbrook, Toxicity of coal-tar pavement sealants and ultraviolet radiation to *Ambystoma maculatum,* Ecotoxicology 19 (2010) 1147–1156. https://doi.org/10.1007/s10646-010-0498-8

[40] L.L. Thurman, T.S. Garcia, P.D. Hoffman, Elevational differences in trait response to UV-B radiation by long-toed salamander populations, Oecologia 175 (2014) 835–845. https://doi.org/10.1007/s00442-014-2957-z

[41] S. Yu, S. Tang, G.D. Mayer, G.P. Cobb, J.D. Maul, Interactive effects of ultraviolet-B radiation and pesticide exposure on DNA photo-adduct accumulation and expression of DNA damage and repair genes in *Xenopus laevis* embryos, Aquat. Toxicol., 159 (2015) 256-266. https://doi.org/10.1016/j.aquatox.2014.12.004

[42] L. Franco-Belussi, H.N. Sköld, C. Oliveira, Internal pigment cells respond to external UV radiation in frogs, J. Exp. Biol. (2016) jeb-134973. https://doi.org/10.1242/jeb.134973

[43] J.E.L. Londero, C.P. Santos, A.L.A. Segatto, A.P. Schuch, Impacts of UVB radiation on food consumption of forest specialist tadpoles, Ecotoxicol. Environ. Saf. 143 (2017) 12–18. https://doi.org/10.1016/j.ecoenv.2017.05.002

[44] L. Franco-Belussi, L.Z. Fanali, C. Oliveira, UV-B affects the immune system and promotes nuclear abnormalities in pigmented and non-pigmented bullfrog tadpoles, J. Photochem. Photobiol. B 180 (2018) 109–117. https://doi.org/10.1016/j.jphotobiol.2018.01.022

[45] C.P. Santos, J.E.L. Londero, M.B. Santos, R.S. Feltrin, L. Loebens, L.B. Moura, S.Z. Cechin, A.P. Schuch, Sunlight-induced genotoxicity and damage in keratin structures decrease tadpole performance. J. Photochem. Photobiol. B 181 (2018) 134–142. https://doi.org/10.1016/j.jphotobiol.2018.03.013

[46] E. Ceccato, R.L. Cramp, F. Seebacher, C.E. Franklin, Early exposure to ultraviolet-B radiation decreases immune function later in life, Conserv. Physiol. 4 (2016) 4 cow037. https://doi.org/10.1093/conphys/cow037

[47] M. Pahkala, A. Laurila, J. Merilä, Carry–over effects of ultraviolet–B radiation on larval fitness in Rana temporaria, Proc. R. Soc. Lond. B Biol. Sci. 268 (2001) 1699-1706. https://doi.org/10.1098/rspb.2001.1725

[48] E. Sage, P.M. Girard, S. Francesconi, Unravelling UVA-induced mutagenesis. Photochem. Photobiol. Sci. 11 (2012) 74-80. https://doi.org/10.1039/c1pp05219e

[49] L.E. Richard, B.M. Peake, S.A. Rusak, W.J. Cooper, D.J. Burritt, Production and decomposition dynamics of hydrogen peroxide in freshwater, Environ. Chem. 4 (2007) 49-54. https://doi.org/10.1071/EN06068

[50] R. Wolf, T. Andersen, D.O. Hessen, K. Hylland, The influence of dissolved organic carbon and ultraviolet radiation on the genomic integrity of *Daphnia magna*, Funct. Ecol. 31 (2017) 848-855. https://doi.org/10.1111/1365-2435.12730

[51] D.P. Morris, B.R. Hargreaves, The role of photochemical degradation of dissolved organic carbon in regulating the UV transparency of three lakes on the Pocono Plateau, Limnol. Oceanogr., 42 (1997) 239-249. https://doi.org/10.4319/lo.1997.42.2.0239

[52] A.P. Roberts, M.M. Alloy, J.T. Oris, Review of the photo-induced toxicity of environmental contaminants, Comp Biochem Physiol C Toxicol Pharmacol. 191 (2017) 160-167. https://doi.org/10.1016/j.cbpc.2016.10.005

[53] B.E. Miner, P.M. Kulling, K.D. Beer, B. Kerr, Divergence in DNA photorepair efficiency among genotypes from contrasting UV radiation environments in nature, Mol. Ecol. 24 (2015) 6177-6187. https://doi.org/10.1111/mec.13460

[54] P.C. Hanawalt, Historical perspective on the DNA damage response, DNA repair 36 (2015) 2-7. https://doi.org/10.1016/j.dnarep.2015.10.001

[55] G. Giglia-Mari, A. Zotter, W. Vermeulen, DNA damage response. Cold Spring Harb. Perspect. Biol. (2010) a000745. https://doi.org/10.1101/cshperspect.a000745

[56] S.E. Ullrich, Mechanisms underlying UV-induced immune suppression. Mutat. Res. - Fund. Mol. M. 571 (2005) 185-205. https://doi.org/10.1016/j.mrfmmm.2004.06.059

[57] M. Pahkala, A. Laurila, J. Merilä, Ambient ultraviolet-B radiation reduces hatchling size in the common frog *Rana temporaria*. Ecography, 23 (2000) 531-538. https://doi.org/10.1111/j.1600-0587.2000.tb00171.x

[58] L.A. Alton, C.R. White, R.S. Wilson, C.E. Franklin, The energetic cost of exposure to UV radiation for tadpoles is greater when they live with predators, Funct. Ecol. 26 (2012) 94–103. https://doi.org/10.1111/j.1365-2435.2011.01900.x

Figure captions

Figure 1. Representative diagram of the factors influencing the incidence of solar UV radiation on chromosomes of the embryonic and larval stages of amphibians. See details in the text. UVAC: Ultraviolet absorbing compounds; DOM: Dissolved organic matter.

Figure 2. UV-induced DNA lesions and repair mechanisms. See details in the text. Graphical example of a normal DNA strand (A) and the lesions, cyclobutane pyrimidine dimer (CPD) (B); pyrimidine-pyrimidone (6-4) photoproducts (6-4PP) (C); 8-oxo-7,8-dihydroguanine (8oxod-G) (D); and single strand break (SSB) (E). UV-induced DNA lesions can result in SSBs or DSB due to the instability caused during the DNA transcription/replication processes. CPD PHR: CPD photolyase; 6-4 PHR: 6-4 photolyase; NER: nucleotide excision repair; TC-NER: transcription-coupled NER; GG-NER: global genome NER; BER: base excision repair; SP-BER: short-patch BER; LP-BER; long-patch BER.

Figure 1

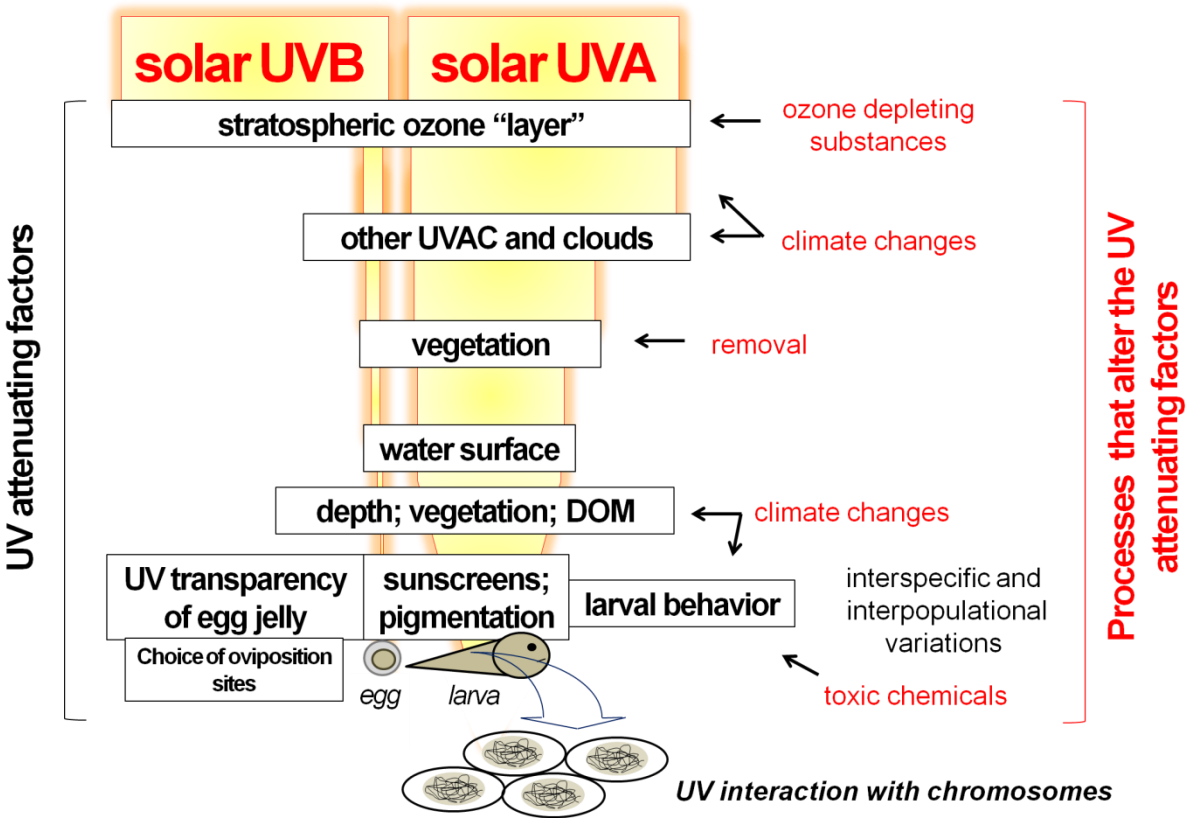
solar UVB
solar UVA
stratospheric ozone "layer"
ozone depleting substances
other UVAC and clouds
climate changes
vegetation
removal
water surface
depth; vegetation; DOM
climate changes
UV transparency of egg jelly
sunscreens; pigmentation
larval behavior
interspecific and interpopulational variations
Choice of oviposition sites
egg
larva
toxic chemicals
UV interaction with chromosomes
UV attenuating factors
Processes that alter the UV attenuating factors

Figure 2

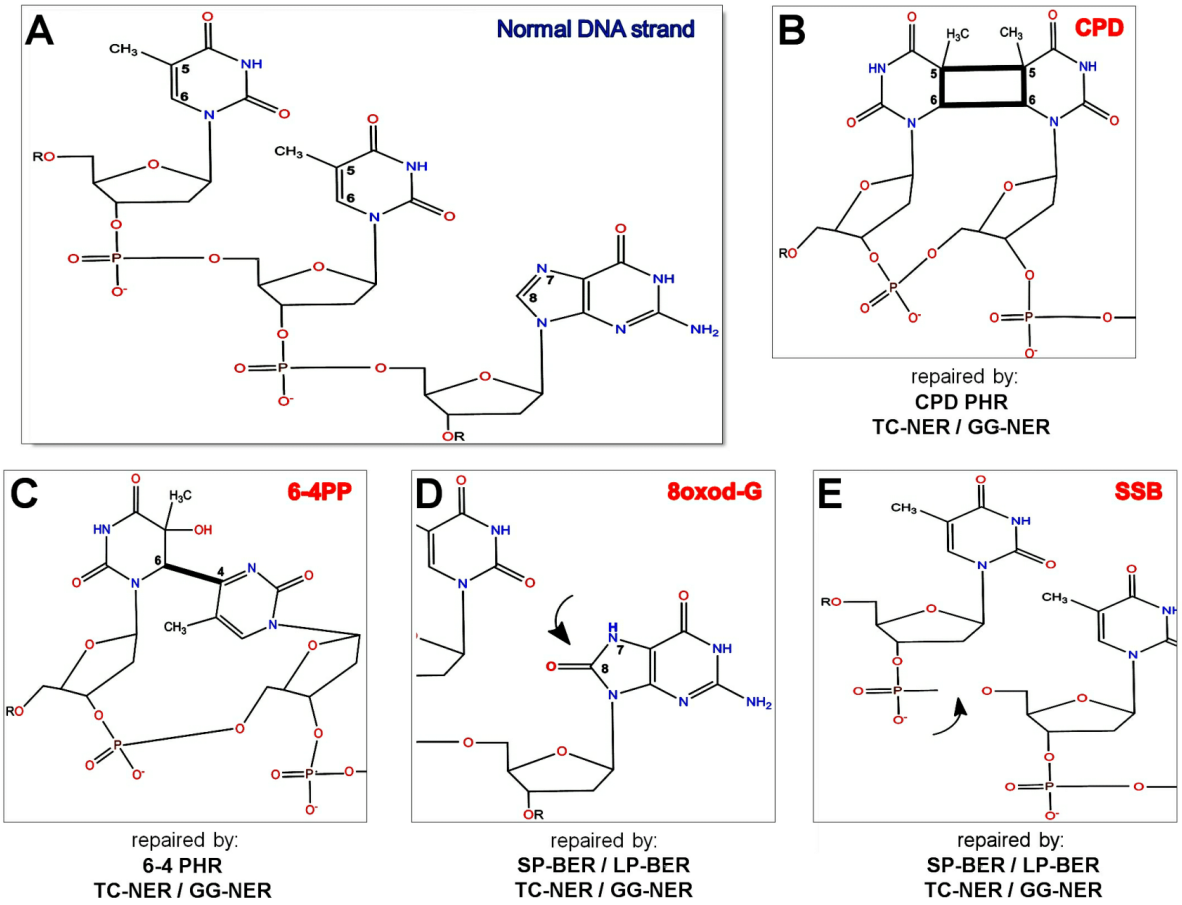
A
Normal DNA strand
B
CPD
repaired by:
CPD PHR
TC-NER / GG-NER
C
6-4PP
repaired by:
6-4 PHR
TC-NER / GG-NER
D
8oxod-G
repaired by:
SP-BER / LP-BER
TC-NER / GG-NER
E
SSB
repaired by:
SP-BER / LP-BER
TC-NER / GG-NER

3 ARTIGO 2 – IMPACTS OF UVB RADIATION ON FOOD CONSUMPTION OF FOREST SPECIALIST TADPOLES

Este estudo o papel do impacto genotóxico induzido por uma dose de radiação UVB ambiental e da ineficiência do fotorreparo de DNA no processo de perda de desempenho alimentar observado em girinos de uma espécie de perereca especialista florestal ameaçada de extinção e restrita de fragmentos de Mata Atlântica da porção sul. Os resultados geram insights ecológicos que estendem a espécie utilizada neste estudo, e trazem uma contribuição substancial para a investigação do papel da radiação UV solar no declínio enigmático de espécies de anfíbios. O presente capítulo encontra-se publicado na revista científica *Ecotoxicology and Environmental Safety* (LONDERO et al., 2017).

Ecotoxicology and Environmental Safety 143 (2017) 12–18

Contents lists available at ScienceDirect

Ecotoxicology and Environmental Safety

journal homepage: www.elsevier.com/locate/ecoenv

Impacts of UVB radiation on food consumption of forest specialist tadpoles

James Eduardo Lago Londero[a,b], Caroline Peripolli dos Santos[a,b], Ana Lúcia Anversa Segatto[a], André Passaglia Schuch[a,b,*]

[a] Department of Biochemistry and Molecular Biology, Federal University of Santa Maria, RS, Brazil
[b] Southern Regional Space Research Center, CRS/INPE-MCTIC, Santa Maria, RS, Brazil

ARTICLE INFO

Keywords:
Sunlight
DNA damage
DNA repair
Treefrog
Weight loss
Amphibian decline

ABSTRACT

Solar ultraviolet radiation B (UVB) is an important environmental stressor for amphibian populations due to its genotoxicity, especially in early developmental stages. Nonetheless, there is an absence of works focused on the UVB effects on tadpoles' food consumption efficiency. In this work, we investigated the effects of the exposure to a low environmental-simulated dose of UVB radiation on food consumption of tadpoles of the forest specialist *Hypsiboas curupi* [Hylidae, Anura] species. After UVB treatment tadpoles were divided and exposed to a visible light source or kept in the dark, in order to indirectly evaluate the efficiency of DNA repair performed by photolyases and nucleotide excision repair (NER), respectively. The body mass and the amount of food in tadpoles' guts were verified in both conditions and these data were complemented by the micronuclei frequency in blood cells. Furthermore, the keratinized labial tooth rows were analyzed in order to check for possible UVB-induced damage in this structure. Our results clearly show that the body weight decrease induced by UVB radiation occurs due to the reduction of tadpoles' food consumption. This behavior is directly correlated with the genotoxic impact of UVB light, since the micronuclei frequency significantly increased after treatments. Surprisingly, the results indicate that photoreactivation treatment was ineffective to restore the food consumption activity and body weight values, suggesting a low efficiency of photolyases enzymes in this species. In addition, UVB treatments induced a higher number of breaks in the keratinized labial tooth rows, which could be also associated with the decrease of food consumption. This work contributes to better understand the process of weight loss observed in tadpoles exposed to UVB radiation and emphasizes the susceptibility of forest specialist amphibian species to sunlight-induced genotoxicity.

1. Introduction

Amphibians are ectotherms characterized by having permeable exposed skin and eggs that may readily absorb substances from the environment (Blaustein and Belden, 2003). Moreover, many species have complex life cycles that can potentially expose them to both aquatic and terrestrial environmental changes (Blaustein and Belden, 2003). In addition, amphibian populations around the world have been suffering a general decline that culminated in the extinction of several species (Stuart et al., 2004). Several factors may be contributing to this phenomenon, such as climate changes (Foden et al., 2013), the pathogenic fungus *Batrachochytrium dendobatidis* (Carvalho et al., 2017), habitat fragmentation and destruction (Cushman, 2006), release of chemicals (Rissoli et al., 2016), and the introduction of exotic species (Kats and Ferrer, 2003). Besides the agents mentioned above, the increased incidence of ultraviolet (UV) radiation due to stratospheric ozone depletion (Kerr and McElroy, 1993) has been proposed as an important factor for amphibian decline due to its genotoxicity on embryonic and larval stages (Alton et al., 2012; Belden and Blaustein, 2002; Blaustein and Belden, 2003; Blaustein et al., 1994; Schuch et al., 2015a, 2015b).

The UV component of sunlight, which corresponds to ultraviolet B (UVB, 280–315 nm) and ultraviolet A (UVA, 315–400 nm) wavelengths, can induce cell death and mutagenesis as a consequence of DNA lesions induction, known as pyrimidine dimers (Pfeifer et al., 2005; Schuch and Menck, 2010; Schuch et al., 2015b). The most frequent DNA lesions induced by UVB radiation are the cyclobutane pyrimidine dimers (CPDs), which constitute ~80–90% of the photoproducts, and pyrimidine-pyrimidone (6-4) photoproducts (6,4PPs), which account for the 10–20% of the UVB lesions (Sancar, 2008). The genotoxicity induced by UVB radiation has been shown to be very detrimental to amphibian species (Schuch et al., 2015a, 2015b).

Abbreviations: UV, ultraviolet radiation; UVA, ultraviolet radiation A; UVB, ultraviolet radiation B; UVC, ultraviolet radiation C; CPDs, cyclobutane pyrimidine dimers; 6-4PPs, pyrimidine (6-4) pyrimidone photoproducts; TSP, Turvo State Park; NER, nucleotide excision repair

* Corresponding author at: Federal University of Santa Maria, Av. Roraima, 1000, P.O. Box 5021, room 3010, Camobi, Santa Maria, RS 97110-970, Brazil.
E-mail address: schuchap@gmail.com (A. Passaglia Schuch).

http://dx.doi.org/10.1016/j.ecoenv.2017.05.002
Received 19 January 2017; Received in revised form 28 April 2017; Accepted 2 May 2017

According to UV-sensitivity hypothesis, the declining amphibian species have lower resistance to UV radiation due to the lower capacity to repair the UV-induced DNA damage (Blaustein et al., 1999, 1994). The DNA damage induced by UV radiation can be repaired by enzymes known as photolyases that use visible/UVA light as an energy source to reverse the DNA damage in an error free process called photoreactivation (Blaustein et al., 1994; Friedberg, 2003). In addition to photolyases, the nucleotide excision repair (NER) pathway can restore the UV-induced DNA damage in a process that needs several proteins and ATP consumption (Sancar and Tang, 1993). However, the role of DNA repair pathways in amphibian decline is still a matter of discussion (Blaustein et al., 1999; Smith et al., 2000; Thurman et al., 2014; Schuch et al., 2015b).

Previous published studies regarding the amphibian foraging behavior were focused on the impact of predation risk, quantity and quality of food (Babbitt, 2001; Eklov and Halvarsson, 2000; Kupferberg, 1997), importance of well-maintained labial tooth row for the feeding knematics (Venesky et al., 2013, 2010b), as well as on the impacts of *Batrachochytrium dendrobatidis* infection on tadpole oral disc (Smith and Weldon, 2007) and foraging efficiency (Venesky et al., 2009). Despite the well documented effects of UVB light on tadpoles' weight (Belden and Blaustein, 2002; Lipinski et al., 2016; Schuch et al., 2015a), there is an absence of works focused on the UVB effects on foraging efficiency, which can have an important role in the tadpoles' weight loss process. Therefore, considering that the UVB radiation reduces tadpoles' normal activity (Alton et al., 2012), and the reduced foraging behavior causes tadpoles to consume less food (Anholt et al., 1996; Skelly, 1994), here we hypothesized that UVB exposure leads to weight loss due to the decrease of food consumption. Furthermore, we also evaluated if the food consumption decrease is a consequence of the UVB-induced genomic instability. Additionally, considering the fact that UVB radiation can alter keratin structures (Biniek et al., 2012), it becomes necessary to evaluate if UVB exposure can disturb tadpoles' food consumption activity due to its impact on the keratinized mouthparts (Venesky et al., 2010b).

In this work we chose the treefrog *Hypsiboas curupi* [Hylidae, Anura] as a model species to evaluate the effects of UVB radiation on tadpoles' food consumption and body weight. This treefrog species is restricted to highly forested areas in the Southern Atlantic Rainforest (Iop et al., 2011), which is part of the Brazilian Atlantic Rainforest biodiversity hotspot (Myers et al., 2000). However, this environment has being severely fragmented during the last century (ICMbio, 2012; SEMA, 2014), and many species, including *H. curupi*, are currently present in both national and state list of endangered species (ICMbio, 2012; SEMA, 2014). After exposures of *H. curupi* tadpoles to a low solar-simulated UVB radiation dose, the food consumption and the total body mass were evaluated. Furthermore, the genotoxic effect of the UVB treatment was assessed through the quantification of micronucleus formation in collected blood samples. In addition, the impact of UVB exposure on tadpoles' keratinized labial tooth rows was evaluated. In all the experiments the results obtained with tadpoles kept in the dark after UVB treatment or with tadpoles exposed to a photoreactivation treatment were compared to evaluate the efficiency of DNA repair pathways to restore UVB-induced DNA damage. The obtained results clearly demonstrate the severe impact of UVB treatment on this endangered treefrog species, as well as the importance of future studies aiming to assess the impact of increased levels of solar UVB radiation on declining forest specialist species of the Hylidae family.

2. Materials and methods

2.1. Animal collection and maintenance

Four freshly laid egg masses of *H. curupi* were collected in a stream at the Turvo State Park (TSP) (27°07'–27°16'S, 53°48'–54°04'W), which is a remaining fragment of the Southern Atlantic Rainforest (SEMA, 2005). The egg masses were packed in plastic sac half filled with air and water from the stream and transported to the laboratory at Federal University of Santa Maria. The collected egg masses were put together in the same plastic tank and kept aerated until the beginning of hatching. The recently hatched tadpoles were then transferred to individual plastic tanks (one tadpole per plastic tank of 14 cm of diameter, 9 cm of height and 42 cm of circumference) filled with dechlorinated water (19 ± 2 °C) to a minimum depth of 55 mm (between 55 and 70 mm). The total volume of water was changed every two days and tadpoles were fed with boiled spinach ad libitum. Tadpoles were maintained under these conditions for about 20–30 days prior to the beginning of the experiments.

2.2. 48-h fasting period, UVB irradiation, photoreactivation treatment and food availability time

Before the beginning of experiments, groups of ten tadpoles (Gosner stage 25–26; Gosner, 1960) were selected based on their similarity in total body length (cm) and mass (g) because we noticed that there was variability regarding these measures inside the same stage. These analyses were made using a stereomicroscope with 40× magnification (Nova Optical Systems, Brazil), an analytical balance (Shimadzu BL3200H, Japan), and a digital 0.01 mm precision caliper rule (Serie 500, Mitutoyo, Brazil). A total of 130 tadpoles were selected for this work (keeping one tadpole per plastic tank). The selected individuals firstly remained in a 48-h fasting period in order to standardize the amount of food in their guts. To prevent tadpoles to use their own feces as a food source, plastic mesh nets were submerged in the water and tadpoles were placed above the nets.

After fasting, tadpoles were divided in two groups: non-irradiated control tadpoles (70 individuals) and UVB-irradiated tadpoles (60 individuals). The UVB dose used in the experiments was 2.0 kJ/m^2 and this simulate 15 min of natural sunlight exposure (12:00–12:15) on a clear sky summer day on a stream located in a deforested area at the TSP (Lipinski et al., 2016). All irradiation was performed using the same 15 W UVB lamp (T15M, Vilber Lourmat, France) filtered with a polycarbonate sheet to block UVC wavelengths. The dose rates of the UVB lamp was 5.9 $J/m^2/s$ and the exposure time to achieve the desired UVB dose was 5 min and 40 s. The UVB dose applied in this work was established through the use of a portable radiometer (UV Monitor MS-211-1, EKO Instruments, Japan). The amount of UVC contamination for the UVB lamp was below the detection limit of the equipment. The spectral characteristic of the UVB lamp was previously presented by Schuch et al. (2015b).

Immediately after UVB exposures, 30 tadpoles were subjected to 3 h of photoreactivation to activate the photolyase enzymes (group UVB L). Photoreactivation was performed by using two 40 W fluorescent lamps (General Electric, Brazil) at a distance of 40 cm from tadpoles. The spectral characteristic of the fluorescent lamps was previously presented by Schuch et al. (2015b). These tadpoles were then maintained in transparent plastic tanks and exposed to a constant photoperiod (12 h light:12 h dark) until the end of the experiment. In parallel, 30 UVB-exposed tadpoles were kept in the dark (each plastic tank was wrapped with aluminum foil) until the end of the experimental period (group UVB D). The same photoreactivation treatment was performed with 40 tadpoles of the non-irradiated control group (group CTL L), while 30 tadpoles from the non-irradiated group were also kept in the dark (group CTL D). Immediately after UVB irradiation, all tadpoles were fed with boiled spinach ad libitum for 3, 24 or 48 h.

2.3. Analysis of the impact of UVB exposure on tadpoles' total body mass and on micronuclei frequency in blood samples

In this experiment, the same tadpole was weighed in three different periods: before fasting (first measurement), after 48 h of fasting (second measurement), and after adding food ad libitum at three different times

after UVB irradiation (3, 24 or 48 h) (third measurement). Ten tadpoles from each treatment were weighed with an analytical balance, and the impact of UVB radiation on tadpoles' total body mass was accessed through two different ratios between mass measurements. The first ratio compared the values (g) of the third measurement with the values of the second measurement: the objective of this ratio was to evaluate if the starving tadpoles exposed to UVB radiation would be able to gain mass when subjected to food ad libitum. On the other hand, the second ratio compared the values of the third measurement with the values of the first measurement: the objective of this ratio was to evaluate if, in the end of the experiment, the tadpoles exposed to UVB radiation would be able to recovery their initial mass values (measured before 48 h of fasting).

In order to confirm the genotoxic potential of UVB radiation, blood samples were collected from five independent tadpoles after each treatment to quantify the micronucleus formation in erythrocytes. Tadpoles were anesthetized with Xylocaine® (lidocaine) 10% and the tails were sectioned transversely at the height of the pelvis. A particular care was taken to collect blood samples free of dirt from the internal organs. The blood samples were placed throughout clean and previously labeled glass slides, fixed in absolute methanol for 8 min, and stained with Giemsa solution (15%) for 8 min. After, the glass slides were subtly washed in running water and dried at room temperature. An Olympus BX41 optical microscope with a magnification of 1000x was used to count at least 1000 erythrocytes per glass slide. The micronuclei frequency was given by the ratio between the number of micronuclei per 1000 erythrocytes counted.

2.4. Impact of UVB exposures on tadpoles' keratinized labial tooth rows

After the body mass measurements and collection of blood samples, the oral disc of ten tadpoles from each treatment was analyzed using a stereomicroscope. In this experiment, each labial tooth row of each individual from all treatment was compared. *H. curupi* tadpoles' oral disc has a complete marginal papillae, without a rostral gap, and the labial tooth row formula is 3(1,3)/5(1) (Garcia et al., 2007). Thus, the amount of tadpoles with A-1, A-2, A-3, P-1, P-2, P-3, P-4 and P-5 keratinized labial tooth row (see Altig and McDiarmid (1999)) with deformities was assessed in each treatment, as well as the normal rows. Nonetheless, in order to increase the accuracy of the determination of UVB-induced deformities in these keratinized structures, this analysis only considered the A-2 labial tooth row, since this is the longest and the most prominent row.

2.5. Impact of UVB exposures on tadpoles' food consumption efficiency

The whole guts of ten tadpoles from each treatment were removed by using a scalpel cut at each end and stretched on white sheets of EVA (Ethylene Vinyl Acetate). Next, it were performed measurements of the total length (mm) and the average diameter of the guts (mm; this average was calculated through three different measures of the guts diameter: at the midpoint and at the two ends) with a vernier caliper (Mitutoyo Absolute IP67 Coolant Caliper: ± 0.001 in). The food consumption efficiency was determined as the proportion of food in the gut, and it was calculated through the ratio between the volume of gut with food and the total volume of the gut. Table 1 summarizes the design of the experiments described above.

2.6. Statistical analysis

The statistics for the total body mass experiment was calculated using the values of tadpoles' mass (g) as the response variable, and the exposure to UVB radiation, photoreactivation or dark treatments (L or D), as well as the food availability time (0, 3, 24 or 48 h) as predictors. The measures of tadpoles' total body mass (g) were expressed as a fold change to compare the mass before fasting, after fasting and after UVB irradiation in each food availability time. In the experiment of food consumption efficiency, we used the proportion of food in tadpoles' guts (expressed as percentage) as the response variable, and the exposure to UVB radiation, photoreactivation or dark treatments (L or D), and food availability time (0, 3, 24 or 48 h) as predictors. For micronuclei frequency, we used the number of micronuclei (expressed as a proportion in relation to 1000 counted cells) as the response variable, and the exposure to UVB radiation, photoreactivation or dark treatments (L or D), and food availability time (0, 3, 24 or 48 h) as predictors. In order to statistically discriminate the entire set of data of each experiment, we performed the Kruskal-Wallis ANOVA test by Ranks. In addition, we also performed a One-way ANOVA, followed by Post Hoc Tukey's tests ($P < 0.05$) using the software RStudio v. 0.99.903 (R Core Team, 2016) with the internal package "car" (Fox and Weisberg, 2011).

Table 1
General scheme of the steps performed in methodology. Before experiment – the selected tadpoles were fed with boiled spinach ad libitum to perform the first measurement of total body mass. **Experiment (prior UVB irradiation) –** tadpoles were fasted for 48 h to perform the second measurement of total body mass. **Experiment (after UVB irradiation) –** third measurement of tadpoles' total body mass (10 tadpoles per group); collection of blood samples (5 tadpoles per group); analysis of mouthparts (10 tadpoles per group); analysis of the proportion of food in the guts (10 tadpoles per group). The same tadpole was weighed in all three different food availability times.

Before experiment	Tadpoles fed with boiled spinach ad libitum	First measurement of the total body mass			
Experiment (prior UVB irradiation)	Tadpoles in the 48-h fasting	Second measurement of total body mass			
Experiment (after UVB irradiation)		Control group		UVB-irradiated	
	Spinach *ad libitium*	L	D	L	D
	0 h	10			
	3 h	10	10	10	10
	24 h	10	10	10	10
	48 h	10	10	10	10

L – tadpoles exposed to photoreactivation treatment; D – tadpoles kept in the dark until the end of the experiment.

3. Results

3.1. Impact of UVB exposure on tadpoles' total body mass

The results of the first ratio are shown in Fig. 1A, and the results of the second ratio are presented in Fig. 1B. The statistics are presented in Table 2.

Fig. 1A demonstrates that while non-irradiated tadpoles (CTL) readily gained weight after 24 and 48 h with food ad libitum, tadpoles from both groups UVB D and UVB L have lost weight during these food availability times. On the other hand, Fig. 1B shows that tadpoles from both groups UVB D and UVB L were unable to return to the mass values measured before 48 h of fasting, even with the administration of food ad libitum for 24 and 48 h. However, all the non-irradiated control tadpoles were able to restore their initial values of mass after 24 and 48 h of food available.

3.2. Impact of UVB exposure on tadpoles' food consumption efficiency

The amount of boiled spinach ingested after both 48 h of fasting and UVB irradiation was quantified for each food availability time by dissecting the tadpoles' guts. The percentage of gut volume with food in relation to the total gut volume was calculated and the result is shown in Fig. 2. The statistics of this result are presented in Table 2.

A similar amount of food was observed in all tadpoles' guts after 3 h of food availability. However, the amount of food found within

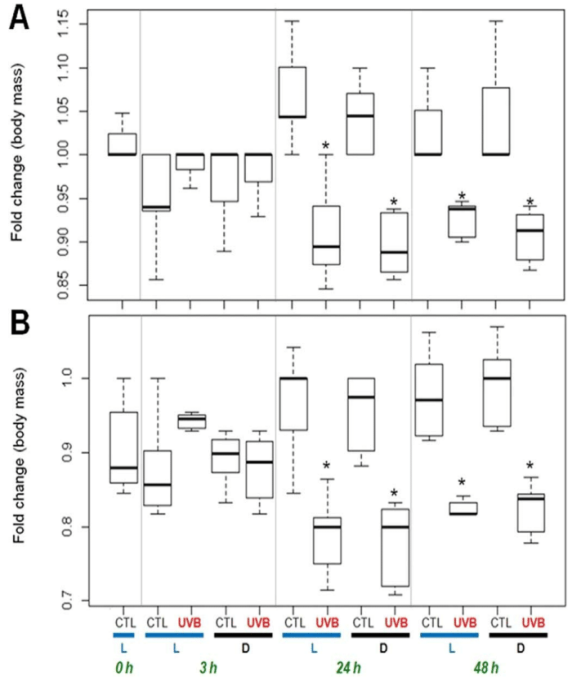

Fig. 1. (A) Ratio between the values of tadpoles' total body mass (g) measured after each food availability time and after 48 h of fasting. **(B)** Ratio between the values of tadpoles' total body mass (g) measured after each food availability time and before 48 h of fasting. CTL – non-irradiated control tadpoles. UVB – tadpoles exposed to 2.0 kJ/m^2 of UVB radiation. L – tadpoles exposed to photoreactivation treatment. D – tadpoles kept in the dark until the end of the experiment. 0, 3, 24 or 48 h – food availability times. * Statistically significant difference in relation to the respective control group ($P < 0.05$).

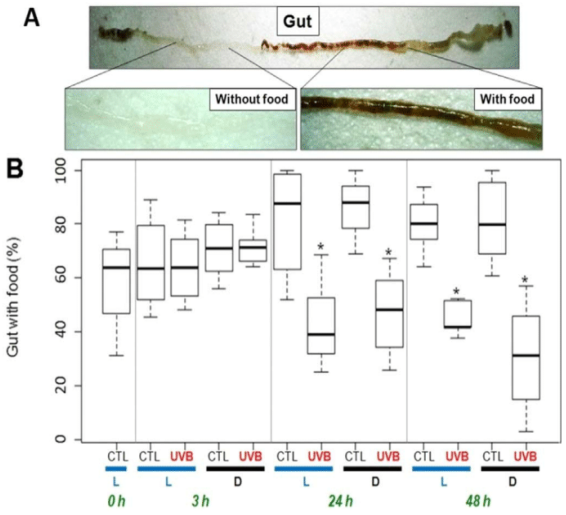

Fig. 2. (A) Representative example of parts of *H. curupi* tadpole's gut with and without food. **(B)** Percentage of gut with food. CTL – non-irradiated control tadpoles. UVB – tadpoles exposed to 2.0 kJ/m^2 of UVB radiation. L – tadpoles exposed to photoreactivation treatment. D – tadpoles kept in the dark until the end of the experiment. 0, 3, 24 or 48 h – food availability times. * Statistically significant difference in relation to the respective control group ($P < 0.05$).

tadpoles' guts of both groups UVB D and UVB L significantly decreased (in relation to their respective non-irradiated controls) during the periods of 24 and 48 h of food available.

3.3. Quantification of micronuclei formation in tadpoles' blood samples

The genotoxicity of the UVB dose applied in this work was analyzed thorough the micronuclei frequency in tadpoles' erythrocytes. This result is shown in Fig. 3 and the statistics are presented in Table 2.

Our result indicates an increase in the micronuclei frequency after 24 and 48 h of UVB exposure, in relation to the non-irradiated control groups. In fact, there was a slight increase in the micronucleus formation in the group UVB L after 24 h compared to their respective non-irradiated control. In contrast, there was a large and statistically significant increase of micronuclei frequency in the group UVB D after 24 h compared to their respective non-irradiated control group. Notably, after 48 h of UVB irradiation both groups UVB L and UVB D presented a large and statistically significant increase of micronucleus formation compared to their respective non-irradiated control groups. It is also important to emphasize that the micronuclei frequency was similar between the groups UVB D and UVB L after 48 h of UVB treatment.

3.4. Impact of UVB exposure on tadpoles' keratinized labial tooth rows

In order to check if keratinized labial tooth rows were deformed after UVB irradiation, the oral disc of all tadpoles were analyzed and the result is presented in Fig. 4.

This result shows that deformed A-2 labial tooth rows were more frequently observed in UVB-irradiated tadpoles than in non-irradiated control tadpoles. After UVB treatment, the amount of tadpoles presenting deformed A-2 row was at least two-fold higher than the non-irradiated control groups that also presented deformities in this row,

Table 2
Statistically significant data of all experiments (ANOVA, followed by Post Hoc Tukey's tests ($p < 0.05$)).

	Treatments	DF	F	P
Body mass: ratio 1	CTL 24 h L vs. UVB 24 h L	12	$F_{(12, 104)} = 72.51$	< 0.0001
	CTL 24 h D vs. UVB 24 h D	12	$F_{(12, 104)} = 72.51$	< 0.0001
	CTL 48 h L vs. UVB 48 h L	12	$F_{(12, 104)} = 72.51$	0.0032
	CTL 48 h D vs. UVB 48 h D	12	$F_{(12, 104)} = 72.51$	< 0.0001
Body mass: ratio 2	CTL 24 h L vs. UVB 24 h L	12	$F_{(12, 103)} = 74.59$	< 0.0001
	CTL 24 h D vs. UVB 24 h D	12	$F_{(12, 103)} = 74.59$	< 0.0001
	CTL 48 h L vs. UVB 48 h L	12	$F_{(12, 103)} = 74.59$	< 0.0001
	CTL 48 h D vs. UVB 48 h D	12	$F_{(12, 103)} = 74.59$	< 0.0001
Gut with food	CTL 24 h L vs. UVB 24 h L	12	$F_{(12, 99)} = 44.95$	0.0002
	CTL 24 h D vs. UVB 24 h D	12	$F_{(12, 99)} = 44.95$	0.0001
	CTL 48 h L vs. UVB 48 h L	12	$F_{(12, 99)} = 44.95$	0.0004
	CTL 48 h D vs. UVB 48 h D	12	$F_{(12, 99)} = 44.95$	< 0.0001
Micronuclei frequency	CTL 24 h D vs. UVB 24 h D	7	$F_{(7, 24)} = 17.50$	0.0061
	CTL 48 h L vs. UVB 48 h L	7	$F_{(7, 24)} = 17.50$	0.0005
	CTL 48 h D vs. UVB 48 h D	7	$F_{(7, 24)} = 17.50$	< 0.0001

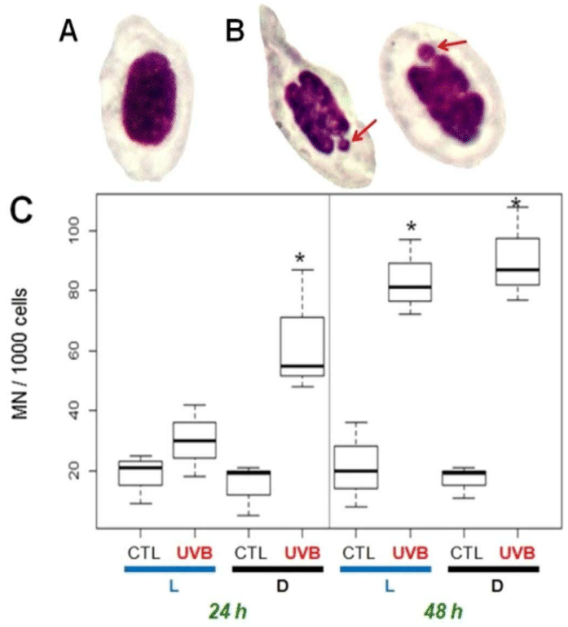

Fig. 3. (A) Representative example of a normal erythrocyte of *H. curupi* tadpole. **(B)** Representative examples of UVB-induced micronuclei in erythrocytes of *H. curupi* tadpoles (the micronuclei are indicated by arrows). **(C)** Number of micronuclei per 1000 counted cells. CTL – non-irradiated control tadpoles. UVB – tadpoles exposed to 2.0 kJ/m^2 of UVB radiation. L – tadpoles exposed to photoreactivation treatment. D – tadpoles kept in the dark until the end of the experiment. 24 or 48 h – food availability times. * Statistically significant difference from the respective control ($P < 0.05$).

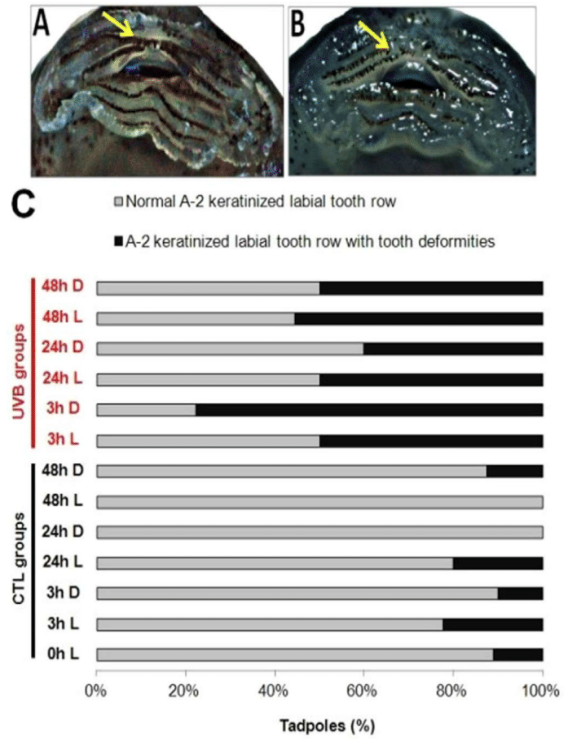

Fig. 4. Representative examples of the oral discs of non-irradiated **(A)** and UVB-irradiated **(B)** tadpoles. In both figures **(A)** and **(B)** the A-2 keratinized labial tooth row is indicated by arrows. **(C)** Percentage of tadpoles with normal A-2 keratinized labial tooth row (grey) and A-2 keratinized labial tooth row with deformities (black). CTL – non-irradiated control tadpoles. UVB – tadpoles exposed to 2.0 kJ/m^2 of UVB radiation. L – tadpoles exposed to photoreactivation treatment. D – tadpoles kept in the dark until the end of the experiment. 0, 3, 24 or 48 h – food availability times.

while it was seven-fold higher if compared to the non-irradiated control tadpoles without deformity in the A-2 row.

4. Discussion

The negative effects of UVB radiation on *H. curupi* tadpoles' body mass (Fig. 1) that were kept in the dark (group UVB D) is in accordance with a previously published work of our group performed with tadpoles of the *Hypsiboas pulchellus* species (Schuch et al., 2015a). However, the authors demonstrated that *H. pulchellus* tadpoles exposed to photoreactivation treatment after UVB irradiation did not lose weight. In contrast, our results indicate that even after photoreactivation treatment, the *H. curupi* tadpoles lost weight and failed to return to their initial mass values when exposed to food ad libitum for 48 h.

Our results provide strong evidence that the exposure to low doses of UVB radiation drastically reduces feeding efficiency in *H. curupi* tadpoles. This is the first work that shows the negative impact of a genotoxic agent, in this case UVB radiation, on tadpoles' food consumption efficiency. The amount of food in the gut of UVB-irradiated tadpoles, even in those exposed to the photoreactivation treatment, was much lower than the amount of food found in the gut of non-irradiated control tadpoles after 24 h and 48 h of food available; although in the time of 3 h it did not show significant difference (Fig. 2). Despite some previous published works explored tadpole's foraging efficiency using treatments of 3 h with food ad libitum (Venesky et al., 2010b, 2009), our results indicate that the food availability time after UVB treatment must be extended to at least 48 h in order to allow the induction of biological effects of DNA lesions generated by this genotoxic agent. Thus, the micronuclei frequency of UVB-irradiated tadpoles kept in the dark was elevated after 24 h, but the peak was observed after 48 h of UVB irradiation, for both tadpoles kept in the dark and exposed to the photoreactivation treatment (Fig. 3). Moreover, this result indicates that this forest specialist species is very sensitive to UVB radiation, probably due to an inefficient DNA repair performed by both photolyases and NER pathways, which could explain the large amount of chromosomal breaks formed 48 h after UVB exposure in both groups (D and L).

The UVB-induced DNA damage may have decreased tadpoles' metabolism as observed in freshwater cladoceran *Daphnia catawba* (Fischer et al., 2006). In common toad (*Bufo bufo*) tadpoles UVB radiation causes decrease in oxygen consumption (Formicki et al., 2003). Thus, the changes in the oxygen uptake of anuran larvae induced by UVB radiation may limit the amount of energy devoted to developmental processes and to behavioral reactions such as feeding, making tadpoles more susceptible to ecologically relevant pathogens (Formicki et al., 2003). The changes in metabolism that arise as consequences of UVB-induced cellular damage may cause alterations in the tadpole activity, as seen in Alton et al. (2012). The reduced activity levels can make tadpoles less active and less foragers, resulting in a lower ingestion of food (Anholt et al., 1996; Skelly, 1994).

In fact, in our food consumption experiment it could be observed that the foraging efficiency of UVB-irradiated tadpoles was compromised. Probably, the use of energy to repair the UVB-induced DNA damage could have affected other metabolic processes, thus impacting the tadpoles' total body mass. Hence, it is known that DNA repair performed by NER pathway demand additional and not foreseen energy expenditure. On the other hand, reduced carbohydrate and nutrients stocks in tadpoles limits the ATP production that is essential for NER (Sancar and Tang, 1993), as well as for other cellular processes (Dimroth et al., 2006). Furthermore, the association between several micronutrients and genome stability is well established, demonstrating that micronutrients play a key role in maintaining genomic integrity (Ames and Wakimoto, 2002; Fenech, 2003). Therefore, we suggest that the impairment of tadpoles' food consumption by UVB radiation results in a reduced micronutrients provision and energy necessary to repair all induced DNA lesions, increasing genomic instability. Probably, the

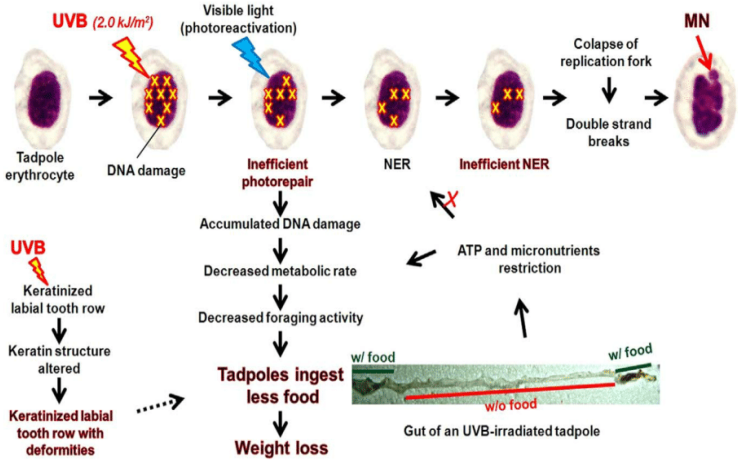

Fig. 5. Scheme showing how the UVB-induced genotoxicity and keratinized labial tooth rows deformities in *H. curupi* tadpoles affects their food consumption inducing weight loss. w/ food – with food; w/o food – without food.

excessive number of DNA damage that has not been repaired by photolyases and NER decreases tadpoles' metabolic rates, then decrease tadpoles' food consumption and the total body mass. On the other hand, it is important to consider that UV radiation is also able to trigger the formation of oxidative DNA damage through the production of reactive oxygen species (ROS) (Schuch et al., 2017). Since this type of DNA lesion is preferentially repaired by the ATP-dependent base excision repair (BER) pathway (Petermann et al., 2003), probably the disruption of this DNA repair mechanism can also contribute for the reduction of food consumption. However, this hypothesis must be interpreted cautiously because UVB is not effective as UVA radiation in producing ROS (Schuch et al., 2017). It is also important to mention that the energetic cost of UVB irradiation can be larger if tadpoles are exposed to other environmental stressors (Alton et al., 2012).

In parallel, it was possible to observe a large number of UVB-irradiated tadpoles with A-2 keratinized labial tooth row with deformities (Fig. 4). In *Lithobates sphenocephalus* tadpoles, a ranid species, it was verified that their feeding kinematics was altered after removal of a single labial tooth row (P-3), which reveals that teeth loss affects the feeding (Venesky et al., 2010b). The labial tooth loss increases the speed of entire gape cycle and the efficiency in obtain food is compromised by spending more energy on increased numbers of gape cycles (Venesky et al., 2010b). Another consequence of this extra energetic spend in acquiring food is the reduction of tadpoles' body size, since less resources are allocated to growth and metamorphose. It is important to note that the pathogenic fungus *Batrachochytrium dendrobatidis* can also attack the keratinized mouthparts of tadpoles and it is already known that it causes decrease in foraging efficiency (Venesky et al., 2010a). Thus, our results suggest that the feeding kinematics of *H. curupi* tadpoles may also have been affected by tooth deformities induced by UVB radiation. However, this result must be interpreted cautiously because natural UVB exposure of tadpoles is more complex than in the laboratory. It is known that aquatic oxygen consumption decreased steadily after the developmental stage 20 of bullfrog *(Rana catesbeiana)* tadpoles, which results in a change from facultative air-breathing to obligate air-breathing at about stage 22 (Crowder et al., 1998). Additionally, tadpoles of *Rana* and *Xenopus* genera present an extremely rapid air-breathing action, exposing them at the water's surface for approximately 170 ms (Wassersug and Yamashita, 2000). However, it is important to note that in hypoxic water tadpoles must bubbling up more times for air-breathing (Wassersug and Seibert, 1975), which can make its labial tooth rows more susceptible to the harmful effects of UVB radiation.

H. curupi is an anuran species restricted to well-maintained forest environment where the solar rays practically do not reach the surface (Lipinski et al., 2016). Previous works have demonstrated that species that lay their eggs in places protected from sunlight are naturally more susceptible to UV damage (Blaustein and Belden, 2003). Therefore, our results suggest that this species must be extremely sensitive to solar UVB radiation, indicating that it does not seems to be adapted to sun exposure. However, more studies are still necessary to confirm this hypothesis.

5. Conclusions

Our results show that UVB radiation exposure reduces the food consumption efficiency and the total body mass of *H. curupi* tadpoles. Also, the micronuclei frequency was higher in tadpoles submitted to UVB treatments, and it was verified a higher number of A-2 keratinized labial tooth row with deformities in UVB-irradiated tadpoles compared to non-irradiated control tadpoles. Therefore, we suggest a new insight regarding the tadpoles' weight loss process induced by UVB radiation, and a scheme is presented in Fig. 5.

In summary, we suggest that the UVB-induced DNA damage was not efficiently repaired by photolyases, and this may have contributed to the reduction of tadpole's metabolic rates. Consequently, the foraging activity was committed, resulting in a decrease of food consumption and weight loss. In addition, the restriction of micronutrients (and ATP) could also have impaired DNA repair performed by NER pathway, increasing genomic instability and chromosomal breaks. In parallel, UVB-induced deformities in the A-2 labial tooth row may have also helped to decrease food consumption. Therefore, this work contributes to better understand the process of weight loss observed in tadpoles exposed to UVB radiation and emphasizes the susceptibility of this forest specialist anuran species to sunlight-induced genotoxicity.

Competing interests

The authors declare no competing or financial interests.

Acknowledgments

We thank to CNPq (Brasília, Brazil) for the financial support (proc. 441407/2014-5) and the Ethics Committee on Animal Use of the Federal University of Santa Maria (022/2013) and the Authorization and Information System on Biodiversity of the Brazilian Ministry of Environment (37928-2) for the access to field sites and for allowing us to conduct the experiments. We also thank to Prof. Dr. Élgion Lúcio da Silva Loreto and Profa. Dra Sonia Zanini Cechin from Federal University of Santa Maria for providing the use of optical microscope and other

equipments, Dr. Victor Mendes Lipinski for collecting the *Hypsiboas curupi* egg masses at the Turvo State Park, Me. Luiza Loebens and Me. Livia Bataioli Moura for helping with oral disc analyzes, and Dr. Maurício Beux dos Santos for helping with statistical analyzes.

References

Altig, R.A., McDiarmid, R.W., 1999. Body plan: development and morphology. In: Altig, R.A., McDiarmid, R.W. (Eds.), Tadpoles: The Biology of Anuran Larvae. University of Chicago Press, Chicago, pp. 24–51.

Alton, L.A., White, C.R., Wilson, R.S., Franklin, C.E., 2012. The energetic cost of exposure to UV radiation for tadpoles is greater when they live with predators. Funct. Ecol. 26, 94–103.

Ames, B.N., Wakimoto, P., 2002. Are vitamin and mineral deficiencies a major cancer risk? Nat. Rev. Cancer 2, 694–704.

Anholt, B.R., Skelly, D.K., Werner, E.E., 1996. Factors modifying Antipredator behavior in larval toads. Herpetologica 52, 301–313.

Babbitt, K.J., 2001. Behaviour and growth of southern leopard frog (*Rana sphenocephala*) tadpoles: effects of food and predation risk. Can. J. Zool. 79, 809–814.

Belden, L.K., Blaustein, A.R., 2002. Exposure of red-legged frog embryos to ambient UV-B radiation in the field negatively affects larval growth and development. Oecologia 130, 551–554.

Biniek, K., Levi, K., Dauskardt, R.H., 2012. Solar UV radiation reduces the barrier function of human skin. Proc. Natl. Acad. Sci. USA 109, 17111–17116.

Blaustein, A.R., Belden, L.K., 2003. Amphibian defenses against ultraviolet-B radiation. Evol. Dev. 5, 89–97.

Blaustein, A.R., Hays, J.B., Hoffman, P.D., Chivers, D.P., Kiesecker, J.M., Leonard, W.P., Marco, A., Olson, D.H., Reaser, J.K., Anthony, R.G., 1999. DNA repair and resistance to UV-B radiation in western spotted frogs. Ecol. Appl. 9, 1100–1105.

Blaustein, A.R., Hoffman, P.D., Hokit, D.G., Kiesecker, J.M., Walls, S.C., Hays, J.B., 1994. UV repair and resistance to solar UV-B in amphibian eggs: a link to population declines? Proc. Natl. Acad. Sci. USA 91, 1791–1795.

Carvalho, T., Becker, C.G., Toledo, L.F., 2017. Historical amphibian declines and extinctions in Brazil linked to chytridiomycosis. Proc. R. Soc. B 284, 20162254.

Crowder, W.C., Nie, M., Ultsch, R.G., 1998. Oxygen uptake in bullfrog tadpoles (*Rana catesbeiana*). J. Exp. Zool. 280, 121–134.

Cushman, S.A., 2006. Effects of habitat loss and fragmentation on amphibians: a review and prospectus. Biol. Conserv. 128, 231–240.

Dimroth, P., von Ballmoos, C., Meier, T., 2006. Catalytic and mechanical cycles in F-ATP synthases. EMBO Rep. 7, 276–282.

Eklov, P., Halvarsson, C., 2000. The trade-off between foraging activity and predation risk for *Rana temporaria* in different food environments. Can. J. Zool. 78, 734–739.

Fenech, M., 2003. Nutritional treatment of genome instability: a paradigm shift in disease prevention and in the setting of recommended dietary allowances. Nutr. Res. Rev. 16, 109–122.

Foden, W.B., Butchart, S.H.M., Stuart, S.N., Vié, J.C., Akçakaya, H.R., Angulo, A., DeVantier, L.M., Gutsche, A., Turak, E., Cao, L., Donner, S.D., Katariya, V., Bernard, R., Holland, R.A., Hughes, A.F., O'Hanlon, S.E., Garnett, S.T., Şekercioğlu, Ç.H., Mace, G.M., 2013. Identifying the world's most climate change vulnerable species: a systematic trait-based assessment of all birds, amphibians and corals. PLoS One 8, e65427.

Formicki, G., Zamachowski, W., Stawarz, R., 2003. Effects of UV-A and UV-B on oxygen consumption in common toad (*Bufo bufo*) tadpoles. J. Zool. 259, 317–326.

Fox, F., Weisberg, S., 2011. An {R} Companion to Applied Regression, Second edition. Sage, Thousand Oaks CA (URL). ⟨http://socserv.socsci.mcmaster.ca/jfox/Books/Companion⟩.

Friedberg, E.C., 2003. DNA damage and repair. Nature 421, 436–440.

Garcia, P.C.A., Faivovich, J.N., Haddad, C.F.B., 2007. Redescription of *Hypsiboas semiguttatus*, with the description of a new species of the *Hypsiboas pulchellus* group. Copeia 4, 933–951.

Gosner, K.L., 1960. A simplified table for staging anuran embryos and larvae with notes on identification. Herpetologica 16, 183–190.

ICMbio, 2012. Sumário Executivo do Plano de Ação Nacional para a Conservação dos anfíbios e répteis ameaçados da região sul do Brasil: PAN Herpetofauna Sul.

Iop, S., Caldart, V.M., dos Santos, T.G., Cechin, S.Z., 2011. Anurans of Turvo State Park: testing the validity of Seasonal Forest as a new biome in Brazil. J. Nat. Hist. 45, 2443–2461.

Kats, L.B., Ferrer, R.P., 2003. Alien predators and amphibian declines: review of two decades of science and the transition to conservation. Divers. Distrib. 9, 99–110.

Kerr, J.B., McElroy, C.T., 1993. Evidence for large upward trends of ultraviolet-B radiation linked to ozone depletion. Nature 262, 1032–1034.

Kupferberg, S.J., 1997. The role of larval diet in anuran metamorphosis. Am. Zool. 37, 146–159.

Lipinski, V.M., dos Santos, T.G., Schuch, A.P., 2016. An UV-sensitive anuran species as an indicator of environmental quality of the Southern Atlantic Rainforest. J. Photochem. Photobiol. B 165, 174–181.

Myers, N., Mittermeier, R.A., Mittermeier, C.G., da Fonseca, G.A.B., Kent, J., 2000. Biodiversity hotspots for conservation priorities. Nature 403, 853–858.

Petermann, E., Ziegler, M., Oei, S.L., 2003. ATP-dependent selection between single nucleotide and long patch base excision repair. DNA Repair 2, 1101–1114.

Pfeifer, G.P., You, Y.-H., Besaratinia, A., 2005. Mutations induced by ultraviolet light. Mutat. Res. 571, 19–31.

R Core Team, 2016. R: a Language and Environment for Statistical Computing. R Foundation for Statistical Computing, Vienna, Austria (URL). ⟨https://www.R-project.org/⟩.

Rissoli, R.Z., Abdalla, F.C., Costa, M.J., Rantin, F.T., Mckenzie, D.J., Kalinin, A.L., 2016. Effects of glyphosate and the glyphosate based herbicides Roundup Original® and Roundup Transorb® on respiratory morphophysiology of bullfrog tadpoles. Chemosphere 156, 37–44.

Sancar, A., 2008. Structure and function of photolyase and in vivo enzymology: 50th anniversary. J. Biol. Chem. 283, 32153–32157.

Sancar, A., Tang, M.-S., 1993. Nucleotide excision repair. Photochem. Photobiol. 57, 905–921.

Schuch, A.P., dos Santos, M.B., Lipinski, V.M., Peres, L.V., dos Santos, C.P., Cechin, S.Z., Schuch, N.J., Pinheiro, D.K., Loreto, E.L.S., 2015a. Identification of influential events concerning the Antarctic ozone hole over southern Brazil and the biological effects induced by UVB and UVA radiation in an endemic treefrog species. Ecotoxicol. Environ. Saf. 118, 190–198.

Schuch, A.P., Menck, C.F.M., 2010. The genotoxic effects of DNA lesions induced by artificial UV-radiation and sunlight. J. Photochem. Photobiol. B 99, 111–116.

Schuch, A.P., Moreno, N.C., Schuch, N.J., Menck, C.F.M., Garcia, C.C.M., 2017. Sunlight damage to cellular DNA: focus on oxidatively generated lesions. Free Radic. Biol. Med. http://dx.doi.org/10.1016/j.freeradbiomed.2017.01.029.

Schuch, A.P., Lipinski, V.M., Santos, M.B., Santos, C.P., Jardim, S.S., Cechin, S.Z., Loreto, E.L.S., 2015b. Molecular and sensory mechanisms to mitigate sunlight-induced DNA damage in treefrog tadpoles. J. Exp. Biol. 218, 3059–3067.

SEMA, 2005. Plano de Manejo do Parque Estadual do Turvo.

SEMA, 2014. Lista de espécies da fauna ameaçada do Rio Grande do Sul.

Skelly, D.K., 1994. Activity level and the susceptibility of anuran larvae to predation. Anim. Behav. 48, 465–468.

Smith, K.G., Weldon, C., 2007. A conceptual framework for detecting oral chytridiomycosis in tadpoles. Copeia 4, 1024–1028.

Smith, M.A., Kapron, C.M., Berrill, M., 2000. Induction of photolyase activity in wood frog (*Rana sylvatica*) embryos. Photochem. Photobiol. 72, 575–578.

Stuart, S.N., Chanson, J.S., Cox, N.A., Young, B.E., Rodrigues, A.S.L., Fischman, D.L., et al., 2004. Status and trends of amphibian declines and extinctions worldwide. Science 306, 1783–1786.

Thurman, L.L., Garcia, T.S., Hoffman, P.D., 2014. Elevational differences in trait response to UV-B radiation by long-toed salamander populations. Oecologia 175, 835–845.

Venesky, M.D., Parris, M.J., Storfer, A., 2009. Impacts of *Batrachochytrium dendrobatidis* infection on tadpole foraging performance. Ecohealth 6, 565–575.

Venesky, M.D., Rossa-Feres, D.C., Nomura, F., de Andrade, G.V., Pezzuti, T.L., de Sousa, V.T.T., Anderson, C.V., Wassersug, R.J., 2013. Comparative feeding kinematics of tropical hylid tadpoles. J. Exp. Biol. 216, 1928–1937.

Venesky, M.D., Wassersug, R.J., Parris, M.J., 2010a. Fungal pathogen changes the feeding kinematics of larval anurans. J. Parasitol. 96, 552–557.

Venesky, M.D., Wassersug, R.J., Parris, M.J., 2010b. How does a change in labial tooth row number affect feeding kinematics and foraging performance of a ranid tadpole (*Lithobates sphenocephalus*)? Biol. Bull. 218, 160–168.

Wassersug, R.J., Seibert, E.A., 1975. Behavioral responses of amphibian larvae to variation in dissolved oxygen. Copeia 1975, 86–103.

Wassersug, R.J., Yamashita, M., 2000. The mechanics of air-breathing in anuran larvae: implications to the development of amphibians in microgravity. Adv. Space Res. 24, 2007–2013.

4 ANÁLISE *IN SILICO* DAS ENZIMAS FOTOLIASES DE ANFÍBIOS

4.1 INTRODUÇÃO

Nas últimas décadas, um declínio global de populações de anfíbios tem sido observado e várias hipóteses têm sido propostas para explicar este fenômeno, tais como o aumento da incidência de radiação UV solar (STUART et al., 2004; SCHUCH et al., 2015b; HADER et al., 2015; LIPINSKI et al, 2016). O principal impacto negativo da radiação UV solar depende de sua capacidade de danificar a molécula de DNA (SCHUCH et al., 2017). Em vista disso, ao longo da evolução, estratégias foram utilizadas pelos anfíbios para evitar os efeitos genotóxicos induzidos pela radiação UV solar.

Uma das linhas de defesa dos anfíbios contra o impacto genotóxico da radiação UV consiste na reparação dos dímeros de pirimidina já estabelecidos no DNA (FRIEDBERG et al., 2003; RASTOGI et al., 2010). O fotorreparo é o principal mecanismo para reparar estes tipos de danos induzidos pela radiação UV em anfíbios e envolve a foto-ativação das enzimas fotoliases (PHR) e quebra dos dímeros de pirimidina (BLAUSTEIN et al., 1994; MENCK 2002; ZHONG, 2015). Outra linha de defesa contra a genotoxicidade induzida pela radiação UV pode ser fornecida por protetores solares naturais e pigmentos em embriões e larvas, bem como por alterações comportamentais em larvas devido à luz UV incidente (BLAUSTEIN e BELDEN, 2003). Larvas de várias espécies de anfíbios são capazes de perceber os raios UV e migrar para regiões onde estes comprimentos de onda são menos intensos (BLAUSTEIN e BELDEN, 2003; SCHUCH et al., 2015a). Em um contexto evolutivo mais amplo, a estratégia de fuga dos raios UV foi uma pressão seletiva determinante para o desenvolvimento da ritmicidade circadiana, a qual melhora a aptidão dos animais em ambientes constantes ou em mudança (PITTENDRIGH, 1993; PARANJPE e SHARMA, 2005). As variações de luz rítmica fornecem informações vitais para sincronizar os fenômenos biológicos básicos, permitindo que as espécies otimizem seu crescimento, propagação e sobrevivência (DODD et al., 2005; ROENNEBERG e MERROW, 2005). A incapacidade de responder molecular ou sensorialmente à UV e/ou luz visível solar pode ser uma desvantagem evolutiva para espécies de anfíbios (CHAVES et al., 2011; SCHUCH et al., 2015a).

O ritmo circadiano tem como principais elementos funcionais as enzimas chamadas criptocromos (CRY), que possuem as fotoliases como ancestrais, porém, em geral não possuem função de reparo dos dímeros de pirimidina induzidos pela radiação UV (SANCAR, 2003). Assim, criptocromos e fotoliases formam uma família de proteínas fotorreceptoras, as quais possuem semelhanças gerais em suas sequências e domínios. Estas proteínas

apresentam no domínio terminal N, o subdomínio conservado chamado “DNA photolyase” e o subdomínio “de ligação FAD” (MEI e DVORNYK, 2015). Além disso, criptocromos de plantas e animais possuem o domínio terminal C de comprimento variável que está ausente ou possuem comprimento reduzido nas proteínas CRY-DASH, 6-4 PHR e CPD PHR (LIN e TODO, 2005) A variação no comprimento do domínio terminal C acarreta em diversidade funcional entre criptocromos (CHAVES et al., 2006) (**Figura 2**).

Figura 2 – Arquitetura de domínios da família PHR/CRY. CRY2: *Homo sapiens*; CRY vegetal: *Arabidopsis thaliana*; CRY-DASH: *Xenopus laevis*; 6-4 PHR: *Danio rerio*; CPD PHR: *Danio rerio*. FAD: dinucleótido de flavina e adenina.

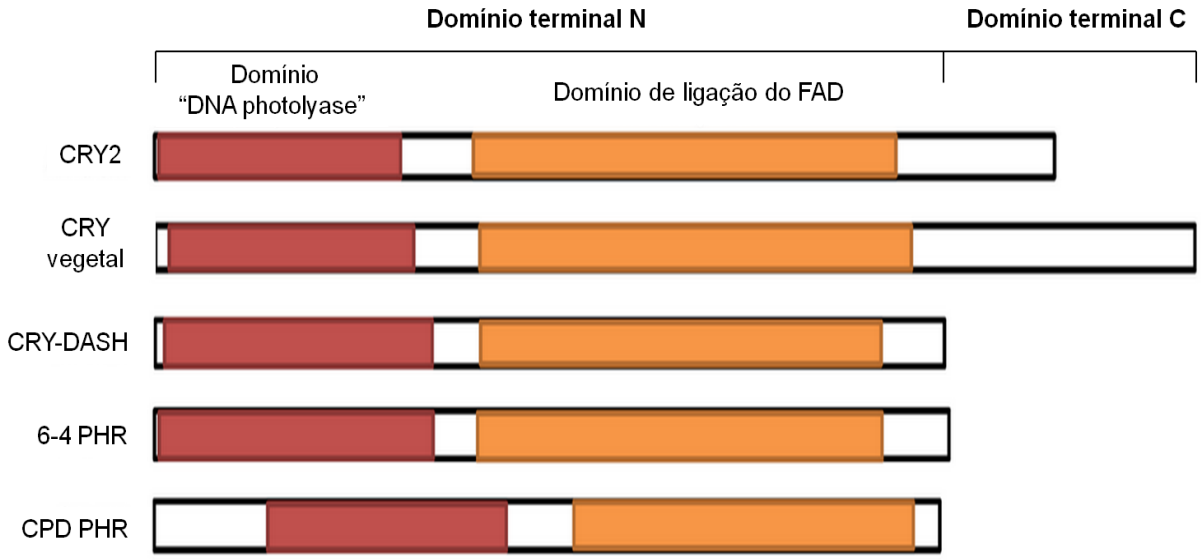

Fonte: Adaptado de MEI e DVORNYK (2015).

Coenzimas podem se ligar aos subdomínios e agirem como cromóforos que absorvem luz. Criptocromos podem possuir dois cromóforos, o MTHF (“methenyltetrahydrofolate”) e o FAD (dinucleótido de flavina e adenina), que se ligam como coenzimas ao subdomínio “DNA photolyase” e ao subdomínio “de ligação FAD”, respectivamente (MALHOTRA et al., 1995). No entanto, criptocromos podem possuir apenas o FAD, como observado em CRY de *Drosophila melanogaster* (OZTURK, 2017). Já as fotoliases podem possuir o cromóforo MTHF ou 8-HDF (“8-hydroxy-5-deazaflavin”), além do cromóforo FAD (SANCAR, 2003; OZTURK, 2017). No domínio terminal N estão localizados o subdomínio α/β e o subdomínio helicoidal α, que na estrutura 3D, são conectados por um loop variável. Os dois lobos do domínio helicoidal α formam um sulco, que é chamado de cavidade de acesso FAD, local

onde os dímeros de pirimidina são reparados (PARK et al., 1995; MEI e DVORNYK et al., 2015) (**Figura 3**).

Figura 3 – Representação esquemática dos domínios e coenzimas que compõem a estrutura 3D das enzimas da família PHR/CRY. (A) Indicação dos sítios aproximados de ligação das duas coenzimas MTHF e FAD. (B) Diagrama *Ribbon* da estrutura cristal da fotoliase de *Escherichia coli*, apresentando os domínios terminais e as posições das coenzimas. (C) Representação do potencial de superfície da estrutura cristal da fotoliase de *Escherichia coli* apresentando os resíduos expostos. A demarcação demonstra o buraco que leva ao FAD no núcleo do domínio helicoidal α. MTHF: methenyltetrahydrofolate; FAD: dinucleótido de flavina e adenina.

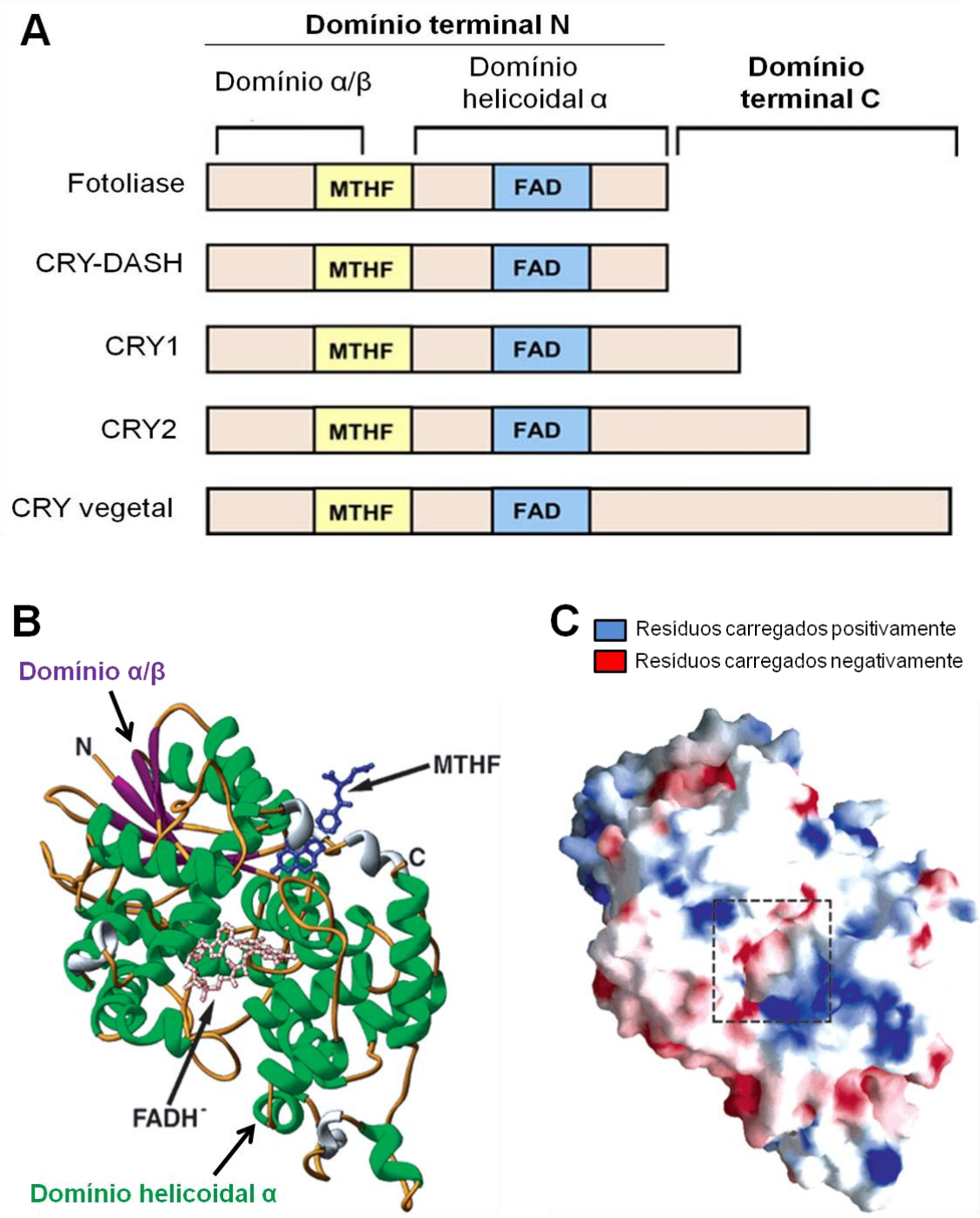

Fonte: Adaptado de SANCAR (2003), SANCAR (2008) e KAVAKLI et al. (2017).

A habilidade de uma macromolécula desempenhar adequadamente seu papel biológico é dependente da sua capacidade de assumir uma estrutura tridimensional funcional (ANFINSEN, 1973; FERSHT, 1999). Desta forma, anormalidades em ácidos nucleicos e proteínas devido a mutações ou mudanças ambientais podem torná-los incapazes de desempenhar suas funções biológicas (LEVY et al., 2001; GRANT et al., 2009; UVERSKY, 2009; NEUDECKER et al., 2012). Portanto, investigar a estrutura e a dinâmica

macromolecular das fotoliases e criptocromos é fundamental para a compreensão de como estas enzimas conduzem suas funções dentro das células de anfíbios. Entretanto, a estrutura cristalográfica de fotoliases e criptocromos de anfíbios ainda não foi relatada, mesmo nos organismos modelos *Xenopus laevis* e *Xenopus tropicalis*. Avanços significativos têm sido feitos *in silico* para realização de análises preditivas da estrutura 3D de proteínas, de forma a complementar experimentos laboratoriais (SCHMIDT et al., 2013; SHAMRIZ e OFOGHI., 2016).

Anfíbios têm ciclos de vida complexos que podem potencialmente expô-los a mudanças ambientais tanto aquáticas quanto terrestres (BLAUSTEIN e BELDEN, 2003), como o aumento da exposição aos raios UV e mudanças no regime de luz. É provável que a luz e o ritmo circadiano regulem mudanças diárias na sensibilidade de anfíbios à radiação UVB (TAKAHASHI et al., 2002; HORAK e FARRÉ, 2015), porém, este tópico ainda não foi pesquisado. Considerando que os membros da família PHR/CRY (1) representam um grupo antigo de proteínas ativadas pela luz UVA/luz visível, (2) são amplamente distribuídos e (3) possuem múltiplos papéis na biologia de anfíbios e que (4) trabalhos anteriores abordaram superficialmente os membros da família de PHR/CRY de anfíbios em um contexto mais amplo juntamente com vários outros clados de árvore da vida; torna-se necessário investigar detalhadamente as relações filogenéticas, estruturais e funcionais dentro da família PHR/CRY de anfíbios. Portanto, este estudo visa compreender as bases moleculares da família PHR/CRY de anfíbios através da identificação *in silico* de (1) genes, (2) estrutura gênica e proteica, (3) conservação de resíduos, (4) estruturas 3D preditas, (5) funções preditas a partir das estruturas 3D geradas, e (5) análises filogenéticas.

4.2 MÉTODOS

4.2.1 Disponibilidade de sequências

Apenas quatro espécies de anfíbios possuem seu genoma totalmente sequenciado: *Xenopus tropicalis*, *Xenopus laevis*, *Nanorana parkeri* e *Ambystoma mexicanum* (HELLSTEN et al., 2010; SUN et al., 2015; SESSION et al., 2016; NOWOSHILOW et al., 2018). Os quatro genomas foram divulgados em artigos científicos entre 2010 e 2018. Em 2018, o genoma da espécie de salamandra *Ambystoma mexicanum* foi publicado (NOWOSHILOW et al., 2018) e novas sequências estão disponíveis nos bancos de dados, porém ainda precisam ser anotadas e curadas. Desta forma, elas ainda não compõem o banco de dados RefSeq (ver abaixo), utilizado nas nossas análises. A incorporação de sequências desta espécie será considerada, a fim de tornar o trabalho mais robusto com a utilização de quatro genomas

totalmente sequenciados. A espécie *A. mexicanum* está criticamente ameaçada de extinção em nível global, diferentemente das outras três espécies, que possuem o status de "Pouco preocupante" em relação à perigo de extinção (IUCN, 2018). Tendo em vista a pouca disponibilidade de sequências genômicas, sequências de transcriptomas anotadas e curadas foram adicionadas neste trabalho. Entre as sequências de transcriptomas, encontra-se a espécie *A. mexicanum*.

4.2.2 Pesquisa por sequências

Sequências proteicas de fotoliases e criptocromos de anfíbios foram obtidas a partir da seção de proteínas do NCBI (https://www.ncbi.nlm.nih.gov/protein/), (1) usando a isca "photolyase xenopus"; (2) marcando o banco de dados RefSeq afim de obter sequências curadas e estáveis (O'LEARY et al, 2016); (3) marcando como filtro os táxons *Xenopus laevis* (Xla) e *X. tropicalis* (Xtr), uma vez que as sequências proteicas destas espécies foram melhor caracterizadas e anotadas; (4) dando preferência para sequências não preditas, e (5) selecionando apenas uma sequência por tipo de proteína disponível.

4.2.3 Pesquisa por sequências similares a partir de sequências de consulta

A ferramenta BLASTP (STEPHEN et al., 1997) foi usada para obter sequências proteicas homólogas a partir das sequências proteicas selecionadas mencionadas acima. O banco de dados RefSeq Protein (RSP) foi usado como "search set" e três espécies com sequências RSP disponíveis foram selecionadas na seção "organism section' (*Xenopus laevis*, *X. tropicalis* and *Nanorana parkeri*).

A fim de pesquisar por banco de dados de nucleotídeos em diferentes espécies de anfíbios a partir de nossas sequências proteicas de consulta, a ferramenta TBLASTN (STEPHEN et al., 1997) foi usada e o banco de dados "Transcriptome Shotgun Assembly (TSA)" foi marcado como "search set". 25 espécies com sequências TSA disponíveis foram marcadas no item "organism section". Estas sequências são "contigs" não anotados. Estes procedimentos foram realizados até janeiro de 2018.

4.2.4 Seleção de sequências

Para os resultados do BLASTP e TBLASTN, o E-value menor de 10^{-6} e o *score* de corte de 200 foi aplicado como um limite inferior da seleção de sequências.

4.2.5 Análise de ocorrência

A verificação da ocorrência das proteínas da família PHR/CRY nas espécies de anfíbios foi feita com base nos resultados do BLASTP e TBLASTN. O critério de análise foi simplesmente verificar a presença de sequências de cada espécie nas sublistas de cada tipo de proteína. Quando uma mesma sequência estava localizada em mais de uma lista (por exemplo, em 6-4 PHR e CRY1 e CRY2), o maior *score*, seguido pela maior cobertura de sequência e maior valor de *E*, foram utilizados como medida seletiva para determinar o tipo de proteína daquela sequência.

4.3 RESULTADOS PRELIMINARES

4.3.1 Sequências consulta selecionadas

As sequências proteicas selecionadas foram CPD PHR Xla (NP_001089127.1), 6-4 PHR Xla (NP_001081421.1), CRY-DASH Xla (NP_001084438.1), CRY1 Xla (NP_001081129.1) CRY2 Xla (NP_001083936.1) e CRY4 Xtr (NP_001123706.1). Estas sequências foram usadas como sequências proteicas de consulta nas ferramentas BLASTP e TBLASTN para encontrar sequências homólogas de anfíbios.

4.3.2 Sequências homólogas obtidas

A **Tabela 1** apresenta a diversidade de espécies de anfíbios resgatada a partir das buscas. As espécies estão distribuídas em diferentes clados da árvore filogenética dos anfíbios (PYRON e WIENS, 2011). Todas as sequências proteicas (BLASTP) e nucleotídicas (TBLASTN) obtidas estão listadas na **Tabela 2** and **Tabela 3**, respectivamente.

Tabela 1. Diversidade de espécies de anfíbios resgatadas a partir das buscas do BLASTP e TBLASTN (sequências de RSP and TSA selecionadas). RSP: Reference Sequence Protein; TSA; Transcritpome Shotgun Assembly.

Família	Espécie	Banco de dados	Taxid
Hynobiidae	*Hynobius chinensis*	TSA	288313
	Hynobius retardatus	TSA	36312
Ambystomatidae	*Ambystoma mexicanum*	TSA	8296
	Ambystoma maculatum	TSA	43114
	Ambystoma tigrinum	TSA	8305
	Ambystoma laterale	TSA	8298
	Ambystoma texanum	TSA	8304
Salamandridae	*Tylototriton wenxianensis*	TSA	385678

Bombinatoridae	*Bombina bombina*	TSA	8345
	Bombina orientalis	TSA	8346
	Bombina variegata	TSA	8348
Pipidae	*Xenopus laevis*	**RSP**	8355
	Xenopus tropicalis	**RSP**	8364
Megophryidae	*Leptobrachium boringii*	TSA	265040
Hylidae	*Pseudacris regilla*	TSA	47562
	Dryophytes cinereus	TSA	8422
Bufonidae	*Bufotes viridis*	TSA	30338
	Rhinella marina	TSA	8386
Hylodidae	*Oreobates cruralis*	TSA	448617
Ranidae	*Nanorana parkeri*	**RSP**	125878
	Lithobates clamitans	TSA	145282
	Lithobates catesbiana	TSA	8400
	Pelophylax nigromaculatus	TSA	8409
	Odorrana margaretae	TSA	121156
Rhacophoridae	*Rhacophorus omeimontis*	TSA	462328
	Rhacophorus dennysi	TSA	143444
	Polypedates megacephalus	RSG	68449

Tabela 2. Todas as sequências proteicas obtidas por similaridade a partir de cada sequência de consulta usando a ferramenta BLASTP.

Sequência de consulta	**Resultado**	**Nº de acesso**	***Score***	**Cobertura**	***E*-value**
6-4 photolyase [Xenopus laevis]	6-4 photolyase [Xenopus laevis]	NP_001081421.1	1095	100%	0
	uncharacterized protein LOC100144974 [Xenopus tropicalis]	NP_001120012.1	1012	99%	0
	PREDICTED: cryptochrome-1-like [Nanorana parkeri]	XP_018420471.1	904	96%	0
	cryptochrome-1 [Xenopus tropicalis]	NP_001017311.2	656	93%	0
	cryptochrome-1 [Xenopus laevis]	NP_001081129.1	656	93%	0
	PREDICTED: cryptochrome-1 [Xenopus laevis]	XP_018110342.1	654	93%	0
	cryptochrome circadian regulator 2 S homeolog [Xenopus laevis]	NP_001083936.1	634	92%	0
	cryptochrome 2a [Xenopus laevis]	NP_001082139.1	627	92%	0
	PREDICTED: LOW QUALITY PROTEIN: cryptochrome-1 [Nanorana parkeri]	XP_018413653.1	620	93%	0
	PREDICTED: cryptochrome-2 [Nanorana parkeri]	XP_018410013.1	619	92%	0
	PREDICTED: cry1 protein isoform X1 [Xenopus laevis]	XP_018100773.1	572	92%	0
	Cry1 protein [Xenopus laevis]	NP_001088990.1	572	92%	0
	cryptochrome 4 [Xenopus tropicalis]	NP_001123706.1	569	98%	0
	PREDICTED: cryptochrome-2 [Xenopus tropicalis]	XP_002934138.2	567	83%	0
	PREDICTED: cryptochrome 4 isoform X1 [Xenopus tropicalis]	XP_012812443.1	563	98%	0
CPD photolyase-like L homeolog [Xenopus laevis]	CPD photolyase-like L homeolog [Xenopus laevis]	NP_001089127.1	1165	100%	0
	PREDICTED: CPD photolyase-like L homeolog isoform X1 [Xenopus laevis]	XP_018096830.1	1164	100%	0
	PREDICTED: CPD photolyase-like L homeolog isoform X2 [Xenopus laevis]	XP_018096831.1	1164	100%	0
	PREDICTED: deoxyribodipyrimidine photo-lyase-like [Nanorana parkeri]	XP_018427648.1	912	97%	0

	PREDICTED: deoxyribodipyrimidine photo-lyase-like [Xenopus tropicalis]	XP_017949882.1	343	30%	3.00E-116
	CPD photolyase-like [Xenopus tropicalis]	NP_001135721.1	262	27%	6.00E-85
Cryptochrome-1 [Xenopus laevis]					
	cryptochrome-1 [Xenopus laevis]	NP_001081129.1	1285	100%	0
	cryptochrome-1 [Xenopus tropicalis]	NP_001017311.2	1254	100%	0
	PREDICTED: cryptochrome-1 [Xenopus laevis]	XP_018110342.1	1177	100%	0
	PREDICTED: LOW QUALITY PROTEIN: cryptochrome-1 [Nanorana parkeri]	XP_018413653.1	1130	100%	0
	cryptochrome 2a [Xenopus laevis]	NP_001082139.1	870	85%	0
	cryptochrome circadian regulator 2 S homeolog [Xenopus laevis]	NP_001083936.1	867	87%	0
	PREDICTED: cryptochrome-2 [Nanorana parkeri]	XP_018410013.1	857	85%	0
	PREDICTED: cryptochrome-2 [Xenopus tropicalis]	XP_002934138.2	788	75%	0
	6-4 photolyase [Xenopus laevis]	NP_001081421.1	656	79%	0
	uncharacterized protein LOC100144974 [Xenopus tropicalis]	NP_001120012.1	649	82%	0
	PREDICTED: cryptochrome-1-like [Nanorana parkeri]	XP_018420471.1	629	83%	0
	PREDICTED: cry1 protein isoform X1 [Xenopus laevis]	XP_018100773.1	584	79%	0
	Cry1 protein [Xenopus laevis]	NP_001088990.1	584	79%	0
	cryptochrome 4 [Xenopus tropicalis]	NP_001123706.1	577	79%	0
	PREDICTED: cryptochrome 4 isoform X1 [Xenopus tropicalis]	XP_012812443.1	572	79%	0
Cryptochrome circadian regulator 2 S homeolog [Xenopus laevis]					
	cryptochrome circadian regulator 2 S homeolog [Xenopus laevis]	NP_001083936.1	1186	100%	0
	cryptochrome 2a [Xenopus laevis]	NP_001082139.1	1103	100%	0
	PREDICTED: cryptochrome-2 [Nanorana parkeri]	XP_018410013.1	1019	100%	0
	PREDICTED: cryptochrome-2 [Xenopus tropicalis]	XP_002934138.2	996	90%	0

	cryptochrome-1 [Xenopus laevis]	NP_001081129.1	867	95%	0
	PREDICTED: cryptochrome-1 [Xenopus laevis]	XP_018110342.1	864	93%	0
	cryptochrome-1 [Xenopus tropicalis]	NP_001017311.2	861	88%	0
	PREDICTED: LOW QUALITY PROTEIN: cryptochrome-1 [Nanorana parkeri]	XP_018413653.1	815	88%	0
	6-4 photolyase [Xenopus laevis]	NP_001081421.1	634	85%	0
	uncharacterized protein LOC100144974 [Xenopus tropicalis]	NP_001120012.1	627	85%	0
	PREDICTED: cryptochrome-1-like [Nanorana parkeri]	XP_018420471.1	613	85%	0
	PREDICTED: cry1 protein isoform X1 [Xenopus laevis]	XP_018100773.1	559	84%	0
	Cry1 protein [Xenopus laevis]	NP_001088990.1	559	84%	0
	cryptochrome 4 [Xenopus tropicalis] 556 0.0 54%	NP_001123706.1	556	85%	
	PREDICTED: cryptochrome 4 isoform X1 [Xenopus tropicalis]	XP_012812443.1	553	85%	
Cryptochrome 4 [Xenopus tropicalis]	cryptochrome 4 [Xenopus tropicalis]	NP_001123706.1	1169	100%	0
	PREDICTED: cryptochrome 4 isoform X1 [Xenopus tropicalis]	XP_012812443.1	1162	100%	0
	PREDICTED: cry1 protein isoform X1 [Xenopus laevis]	XP_018100773.1	1064	100%	0
	Cry1 protein [Xenopus laevis]	NP_001088990.1	1064	100%	0
	cryptochrome-1 [Xenopus laevis]	NP_001081129.1	577	87%	0
	cryptochrome-1 [Xenopus tropicalis]	NP_001017311.2	574	87%	0
	PREDICTED: cryptochrome-1 [Xenopus laevis]	XP_018110342.1	572	87%	0
	6-4 photolyase [Xenopus laevis]	NP_001081421.1	569	96%	0
	uncharacterized protein LOC100144974 [Xenopus tropicalis]	NP_001120012.1	566	89%	0
	cryptochrome 2a [Xenopus laevis]	NP_001082139.1	558	87%	0
	cryptochrome circadian regulator 2 S homeolog [Xenopus laevis]	NP_001083936.1	556	87%	0

	PREDICTED: cryptochrome-2 [Nanorana parkeri]	XP_018410013.1	554	87%	0
	PREDICTED: cryptochrome-1-like [Nanorana parkeri]	XP_018420471.1	549	86%	0
	PREDICTED: LOW QUALITY PROTEIN: cryptochrome-1 [Nanorana parkeri]	XP_018413653.1	545	89%	0
Cryptochrome DASH [Xenopus laevis]	Cryptochrome DASH [Xenopus laevis]	NP_001084438.1	1093	100%	0
	PREDICTED: cryptochrome DASH [Nanorana parkeri]	XP_018408992.1	943	100%	0
	PREDICTED: LOW QUALITY PROTEIN: cryptochrome DASH-like [Xenopus tropicalis]	XP_012820544.1	818	100%	0

Tabela 3. Todas as sequências de transcritos obtidas por similaridade a partir de cada sequência de consulta usando a ferramenta TBLASTN , sem repetições. Estas sequências de RNA primário passaram pela análise do Transdecoder para manutenção apenas de regiões codificantes.

Sequência de consulta	Resultados	Nº de acesso	*Score*	Cobertura	*E*-value
6-4 photolyase [Xenopus laevis]	TSA: Polypedates megacephalus comp58400_c0 transcribed RNA sequence	GEGH01033891.1	956	100%	0
	TSA: Rana catesbeiana contig-159444 transcribed RNA sequence	GDDO01042491.1	951	100%	0
	TSA: Dryophytes cinereus TR804319_c0_g1_i10 transcribed RNA sequence	GENE01043012.1	949	100%	0
	TSA: Odorrana margaretae comp92855_c0 transcribed RNA sequence	GEGJ01008314.1	946	100%	0
	TSA: Hynobius retardatus mRNA, contig: comp181653_c0_seq1, mRNA sequence	LE143480.1	943	100%	0
	TSA: Ambystoma maculatum c446684_g1_i1 transcribed RNA sequence	GFMY01065621.1	938	100%	0
	TSA: Rhinella marina Rm22464d7460467t2 transcribed RNA sequence	GFMT01018198.1	934	93%	0
	TSA: Ambystoma mexicanum A-MEXTC_0340000012721 transcribed RNA sequence	GFZP01123555.1	929	100%	0
	TSA: Leptobrachium boringii comp40268_c0 transcribed RNA sequence	GEGK01041188.1	919	99%	0
	TSA: Oreobates cruralis Unigene150829_c4_g2_i1_Oreobates_cruralis transcribed RNA sequence	GFNJ01017291.1	703	72%	0
	TSA: Bombina variegata variegata, contig c15188_g1_i1, transcribed RNA sequence	HADR01012715.1	656	93%	0
	TSA: Bombina bombina, contig c22651_g1_i2, transcribed RNA sequence	HADQ01021572.1	656	93%	0
	TSA: Bombina orientalis, contig c28403_g2_i1, transcribed RNA sequence	HADT01029591.1	655	93%	0
	TSA: Pelophylax nigromaculatus comp51682_c2	GEGI01005372.1	652	93%	0

	transcribed RNA sequence				
	TSA: Tylototriton wenxianensis Tw_m.19227 transcribed RNA sequence	GESS01043110.1	649	92%	0
	TSA: Rhacophorus dennysi comp56514_c1 transcribed RNA sequence	GEGG01061150.1	647	93%	0
	TSA: Hynobius chinensis comp55479_c0_seq1 transcribed RNA sequence	GAQK01097722.1	399	42%	1.00E-135
	TSA: Rana clamitans Lithobates.clamitans_contig_6299 mRNA sequence	GAEG01006299.1	301	50%	1.00E-95
	TSA: Odorrana margaretae comp78368_c0 transcribed RNA sequence	GEGJ01048240.1	273	43%	9.00E-85
	TSA: Ambystoma tigrinum ATi_cds.comp27842_c2_seq1.m.15600 transcribed RNA sequence	GFLI01009102.1	248	41%	1.00E-76
	TSA: Bufotes viridis Unigene100616_Bufo_viridis transcribed RNA sequence	GDRL01071324.1	242	38%	1.00E-74
CPD photolyase-like L homeolog [Xenopus laevis]	TSA: Pelophylax nigromaculatus comp50783_c0 transcribed RNA sequence	GEGI01021429.1	903	94%	0
	TSA: Rhinella marina Rm2227d9340907t7 transcribed RNA sequence	GFMT01022267.1	901	94%	0
	TSA: Bombina variegata variegata, contig c15755_g1_i1, transcribed RNA sequence	HADR01013115.1	899	94%	0
	TSA: Bombina orientalis, contig c46906_g1_i1, transcribed RNA sequence	HADT01052142.1	895	94%	0
	TSA: Leptobrachium boringii comp34429_c0 transcribed RNA sequence	GEGK01015219.1	894	99%	0
	TSA: Bombina bombina, contig c25276_g1_i2, transcribed RNA sequence	HADQ01025428.1	894	94%	0
	TSA: Bombina variegata scabra, contig c6078_g1_i1, transcribed RNA sequence	HADS01005325.1	889	94%	0
	TSA: Pseudacris regilla Pseudacris.regilla_contig_671 mRNA sequence	GAEI01000671.1	887	93%	0
	TSA: Oreobates cruralis Unigene150466_c1_g2_i9_Oreobates_cruralis transcribed	GFNJ01006097.1	886	94%	0

	RNA sequence				
	TSA: Rana catesbeiana contig-280574 transcribed RNA sequence	GDDO01102518.1	882	85%	0
	TSA: Ambystoma maculatum c479575_g2_i2 transcribed RNA sequence	GFMY01058775.1	868	85%	0
	TSA: Ambystoma mexicanum AMEXTC_0340000168533 transcribed RNA sequence	GFZP01161266.1	868	85%	0
	TSA: Tylototriton wenxianensis Tw_m.124841 transcribed RNA sequence	GESS01057049.1	867	86%	0
	TSA: Ambystoma mexicanum Ambymex_c1074295_g2_i1 transcribed RNA sequence	GFBM010733838.1	866	85%	0
	TSA: Hynobius retardatus mRNA, contig: comp186306_c2_seq1, mRNA sequence	LE160722.1	864	86%	0
	TSA: Polypedates megacephalus comp54851_c0 transcribed RNA sequence	GEGH01017630.1	862	99%	0
	TSA: Rhacophorus dennysi comp48612_c0 transcribed RNA sequence	GEGG01052580.1	855	85%	0
	TSA: Rana clamitans Lithobates.clamitans_contig_5162 mRNA sequence	GAEG01005162.1	649	65%	0
	TSA: Rhacophorus omeimontis comp199045_c2 transcribed RNA sequence	GEGF01035370.1	578	56%	0
	TSA: Bufotes viridis Unigene104222_Bufo_viridis transcribed RNA sequence	GDRL01074928.1	479	47%	3.00E-166
	TSA: Hynobius chinensis comp6716_c1_seq1 transcribed RNA sequence	GAQK01103477.1	415	38%	4.00E-141
cryptochrome-1 [Xenopus laevis]	TSA: Bombina bombina, contig c22651_g1_i2, transcribed RNA sequence	HADQ01021572.1	1180	100%	0
	TSA: Rana catesbeiana contig-302143 transcribed RNA sequence	GDDO01003453.1	1174	100%	0
	TSA: Polypedates megacephalus comp61682_c0 transcribed RNA sequence	GEGH01000038.1	1174	100%	0
	TSA: Bombina variegata variegata, contig c15188_g1_i1, transcribed RNA sequence	HADR01012715.1	1174	100%	0

TSA: Pelophylax nigromaculatus comp51682_c2 transcribed RNA sequence	GEGI01005372.1	1172	100%	0
TSA: Rhacophorus dennysi comp56514_c1 transcribed RNA sequence	GEGG01061150.1	1171	100%	0
TSA: Rhinella marina Rm23122d9381937t1 transcribed RNA sequence	GFMT01029465.1	1169	100%	0
TSA: Bombina orientalis, contig c28403_g2_i1, transcribed RNA sequence	HADT01029591.1	1169	100%	0
TSA: Leptobrachium boringii comp34550_c0 transcribed RNA sequence	GEGK01045838.1	1160	100%	0
TSA: Hynobius retardatus mRNA, contig: comp183139_c0_seq2, mRNA sequence	LE148515.1	1088	100%	0
TSA: Tylototriton wenxianensis Tw_m.19227 transcribed RNA sequence	GESS01043110.1	1071	99%	0
TSA: Ambystoma mexicanum Ambymex_c1071668_g2_i1 transcribed RNA sequence	GFBM010714201.1	885	84%	0
TSA: Dryophytes cinereus TR7961 14_c3_g2_i1 transcribed RNA sequence	GENE01035822.1	845	65%	5.00E-121
TSA: Odorrana margaretae comp93145_c0 transcribed RNA sequence	GEGJ01038093.1	835	85%	0
TSA: Ambystoma maculatum c451714_g1_i2 transcribed RNA sequence	GFMY01017149.1	805	77%	0
TSA: Rhacophorus omeimontis comp203387_c0 transcribed RNA sequence	GEGF01036638.1	768	68%	0
TSA: Oreobates cruralis Unigene146326_c0_g1_i1_Oreobates_cruralis transcribed RNA sequence	GFNJ01018085.1	715	67%	0
TSA: Ambystoma laterale ATTiL_cds.comp24688_c1_seq1.m.5792 transcribed RNA sequence	GFLO01003504.1	631	60%	0
TSA: Rana clamitans Lithobates.clamitans_contig_4836 mRNA sequence	GAEG01004836.1	447	41%	1.00E-127
TSA: Bufotes viridis Unigene100616_Bufo_viridis transcribed RNA sequence	GDRL01071324.1	420	33%	6.00E-143
TSA: Hynobius chinensis comp55787_c0_seq1	GAQK01098016.1	366	32%	8.00E-122

	transcribed RNA sequence				
	TSA: Ambystoma tigrinum A-Ti_cds.comp27842_c2_seq1.m.15600 transcribed RNA sequence	GFLI01009102.1	355	35%	3.00E-117
cryptochrome circadian regulator 2 S homeolog [Xenopus laevis]	TSA: Polypedates megacephalus comp60877_c0 transcribed RNA sequence	GEGH01018354.1	1009	100%	0
	TSA: Rhacophorus dennysi comp57075_c0 transcribed RNA sequence	GEGG01018958.1	999	98%	0
	TSA: Bombina bombina, contig c22646_g1_i3, transcribed RNA sequence	HADQ01021560.1	984	98%	0
	TSA: Rhinella marina Rm16915d1282795t2 transcribed RNA sequence	GFMT01061620.1	981	94%	0
	TSA: Odorrana margaretae comp93145_c0 transcribed RNA sequence	GEGJ01038093.1	975	96%	0
	TSA: Rana catesbeiana contig-60946 transcribed RNA sequence	GDDO01000735.1	974	95%	0
	TSA: Ambystoma mexicanum Ambmex_c1071668_g3_i1 transcribed RNA sequence	GFBM010714202.1	939	95%	0
	TSA: Hynobius retardatus mRNA, contig: comp183139_c0_seq1, mRNA sequence	LE148514.1	930	95%	0
	TSA: Bombina variegata variegata, contig c15188_g1_i1, transcribed RNA sequence	HADR01012715.1	835	89%	0
	TSA: Bombina orientalis, contig c28403_g2_i1, transcribed RNA sequence	HADT01029591.1	835	89%	0
	TSA: Tylototriton wenxianensis Tw_m.19227 transcribed RNA sequence	GESS01043110.1	825	92%	0
	TSA: Oreobates cruralis Unigene146326_c0_g1_i1_Oreobates_cruralis transcribed RNA sequence	GFNJ01018085.1	775	72%	0
	TSA: Ambystoma laterale AT-TiL_cds.comp24688_c1_seq1.m.5792 transcribed RNA sequence	GFLO01003504.1	659	65%	0
	TSA: Ambystoma maculatum c451714_g1_i2 trans-	GFMY01017149.1	634	64%	0

	cribed RNA sequence				
	TSA: Dryophytes cinereus TR804319_c0_g1_i1 transcribed RNA sequence	GENE01043011.1	618	84%	0
	TSA: Rhinella marina Rm22464d7460467t2 transcribed RNA sequence	GFMT01018198.1	613	86%	0
	TSA: Leptobrachium boringii comp40268_c0 transcribed RNA sequence	GEGK01041188.1	596	92%	0
	TSA: Rhacophorus omeimontis comp203387_c0 transcribed RNA sequence	GEGF01036638.1	565	54%	0
	TSA: Bombina variegata scabra, contig c215_g2_i1, transcribed RNA sequence	HADS01000188.1	532	52%	0
	TSA: Pelophylax nigromaculatus comp46923_c0 transcribed RNA sequence	GEGI01058063.1	491	42%	1.00E-170
	TSA: Rana clamitans Lithobates.clamitans_contig_6299 mRNA sequence	GAEG01006299.1	460	49%	3.00E-157
	TSA: Hynobius chinensis comp55787_c0_seq1 transcribed RNA sequence	GAQK01098016.1	410	37%	1.00E-139
	TSA: Ambystoma tigrinum A-Ti_cds.comp27842_c2_seq1.m.15600 transcribed RNA sequence	GFLI01009102.1	392	38%	2.00E-132
	TSA: Rana clamitans Lithobates.clamitans_contig_1042 mRNA sequence	GAEG01001042.1	322	37%	2.00E-99
	TSA: Bufotes viridis Unigene100616_Bufo_viridis transcribed RNA sequence	GDRL01071324.1	286	36%	4.00E-91
cryptochrome 4 [Xenopus tropicalis]	TSA: Dryophytes cinereus TR804319_c0_g1_i10 transcribed RNA sequence	GENE01043012.1	579	89%	0
	TSA: Rana catesbeiana contig-81 10 transcribed RNA sequence	GDDO01006067.1	578	89%	0
	TSA: Rhacophorus dennysi comp56514_c1 transcribed RNA sequence	GEGG01061150.1	577	89%	0
	TSA: Ambystoma maculatum c446684_g1_i1 transcribed RNA sequence	GFMY01065621.1	576	89%	0
	TSA: Polypedates megacephalus comp61682_c0 transcribed RNA sequence	GEGH01000038.1	575	89%	0

TSA: Pelophylax nigromaculatus comp51682_c2 transcribed RNA sequence	GEGI01005372.1	573	89%	0
TSA: Tylototriton wenxianensis Tw_m.19227 transcribed RNA sequence	GESS01043110.1	573	87%	0
TSA: Bombina bombina, contig c22651_g1_i2, transcribed RNA sequence	HADQ01021572.1	572	89%	0
TSA: Bombina variegata variegata, contig c15188_g1_i1, transcribed RNA sequence	HADR01012715.1	572	89%	0
TSA: Bombina orientalis, contig c28403_g2_i1, transcribed RNA sequence	HADT01029591.1	572	89%	0
TSA: Hynobius retardatus mRNA, contig: comp181653_c0_seq1, mRNA sequence	LE143480.1	572	95%	0
TSA: Polypedates megacephalus comp58400_c0 transcribed RNA sequence	GEGH01033891.1	571	88%	0
TSA: Leptobrachium boringii comp34550_c0 transcribed RNA sequence	GEGK01045838.1	568	89%	0
TSA: Odorrana margaretae comp92855_c0 transcribed RNA sequence	GEGJ01008314.1	565	86%	0
TSA: Rhinella marina Rm16915d1282795t2 transcribed RNA sequence	GFMT01061620.1	556	95%	0
TSA: Ambystoma mexicanum AMEXTC_0340000015558 transcribed RNA sequence	GFZP01003862.1	552	98%	0
TSA: Ambystoma laterale ATTiL_cds.comp24688_c1_seq1.m.5792 transcribed RNA sequence	GFLO01003504.1	397	66%	4.00E-132
TSA: Bombina variegata scabra, contig c215_g2_i1, transcribed RNA sequence	HADS01000188.1	333	40%	1.00E-106
TSA: Rana clamitans Lithobates.clamitans_contig_4836 mRNA sequence	GAEG01004836.1	330	39%	3.00E-89
TSA: Hynobius chinensis comp55787_c0_seq1 transcribed RNA sequence	GAQK01098016.1	276	33%	3.00E-87
TSA: Bufotes viridis Unigene93032_Bufo_viridis transcribed RNA sequence	GDRL01063749.1	235	26%	3.00E-72
TSA: Rhacophorus omeimontis comp190470_c0	GEGF01018072.1	225	46%	7.00E-67

	transcribed RNA sequence				
	TSA: Ambystoma tigrinum A-Ti_cds.comp27842_c0_seq1.m.15598 transcribed RNA sequence	GFLI01009101.1	215	36%	1.00E-63
cryptochrome DASH [Xenopus laevis]	TSA: Bombina variegata variegata, contig c3971_g1_i2, transcribed RNA sequence	HADR01003408.1	931	100%	0
	TSA: Rana catesbeiana CCH-0004-C_S3793690 transcribed RNA sequence	GFBS01155368.1	928	100%	0
	TSA: Polypedates megacephalus comp57652_c0 transcribed RNA sequence	GEGH01068563.1	925	100%	0
	TSA: Dryophytes cinereus TR693797_c0_g1_i1 transcribed RNA sequence	GENE01005796.1	916	99%	0
	TSA: Ambystoma maculatum c452068_g1_i2 transcribed RNA sequence	GFMY01077095.1	902	100%	0
	TSA: Hynobius chinensis comp10443_c0_seq1 transcribed RNA sequence	GAQK01031851.1	895	99%	0
	TSA: Rhinella marina Rm7139d4816037t9 transcribed RNA sequence	GFMT01019882.1	895	98%	0
	TSA: Hynobius retardatus mRNA, contig: comp229999_c0_seq1, mRNA sequence	LE206047.1	894	99%	0
	TSA: Tylototriton wenxianensis Tw_m.104743 transcribed RNA sequence	GESS01002028.1	893	100%	0
	TSA: Ambystoma mexicanum Ambmex_c1069709_g1_i1 transcribed RNA sequence	GFBM010700958.1	889	100%	0
	TSA: Leptobrachium boringii comp39991_c0 transcribed RNA sequence	GEGK01016386.1	886	98%	0
	SA: Bombina orientalis, contig c14493_g1_i1, transcribed RNA sequence	HADT01012028.1	793	86%	0
	TSA: Pelophylax nigromaculatus comp38773_c0 transcribed RNA sequence	GEGI01030788.1	748	79%	0
	TSA: Rhacophorus dennysi comp43909_c0 transcribed RNA sequence	GEGG01046252.1	543	58%	0
	TSA: Ambystoma laterale AT-TiL_cds.comp23022_c1_seq1.m.5016 transcribed	GFLO01002927.1	489	53%	2.00E-170

RNA sequence				
TSA: Bufotes viridis Unigene104856_Bufo_viridis transcribed RNA sequence	GDRL01075562.1	466	51%	4.00E-161
TSA: Bombina bombina, contig c34029_g1_i1, transcribed RNA sequence	HADQ01040819.1	434	46%	8.00E-149
TSA: Oreobates cruralis Unige-ne53867_c0_g1_i1_Oreobates_cruralis transcribed RNA sequence	GFNJ01046791.1	428	43%	5.00E-147
TSA: Ambystoma tigrinum ATi_cds.comp1 1938_c1_seq1.m.1558 transcribed RNA sequence	GFLI01000667.1	397	43%	5.00E-135
TSA: Ambystoma laterale AT-TiL_cds.comp17065_c0_seq1.m.2271 transcribed RNA sequence	GFLO01000935.1	390	45%	2.00E-131
TSA: Ambystoma texanum AT_cds.comp25061_c1_seq1.m.1 1281 transcribed RNA sequence	GFLJ01006804.1	298	30%	5.00E-97
TSA: Pseudacris regilla Pseuda-cris.regilla_contig_26054 mRNA sequence	GAEI01026054.1	293	27%	5.00E-70
TSA: Bombina variegata scabra, contig c9706_g1_i1, transcribed RNA sequence	HADS01008717.1	243	26%	4.00E-76
TSA: Rhacophorus omeimontis comp158767_c0 transcribed RNA sequence	GEGF01022499.1	234	24%	1.00E-72

4.3.3 Ocorrência das enzimas em anfíbios

Um apanhado geral para verificação de presença e ausência de fotoliases e criptocromos nas espécies de anfíbios avaliadas foi feito utilizando as **Tabelas 2** e **3**. Os resultados gerais encontram-se na **Tabela 4**. De forma complementar, a **Figura 4** demonstra graficamente a porcentagem de espécies de anfíbios que apresentam cada tipo de proteína, bem como uma relação entre espécies e quantidade de proteínas da família presentes.

Tabela 4 – Análise de ocorrência das proteínas da família das fotoliases e criptocromos em espécies de anfíbios de diferentes famílias, com base nos métodos utilizados. Quadro verde: proteína presente; Quadro branco: proteína ausente; Quadros amarelos (letra a): uma mesma sequência pode ser mais de um tipo de proteína.

Amphibian family	**Species**	**CPD PHR**	**6-4 PHR**	**CRY-DASH**	**CRY1**	**CRY2**	**CRY4**
Hynobiidae	*H. chinensis*						
	H. retardatus						
Ambystomatidae	*A. mexicanum*						
	A. maculatum						
	A. tigrinum		a		a	a	
	A. laterale						
	A. texanum						
Salamandridae	*T. wenxianensis*						
Bombinatoridae	*B. bombina*						
	B.orientalis						
	B. v. variegata						
	B.v. scabra						
Pipidae	*X. laevis*						
	X. tropicalis						
Megophryidae	*L. boringii*						
Hylidae	*P. regilla*						
	D. cinereus						
Bufonidae	*B. viridis*		a		a	a	
	R. marina						
Hylodidae	*O. cruralis*						
Ranidae	*N. parkeri*						
	L. clamitans						
	L. catesbiana						
	P. nigromaculatus						
	O. margaretae						
Rhacophoridae	*R. omeimontis*						

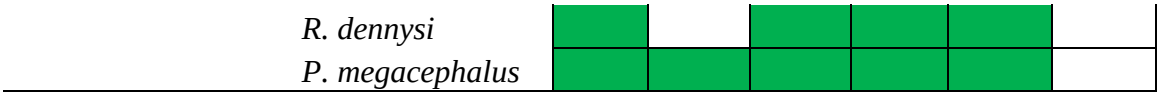

Figura 4 – Ocorrência de fotoliases e criptocromos em anfíbios. **(A)** Porcentagem de espécies de anfíbios que apresentam cada tipo de proteína. **(B)** Relação entre espécies e quantidade de proteínas da família presentes.

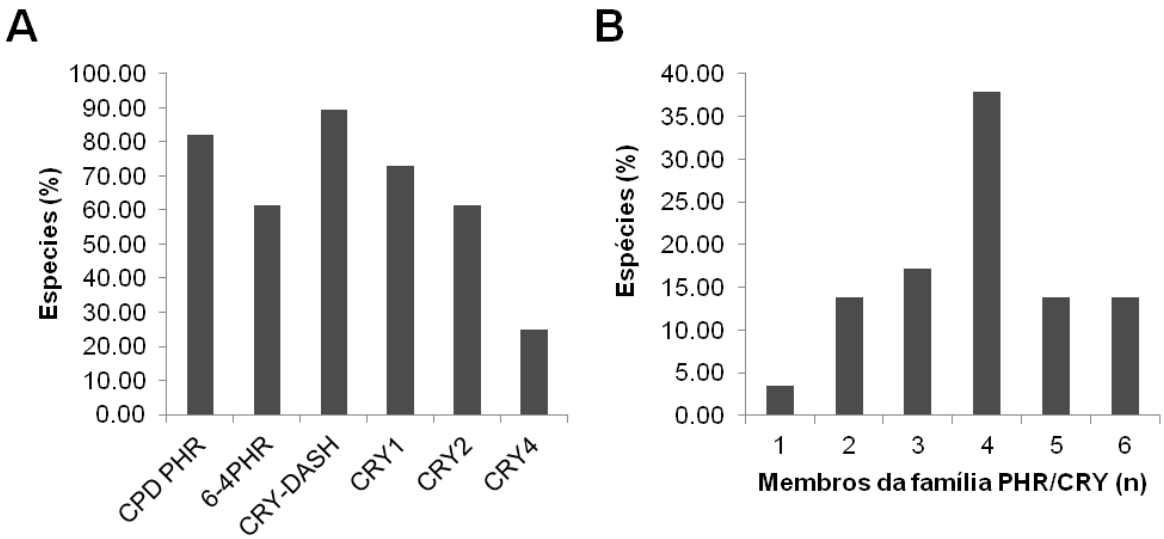

4.4 DISCUSSÃO

Sequências anotadas de *Xenopus laevis* e *X. tropicalis* foram utilizadas para a realização de buscas *in silico* por sequências homólogas em outras espécies de anfíbios. Os resultados das buscas permitiram o cálculo da porcentagem de espécies de anfíbios que apresentam cada tipo de proteína da família das fotoliases e criptocromos homólogas às sequências de *Xenopus* sp. Sequências homólogas à CRY-DASH, CPD PHR, CRY1, CRY2, 6-4 PHR e CRY4 de *Xenopus* sp. foram encontradas nas espécies de anfíbios nas respectivas porcentagens: 89, 82, 73, 61, 61 e 25%. Além disso, foi verificado que 38% das espécies analisadas apresentavam quatro tipos de proteínas homólogas à *Xenopus* sp, embora outras espécies apresentaram um (3%), dois (14%), três (17%), cinco (14%) ou seis (14%) tipos ao mesmo tempo. É importante ressaltar que algumas sequências apresentaram valores de *score* e de cobertura de sequência relativamente baixos em comparação com sequências de outras espécies. Isto pode significar que houve uma maior divergência destas sequências com as sequências consulta de *Xenopus* sp., ou que a sequência encontrada não corresponde exatamente do mesmo tipo de proteína de *Xenopus* sp., ou que a sequência não corresponde a um membro da família PHR/CRY, sendo um falso positivo. Adicionalmente, os resultados do

BLASTP indicam fortemente que as sequências “uncharacterized protein LOC100144974” de *Xenopus tropicalis,* e “PREDICTED; crypochrome-1-like” de *Nanorana parkeri* são na verdade sequências de 6-4 PHR; e que as sequências “PREDICTED: cry1 protein isoform X1” e “Cry1 protein” de *Xenopus laevis* são na verdade sequências de CRY4. Estas sequências foram interpretadas e contabilizadas na **Tabela 4** levando em consideração os resultados do BLASTP a partir de *Xenopus* sp., e não os seus nomes, que podem ter sido anotados erroneamente.

4.5 PERSPECTIVAS

É conhecido que os bancos de dados apresentam sequências com anotações incorretas, em sua maioria baseadas apenas em análises de similaridade. Homologia entre proteínas significa simplesmente que elas possuem uma origem evolutiva comum. Sequências similares de proteínas frequentemente conduzem funções similares, mas similaridade entre proteínas não garante a conservação da função entre elas. Em alguns casos, pequenas diferenças nas sequências podem causar mudanças radicais nas propriedades funcionais, tais como uma mudança na ação enzimática, ou mesmo perda ou ganho de atividade enzimática (LEE et al., 2007; HINZ e THE UNIPROT CONSORTIUM, 2010). Desta forma, predições *in silico* da estrutura 3D e da função a partir das sequências primárias de fotoliases e criptocromos de anfíbios serão conduzidas. Além disso, análises filogenéticas e outras análises estruturais dos genes e proteínas serão realizadas, com o intuito de dar suporte para as predições de estrutura 3D e função das enzimas. Com estes objetivos cumpridos, começaremos nossa análise principal: predizer a eficiência das funções desempenhadas pelas fotoliases e criptocromos de anfíbios. Análises dos resíduos catalíticos e mutações guiadas em aminoácidos terão papel principal para atingir este objetivo. A seguir estão apresentados em detalhes os métodos que serão utilizados.

4.5.1 Edição de sequência

Inicialmente, todas as sequências repetidas serão removidas. Considerando que sequências TSA são sequências de RNA primário e que serão realizadas comparações entre estas sequências com sequências de proteínas obtidas a partir do BLASTP, regiões não codificantes das sequências TSA (RNA primário) serão deletadas utilizando a ferramenta Transdecoder (https://github.com/TransDecoder/TransDecoder/wiki). Serão realizados alinhamentos e comparações destas sequências com sequências de DNA codificantes das

sequências de consulta. As sequências de TSA editadas serão alinhadas e convertidas para sequências proteicas com auxílio do programa MEGA7 (KUMAR et al., 2016).

4.5.2 Análise filogenética

Três tipos de análises filogenéticas serão conduzidos com todas as sequências juntas nos respectivos softwares/ferramentas: Neighboor-Joinning (MEGA), Bayesiana (Beast ou Mr. Bays) e Máxima Verossimilhança (RaxML) (YANG e RANNALA, et al., 2012). As sequências de TSA modeladas pelo Transdecoder serão incorporadas por similaridade juntamente com as sequências referência de proteínas (RSP).

4.5.3 Análise estrutural primária de genes e proteínas

Análises da estrutura de éxon e íntrons dos genes da família PHR/CRY serão conduzidas a partir de sequências dos genomas completos de *X. laevis*, *X. tropicalis* e *N. parkeri*, utilizando o servidor GSDS 2.0 (HU et al., 2014). Os números de éxons e íntrons serão tabelados, bem como as posições nucleotídicas de cada uma destas partes nos genes (exemplo: Éxon 1: nucleotídeos 40-75) e o tamanho dos genes. Além disso, a arquitetura de domínios e as regiões conservadas serão avaliadas nas sequências gênicas e proteicas com o auxílio dos servidores SMART e CDD-NCBI (MARCHLER-BAUER et al., 2014; LETUNIC e BORK, 2017). O software Jalview 2 será utilizado para gerar um diagrama de alinhamento de sequências múltiplas (WATERHOUSE et al., 2009), a fim de verificar a (1) conservação físico-química dos aminoácidos, (2) a sequência consenso, além de (3) melhor caracterizar a estrutura de domínios de cada proteína com o suporte das ferramentas SMART e CDD-NCBI. Cada sequência referência de consulta (por exemplo, *Xenopus laevis* CPD PHR) e suas respectivas sequências proteicas homólogas obtidas com o BLASTP and TBLASTN serão alinhadas no software Jalview 2, assim como todas as sequências proteicas da família inteira, afim de verificar a similaridade entre sequências e resíduos conservados.

O servidor Prot Param (Expasy) será usado para estudar caracteres físico-químicos basais de fotoliases e criptocromos de anfíbios, a partir de suas sequências primárias (GASTEIGER et al., 2005). A estabilidade das proteínas será avaliada a partir de diferentes variáveis tais como: ponto teórico isoelétrico (pI), peso molecular, fórmula molecular, número total de resíduos positivos e negativos, índice de instabilidade (GURUPRASAD et al., 1990), índice alifático (IKAI, 1980) e hidropaticidade média (KYTE e DOOLITHE, 1982).

4.5.4 Análise da estrutura secundária

Elementos de estrutura secundária das proteínas serão determinados usando os servidores *online* Phyre2 e I-TASSER (KELLEY et al., 2015; YANG et al., 2015).

4.5.5 Predição de modelo 3D

A estrutura 3D das proteínas será modelada usando os servidores *online* I-TASSER e SWISS-MODEL (YANG et al., 2015a; YANG et al., 2015b; WATERHOUSE et al., 2018). As sequências primárias de aminoácidos serão carregadas no formato FASTA nos servidores. Os resultados gerarão modelos principais para cada entrada. O modelo que apresentar o melhor ranqueamento será selecionado.

4.5.6 Validação do modelo 3D

A visualização será realizada pelo software PyMOL (DELANO, 2002). Erros estruturais rastreáveis serão corrigidos e a carga global substituída no software Vega ZZ (PEDRETTI et al., 2004). Os gráficos de Ramachandran serão calculados através do software RAMPAGE Ramachandran Plot Assessment (LOVELL et al., 2003). O índice de hidropaticidade será calculado pelo software Marvin (http://www.chemaxon.com). A dinâmica molecular será realizada pelos softwares GROMACS e VMD (HUMPHREY et al., 1996; ABRAHAM et al., 2014). O formato do arquivo PDB será analisado em algorítmo de dinâmica molecular de abordagens MD, e será feita a otimização da geometria, conforme SAMRIZ e OFOGHI (2016).

4.5.7 Análise de simulação

Após o término da simulação, os dados de saída serão analisados de acordo com a energia (energia cinética, potencial e total), desvio da raiz quadrada média (RMSD), raio de rotação e formação/deformação da ligação H (SAMRIZ e OFOGHI, 2016).

4.5.8 Predição de função proteica

Características da sequência e estrutura ajudam a predizer a função de uma proteína. Por exemplo, resíduos que se ligam ao DNA compartilham características físico-químicas e estruturais comuns na maioria das proteínas ligantes de DNA. No entanto, resíduos funcionais podem não ser perfeitamente conservados em proteínas de função similar. Além disso, pequenas alterações ou perturbações do núcleo 3D de um sítio ativo de uma arquitetura estruturada conservada de uma proteína deverão gerar uma séria consequência no

funcionamento desta macromolécula (LEE et al., 2007; HINZ e THE UNIPROT CONSORTIUM, 2010). Desta foram análises funcionais posteriores são também necessárias para uma melhor caracterização enzimática.

A função das proteínas serão preditas utilizando os servidores *online* I-TASSER e ProFunc. O servidor I-TASSER é um dos sistemas *online* mais usados para predição de estrutura proteica e anotação de função baseada na estrutura (YANG et al., 2015a; YANG et al., 2015b). Iniciando a partir da sequência de aminoácidos, o I-TASSER constrói modelos estruturais 3D e percepções biológicas da proteína alvo são deduzidas através da combinação dos modelos estruturais com proteínas conhecidas nos bancos de dados funcionais. O banco de dados funcional BioLiP será utilizado como banco de dados base para predições de função biológica (YANG et al., 2013; YANG et al., 2015a).

O servidor ProFunc (LASKOWSKI et al., 2005) será utilizado de forma complementar ao I-TASSER. A partir da adição de arquivo com proteína com estrutura 3D – no formato PDB gerado pelo SWISS-MODEL e I-TASSER – no servidor *online* ProFunc é possível determinar a função da proteína. O ProFunc combina buscas por BLAST e HMM com análises baseadas no modelo 3D e análises de fissuras superficiais, para identificar proteínas similares, que forneçam sinais da função da proteína que está sendo consultada (LASKOWSKI et al., 2005; LEE et al., 2007).

4.5.9 Mutações guiadas

Trabalhos estruturais com macromoléculas podem ser melhor fundamentados com a adição de análises mutacionais guiadas. A mutação de resíduos pode ser informativa para testar o papel e a importância de um determinado resíduo para o funcionamento de uma enzima. Desta forma, resíduos serão mutados sob o auxílio do método SNAP, o qual quantifica consequências funcionais de substituições de um único aminoácido (BROMBERG e ROST, 2008; BROMBERG et al., 2009).

5 DISCUSSÃO GERAL

Nesta dissertação, três frentes foram utilizadas para avaliar a importância do fotorreparo de DNA em espécies de anfíbios: (1) uma revisão da literatura existente sobre o impacto da radiação UV solar em anfíbios, tendo como foco as respostas biológicas destes animais aos danos de DNA induzidos, as quais incluem a capacidade de fotorreparo de DNA; (2) Um estudo experimental controlado que avaliou a importância do fotorreparo de DNA para a manutenção do desempenho alimentar de girinos especialistas florestais expostos à radiação UVB; e (3) um estudo que tem como objetivo compreender as bases moleculares subjacentes ao fotorreparo de DNA de anfíbios, através de uma caracterização computacional dos genes e proteínas das enzimas fotoliases de diferentes espécies de anfíbios.

A revisão da literatura (primeira frente) destaca o papel da estabilidade genômica no funcionamento celular e sistêmico em anfíbios, o qual pode ser comprometido pelos efeitos genotóxicos da radiação UV solar. Justamente o efeito prejudicial mais relevante da exposição à luz solar, a indução de danos de DNA (SCHUCH et al., 2017), foi medido diretamente em espécies de anfíbios em apenas três estudos. Como consequência, o fotorreparo de DNA, e outras vias de atenuação dos efeitos genotóxicos da radiação UV, são pobremente compreendidos nestes organismos.

A segunda frente enfatiza a susceptibilidade de espécies de anfíbios especialistas florestais à genotoxicidade induzida pela radiação solar e contribui para o entendimento do processo de peso observado em girinos expostos à radiação UVB. Nosso modelo experimental, *Boana curupi* é uma espécie restrita a pequenos fragmentos florestais remanescentes de Mata Atlântica da porção sul, onde os raios UV praticamente não alcançam seus sítios reprodutivos (LIPINSKI et al., 2016; LONDERO et al., 2018). Os resultados sugerem que esta espécie é extremamente sensível à radiação solar, possivelmente devido a ineficiência do mecanismo de fotorreparo de DNA, uma vez que mesmo girinos irradiados com radiação UVB e submetidos a um tratamento adicional de fotorreparo apresentaram instabilidade genômica, perda de peso e redução no consumo de alimento. Por outro lado, girinos de *Boana pulchella*, expostos a uma maior dose de radiação UVB e submetidos ao mesmo tratamento adicional de fotorreparo, conseguiram recuperar um pouco do peso corporal (SCHUCH et al., 2015b). A redução do desempenho alimentar em girinos expostos à radiação UVB foi registrado pela primeira vez na literatura através do nosso estudo com *Boana curupi*.

A terceira frente destaca a importância da compreensão das bases moleculares subjacentes ao fotorreparo de DNA e inicia uma caracterização computacional dos genes e

proteínas da família das fotoliases e criptocromos de anfíbios. Sequências homólogas à CRY-DASH, CPD PHR, CRY1, CRY2, 6-4 PHR e CRY4 de *Xenopus* sp. foram encontradas em 28 espécies de anfíbios nas respectivas porcentagens: 89, 82, 73, 61, 61 e 25%. Foi verificado que 38% das espécies analisadas apresentam quatro tipos de proteínas homólogas à *Xenopus sp*, embora outras espécies apresentaram um (3%), dois (14%), três (17%), cinco (14%) ou seis (14%) tipos ao mesmo tempo. É importante ressaltar que análises estruturais e funcionais deverão ser realizadas para complementar os dados de similaridade. A precisão de técnicas *in silico* tem avançado consideravelmente nos últimos anos, de forma a predizer aspectos evolutivos, estruturais e funcionais de moléculas com grau de fidedignidade alto, tendo como base apenas sequências primárias (nucleotídeos ou aminoácidos) (LEE et al., 2007; HINZ e THE UNIPROT CONSORTIUM, 2010). Como perspectiva, a família das fotoliases e criptocromos de anfíbios será estudada utilizando as sequências obtidas, através de análises filogenéticas, estruturais e funcionais. Espera-se que a caracterização *in silico* da família das fotoliases em espécies de anfíbios seja referência para futuras pesquisas na área de reparo de DNA de anfíbios e lance luz a novas hipóteses, uma vez que vários aspectos da família das fotoliases e criptocromos ao longo da árvore da vida são controversos e desconhecidos ainda (MÜLLER e CARELL, 2009).

6 CONCLUSÃO

Em teoria, o fotorreparo de DNA é o principal e mais eficiente mecanismo para reparar as lesões de DNA induzidas pela radiação UV solar em anfíbios, porém na prática, existem variações interespecíficas na eficiência deste mecanismo. De fato, nosso modelo experimental para girinos especialistas florestais apresentou, através de medidas de desempenho alimentar e análise citogenética, uma baixa eficiência do fotorreparo. Os efeitos da radiação UV solar em anfíbios têm sido relativamente bem estudados, no entanto, os danos de DNA, principal consequência da irradiação de sistemas biológicos à UV, e seus mecanismos atenuadores têm sido muito pobremente avaliados nestes organismos. Portanto, a contribuição da radiação UV solar no declínio de anfíbios e a importância do fotorreparo de DNA para evitar os efeitos genotóxicos da UV em espécies de anfíbios pode se tornar mais evidente em um futuro próximo. Experimentos *in vivo*, *in vitro* e *in silico* (como demonstrado aqui) são bem-vindos para uma melhor compreensão deste mecanismo de reparo de DNA em espécies de anfíbios. A caracterização computacional dos genes e proteínas da família das fotoliases de anfíbios ampliará a compreensão das bases moleculares subjacentes ao fotorreparo de DNA nestes organismos.

REFERÊNCIAS

ABRAHAM, M. J. et al. the GROMACS development team. **GROMACS user manual version**, v. 5, n. 2, 2014.

ALTIG, R.; MCDIARMID, R. W. (Ed.). **Tadpoles: the biology of anuran larvae**. University of Chicago Press, 1999.

ALTON, L. A. et al. The energetic cost of exposure to UV radiation for tadpoles is greater when they live with predators. **Functional Ecology**, v. 26, n. 1, p. 94-103, 2012.

ALTON, L. A.; FRANKLIN, C. E. Drivers of amphibian declines: effects of ultraviolet radiation and interactions with other environmental factors. **Climate Change Responses**, v. 4, n. 1, p. 6, 2017.

ANFINSEN, C. B. Principles that govern the folding of protein chains. **Science**, v. 181, n. 4096, p. 223-230, 1973.

BLAUSTEIN, A. R. et al. Effects of ultraviolet radiation on amphibians: field experiments. **American Zoologist**, v. 38, n. 6, p. 799-812, 1998.

BLAUSTEIN, A. R. et al. UV repair and resistance to solar UV-B in amphibian eggs: a link to population declines?. **Proceedings of the National Academy of Sciences**, v. 91, n. 5, p. 1791-1795, 1994.

BLAUSTEIN, A. R.; BELDEN, L. K. Amphibian defenses against ultraviolet-B radiation. **Evolution & Development**, v. 5, n. 1, p. 89-97, 2003.

BROMBERG, Y. et al. In silico mutagenesis: a case study of the melanocortin 4 receptor. **The FASEB Journal**, v. 23, n. 9, p. 3059-3069, 2009.

BROMBERG, Y.; ROST, B.. Comprehensive in silico mutagenesis highlights functionally important residues in proteins. **Bioinformatics**, v. 24, n. 16, p. i207-i212, 2008.

CHAVES, I. et al. Functional evolution of the photolyase/cryptochrome protein family: importance of the C terminus of mammalian CRY1 for circadian core oscillator performance. **Molecular and Cellular Biology**, v. 26, n. 5, p. 1743-1753, 2006.

CHAVES, I. et al. The cryptochromes: blue light photoreceptors in plants and animals. **Annual Review of Plant Biology**, v. 62, p. 335-364, 2011.

DELANO, W. L. The PyMOL molecular graphics system. **http://www.pymol.org**, 2002.

DODD, A. N. et al. Plant circadian clocks increase photosynthesis, growth, survival, and competitive advantage. **Science**, v. 309, n. 5734, p. 630-633, 2005.

DUELLMAN, W. E.; TRUEB, L. **Biology of amphibians**. JHU press, 1994.

FERSHT, A. **Structure and mechanism in protein science: a guide to enzyme catalysis and protein folding**. Macmillan, 1999.

FRIEDBERG, E. C. DNA damage and repair. **Nature**, v. 421, n. 6921, p. 436, 2003.

GASTEIGER, E. et al. Protein identification and analysis tools on the ExPASy server. In: **The Proteomics Protocols Handbook**. Humana press, 2005. p. 571-607.

GOVERNO DO ESTADO DO RIO GRANDE DO SUL: **Decreto N° 51.797, de 8 de setembro de 2014**. Declara as Espécies da Fauna Silvestre Ameaçadas de Extinção no Estado do Rio Grande do Sul, 2014.

GRANT, B. J.; GORFE, A. A.; MCCAMMON, J. A. Ras conformational switching: simulating nucleotide-dependent conformational transitions with accelerated molecular dynamics. **PLoS Computational Biology**, v. 5, n. 3, p. e1000325, 2009.

GURUPRASAD, K.; REDDY, B.V.B.; PANDIT, M. W. Correlation between stability of a protein and its dipeptide composition: a novel approach for predicting in vivo stability of a protein from its primary sequence. **Protein Engineering, Design and Selection**, v. 4, n. 2, p. 155-161, 1990.

HÄDER, D-P. et al. Effects of UV radiation on aquatic ecosystems and interactions with other environmental factors. **Photochemical & Photobiological Sciences**, v. 14, n. 1, p. 108-126, 2015.

HELLSTEN, U. et al. The genome of the Western clawed frog *Xenopus tropicalis*. **Science**, v. 328, n. 5978, p. 633-636, 2010.

HINZ, U; THE UNIPROT CONSORTIUM. From protein sequences to 3D-structures and beyond: the example of the UniProt knowledgebase. **Cellular and Molecular Life Sciences**, v. 67, n. 7, p. 1049-1064, 2010.

HORAK, E.; FARRÉ, E. M. The regulation of UV-B responses by the circadian clock. **Plant Signaling & Behavior**, v. 10, n. 5, p. e1000164, 2015.

HU, B. et al. GSDS 2.0: an upgraded gene feature visualization server. **Bioinformatics**, v. 31, n. 8, p. 1296-1297, 2014.

HUMPHREY, W.; DALKE, A.; SCHULTEN. VMD: visual molecular dynamics. **Journal of molecular graphics**, v. 14, n. 1, p. 33-38, 1996.

IKAI, A. Thermostability and aliphatic index of globular proteins. **The Journal of Biochemistry**, v. 88, n. 6, p. 1895-1898, 1980.

INTERNATIONAL UNION FOR CONSERVATION OF NATURE. The IUCN Red List of Threatened Species. Version 2018–2. 2018. http://www.iucnredlist.org.

KAO, Y-T. et al. Femtochemistry in enzyme catalysis: DNA photolyase. **Cell Biochemistry and Biophysics**, v. 48, n. 1, p. 32-44, 2007.

KAVAKLI, I. H.et al. The photolyase/cryptochrome family of proteins as DNA repair enzymes and transcriptional repressors. **Photochemistry and Photobiology**, v. 93, n. 1, p. 93-103, 2017.

KELLEY, L. A. et al. The Phyre2 web portal for protein modeling, prediction and analysis. **Nature Protocols**, v. 10, n. 6, p. 845, 2015.

KUMAR, S.; STECHER, G.; TAMURA, K. MEGA7: molecular evolutionary genetics analysis version 7.0 for bigger datasets. **Molecular Biology and Evolution**, v. 33, n. 7, p. 1870-1874, 2016.

KYTE, J.; DOOLITTLE, R. F. A simple method for displaying the hydropathic character of a protein. **Journal of Molecular Biology**, v. 157, n. 1, p. 105-132, 1982.

LASKOWSKI, R. A.; WATSON, J. D.; THORNTON, J. M. ProFunc: a server for predicting protein function from 3D structure. **Nucleic Acids Research**, v. 33, n. suppl_2, p. W89-W93, 2005.

LEE, D.; REDFERN, O.; ORENGO, C. Predicting protein function from sequence and structure. **Nature Reviews Molecular Cell Biology**, v. 8, n. 12, p. 995, 2007.

LETUNIC, I.; BORK, P. 20 years of the SMART protein domain annotation resource. **Nucleic Acids Research**, v. 46, n. D1, p. D493-D496, 2017.

LEVY, G. G. et al. Mutations in a member of the ADAMTS gene family cause thrombotic thrombocytopenic purpura. **Nature**, v. 413, n. 6855, p. 488, 2001.

LIN, C.; TODO, T. The cryptochromes. **Genome Biology**, v. 6, n. 5, p. 220, 2005.

LIPINSKI, V. M.; DOS SANTOS, T. G.; SCHUCH, A. P. An UV-sensitive anuran species as an indicator of environmental quality of the Southern Atlantic Rainforest. **Journal of Photochemistry and Photobiology B: Biology**, v. 165, p. 174-181, 2016.

LIU, Z. et al. Dynamics and mechanism of cyclobutane pyrimidine dimer repair by DNA photolyase. **Proceedings of the National Academy of Sciences**, v. 108, n. 36, p. 14831-14836, 2011.

LONDERO, J.E.L., Interspecific amplexus between two treefrogs of the genus *Boana* Gray, 1825 (Anura: Hylidae) in captivity: male-female and male-male pairings. **Herpetology Notes**, v. 11, p. 413-415, 2018.

LONDERO, J.E.L et al. Impacts of UVB radiation on food consumption of forest specialist tadpoles. **Ecotoxicology and Environmental Safety**, v. 143, p. 12-18, 2017.

LOVELL, S. C. et al. Structure validation by Cα geometry: ϕ, ψ and Cβ deviation. **Proteins: Structure, Function, and Bioinformatics**, v. 50, n. 3, p. 437-450, 2003.

MALHOTRA, K. et al. Putative blue-light photoreceptors from *Arabidopsis thaliana* and *Sinapis alba* with a high degree of sequence homology to DNA photolyase contain the two

photolyase cofactors but lack DNA repair activity. **Biochemistry**, v. 34, n. 20, p. 6892-6899, 1995.

MARCHLER-BAUER, A. et al. CDD: NCBI's conserved domain database. **Nucleic Acids Research**, v. 43, n. D1, p. D222-D226, 2014.

MEI, Q.; DVORNYK, V. Evolutionary history of the photolyase/cryptochrome superfamily in eukaryotes. **PloS ONE**, v. 10, n. 9, p. e0135940, 2015.

MENCK, C. F. M. Shining a light on photolyases. **Nature Genetics**, v. 32, n. 3, p. 338, 2002.

MINISTÉRIO DO MEIO AMBIENTE. Lista Nacional Oficial das Espécies da Fauna Brasileira Ameaçadas de Extinção. **Portaria nº 444, de 17 de dezembro de 2014**. Diário Oficial da República Federativa do Brasil, Brasília, DF. Seção 1, 245, 121-126, 2014.

MÜLLER, M.; CARELL, T.. Structural biology of DNA photolyases and cryptochromes. **Current Opinion in Structural Biology**, v. 19, n. 3, p. 277-285, 2009.

MYERS, N. et al. Biodiversity hotspots for conservation priorities. **Nature**, v. 403, n. 6772, p. 853, 2000.

NEUDECKER, P. et al. Structure of an intermediate state in protein folding and aggregation. **Science**, v. 336, n. 6079, p. 362-366, 2012.

NOWOSHILOW, S. et al. The axolotl genome and the evolution of key tissue formation regulators. **Nature**, v. 554, n. 7690, p. 50, 2018.

O'LEARY, N. A. et al. Reference sequence (RefSeq) database at NCBI: current status, taxonomic expansion, and functional annotation. **Nucleic Acids Research**, v. 44, n. D1, p. D733-D745, 2015.

OZTURK, N. Phylogenetic and functional classification of the photolyase/cryptochrome family. **Photochemistry and Photobiology**, v. 93, n. 1, p. 104-111, 2017.

PARANJPE, D. A.; SHARMA, V. Evolution of temporal order in living organisms. **Journal of Circadian Rhythms**, v. 3, n. 1, p. 7, 2005.

PARK, H.-W.et al. Crystal structure of DNA photolyase from *Escherichia coli*. **Science**, v. 268, n. 5219, p. 1866-1872, 1995.

PEDRETTI, A.; VILLA, L,; VISTOLI, G. VEGA–an open platform to develop chemo-bio-informatics applications, using plug-in architecture and script programming. **Journal of Computer-aided Molecular Design**, v. 18, n. 3, p. 167-173, 2004.

PITTENDRIGH, C. S. Temporal organization: reflections of a Darwinian clock-watcher. **Annual Review of Physiology**, v. 55, n. 1, p. 17-54, 1993.

PYRON, R. A.; WIENS, J. J. A large-scale phylogeny of Amphibia including over 2800 species, and a revised classification of extant frogs, salamanders, and caecilians. **Molecular Phylogenetics and Evolution**, v. 61, n. 2, p. 543-583, 2011.

RASTOGI, R. P. et al. Molecular mechanisms of ultraviolet radiation-induced DNA damage and repair. **Journal of Nucleic Acids**, v. 2010, 2010.

ROENNEBERG, T.; MERROW, M. Circadian clocks - the fall and rise of physiology. **Nature Reviews Molecular Cell Biology**, v. 6, n. 12, p. 965, 2005.

SANCAR, A. Structure and function of DNA photolyase and cryptochrome blue-light photoreceptors. **Chemical Reviews**, v. 103, n. 6, p. 2203-2238, 2003.

SANCAR, A. Structure and function of photolyase and in vivo enzymology: 50th anniversary. **Journal of Biological Chemistry**, v. 283, n. 47, p. 32153-32157, 2008.

SANTOS e LONDERO et al. Sunlight-induced genotoxicity and damage in keratin structures decrease tadpole performance. **Journal of Photochemistry and Photobiology B: Biology**, v. 181, p. 134-142, 2018.

SCHMIDT, M. et al. Protein energy landscapes determined by five-dimensional crystallography. **Acta Crystallographica Section D: Biological Crystallography**, v. 69, n. 12, p. 2534-2542, 2013.

SCHUCH, A. P. et al. Identification of influential events concerning the Antarctic ozone hole over southern Brazil and the biological effects induced by UVB and UVA radiation in an endemic treefrog species. **Ecotoxicology and Environmental Safety**, v. 118, p. 190-198, 2015b.

SCHUCH, A. P. et al. Molecular and sensory mechanisms to mitigate sunlight-induced DNA damage in treefrog tadpoles. **Journal of Experimental Biology**, v. 218, n. 19, p. 3059-3067, 2015a.

SCHUCH, A. P. et al. Sunlight damage to cellular DNA: Focus on oxidatively generated lesions. **Free Radical Biology and Medicine**, v. 107, p. 110-124, 2017.

SESSION, A. M. et al. Genome evolution in the allotetraploid frog *Xenopus laevis*. **Nature**, v. 538, n. 7625, p. 336, 2016.

SHAMRIZ, S.; OFOGHI, H. Design, structure prediction and molecular dynamics simulation of a fusion construct containing malaria pre-erythrocytic vaccine candidate, *PfCelTOS*, and human interleukin 2 as adjuvant. **BMC Bioinformatics**, v. 17, n. 1, p. 71, 2016.

STEBBINS, R. C.; COHEN, N. W. **A natural history of amphibians**. Princeton University Press, 1995.

STEPHEN, F. A. Gapped BLAST and PSI-BLAST: a new generation of protein database search programs. **Nucleic Acids Research**, v. 25, p. 3389-3402, 1997.

STUART, S. N. et al. Status and trends of amphibian declines and extinctions worldwide. **Science**, v. 306, n. 5702, p. 1783-1786, 2004.

SUN, Y.-B. et al. Whole-genome sequence of the Tibetan frog *Nanorana parkeri* and the comparative evolution of tetrapod genomes. **Proceedings of the National Academy of Sciences**, v. 112, n. 11, p. 1257-1262, 2015.

TAKAHASHI, S. et al. Diurnal change of cucumber CPD photolyase gene (CsPHR) expression and its physiological role in growth under UV-B irradiation. **Plant and Cell Physiology**, v. 43, n. 3, p. 342-349, 2002.

UVERSKY, V. N. Intrinsic disorder in proteins associated with neurodegenerative diseases. In: **Protein Folding and Misfolding: Neurodegenerative Diseases**. Springer, Dordrecht, 2009. p. 21-75.

VAN DE MORTEL, T. et al. A comparison of photolyase activity in three Australian tree frogs. **Oecologia**, v. 115, n. 3, p. 366-369, 1998.

WATERHOUSE, A. et al. SWISS-MODEL: homology modelling of protein structures and complexes. **Nucleic Acids Research**, 2018.

WATERHOUSE, A. M. et al. Jalview Version 2—a multiple sequence alignment editor and analysis workbench. **Bioinformatics**, v. 25, n. 9, p. 1189-1191, 2009.

WHILES, M. R. et al. The effects of amphibian population declines on the structure and function of Neotropical stream ecosystems. **Frontiers in Ecology and the Environment**, v. 4, n. 1, p. 27-34, 2006.

YANG, J. et al. The I-TASSER Suite: protein structure and function prediction. **Nature Methods**, v. 12, n. 1, p. 7, 2015b.

YANG, J.; ROY, A.; ZHANG, Y. BioLiP: a semi-manually curated database for biologically relevant ligand–protein interactions. **Nucleic Acids Research**, v. 41, n. D1, p. D1096-D1103, 2013.

YANG, J.; ZHANG, Y. I-TASSER server: new development for protein structure and function predictions. **Nucleic Acids Research**, v. 43, n. W1, p. W174-W181, 2015a.

YANG, Z.; RANNALA, B. Molecular phylogenetics: principles and practice. **Nature Reviews Genetics**, v. 13, n. 5, p. 303, 2012.

ZHONG, D. Electron transfer mechanisms of DNA repair by photolyase. **Annual Review of Physical Chemistry**, v. 66, p. 691-715, 2015.

APÊNDICE A – SÚMULA CURRICULAR

A seguir, a produção científica e atividades realizadas pelo aluno bolsista **(PROEX CAPES – nº 8882.182173/2018-01)** no período vigente do mestrado (março de 2017 – fevereiro de 2019).

Artigos científicos publicados

LONDERO, J.E.L., SANTOS, C.P.; SEGATTO, A.L.A.; SCHUCH, A.P. Impacts of UVB radiation on food consumption of forest specialist tadpoles. ECOTOXICOLOGY AND ENVIRONMENTAL SAFETY, v. 143, p. 12-18, **2017**.

SANTOS, C.P.[§]; **LONDERO, J.E.L.**[§]; SANTOS, M. B.; FELTRIN, R. S.; LOEBENS, L. ; MOURA, L. B. ; CECHIN, S. Z. ; SCHUCH, A. P. Sunlight-induced genotoxicity and damage in keratin structures decrease tadpole performance. JOURNAL OF PHOTOCHEMISTRY AND PHOTOBIOLOGY B-BIOLOGY, v. 181, p. 134-142, **2018**.

***§* Contribuíram igualmente para o presente trabalho.**

LONDERO, J.E.L.; FELTRIN, R.S. ; ROCHA, M.C. ; SCHUCH, A.P. ; SANTOS, M. B. Interspecific amplexus between two treefrogs of the genus *Boana* Gray, 1825 (Anura: Hylidae) in captivity: male-female and male-male pairings. HERPETOLOGY NOTES, v. 11, p. 413-415, **2018**.

Mini-review em processo final de revisão por referees/editor

LONDERO, J.E.L., SANTOS, M.B., SCHUCH, A.P..Impact of solar UV radiation on amphibians: focus on genotoxic stress. MUTATION RESEARCH – GENETIC TOXICOLOGY AND ENVIRONMENTAL MUTAGENESIS.

Trabalhos publicados em anais de eventos

LONDERO, J. E. L.*; SEGATTO, A. L. A. ; SCHUCH, A. P. . Effects of UVB radiation on forest specialist tadpoles' food consumption: the impact of dna photorepair inefficiency. Em: XIII CONGRESSO DA MUTAGEN-BRASIL, 2017, RIBEIRÃO PRETO - SP. LIVRO DE RESUMOS XIII CONGRESSO DA MUTAGEN-BRASIL, **2017**. * **Apresentador**

DOYLE, L. M. M. ; **LONDERO, J. E. L.***; BORIN, B. C. ; FELTRIN, R. S. ; SCHUCH, A. P. Characterization of the genotoxic potential of sunlight in Santa Maria/RS, Brazil. Em: XIII Congresso da MutaGen-Brasil, **2017**, Ribeirão Preto-SP.
***Coorientador de Iniciação Científica**
Resumo/Pôster 1º Lugar na categoria Iniciação Científica na área de Mutagênese Ambiental.

DOYLE, L. M. M. ; **LONDERO, J. E. L.** *; SCHUCH, A. P. . Avaliação dos efeitos genotóxicos da radiação ultravioleta solar em Santa Maria. Em: 32ª Jornada Acadêmica Integrada da UFSM, **2017**, Santa Maria/RS.
***Coorientador de Iniciação Científica**
Resumo/Pôster entre os 40 melhores trabalhos do evento.

BORIN, B.C.; **LONDERO, J.E.L**.*; SCHUCH, A. P. . Caracterização do potencial genotóxico da luz solar em Santa Maria. Em: 33ª Jornada Acadêmica Integrada da UFSM, **2018**, Santa Maria/RS.
***Coorientador de Iniciação Científica**

Cursos e palestras ministrados

LONDERO, J. E. L.. Método alternativo *in vitro* para detecção e quantificação de lesões de DNA (VIII Oficina de Inverno em Bioquímica Toxicológica). **2018**. (Curso Teórico-Prático).

LONDERO, J. E. L.. Respostas ao Estresse Genotóxico - VIII Semana Acadêmica Biologia UFSM-Palmeira das Missões. **2018**. (Ministrante de palestra).

Participação em cursos/eventos

XIII Congresso da MutaGen-Brasil, Ribeirão Preto-SP, **2017**.

Métodos para o estudo dos mecanismos de reparo de DNA; Mutagen-Brasil, Ribeirão Preto/SP - Carga horária: 2 h – **2017**

Phyton para Biologia Molecular, Universidade Federal do Rio Grande do Sul (UFRGS), Brasil - Carga horária: 9 horas – **2018**